APPENDIX 2CC

GROUNDWATER MODEL DEVELOPMENT AND ANALYSIS

Appendix 2CC Table of Contents

APPENDIX 2CC TABLE OF CONTENTS (CONT.)

APPENDIX 2CC TABLE OF CONTENTS (CONT.)

Appendix 2CC List of Tables

Appendix 2CC List of Figures

APPENDIX 2CC LIST OF FIGURES (CONT.)

APPENDIX 2CC LIST OF FIGURES (CONT.)

UNITS

ft	feet
m	meter
cm/s	centimeters per second
ft/day	feet per day
ft/s	feet per second
in/yr	inches per year
ft^2/day	feet squared per day
gpm	gallons per minute
gpd	gallons per day
kg/m^3	kilograms per meter cubed

ABBREVIATIONS

ARM	Absolute Residual Mean
bgs	Below Ground Surface
CCS	Cooling Canal System
COLA	Combined License Application
DEM	Digital Elevation Model
DRN	Drain Package (MODFLOW)
epm	Equivalent Porous Media
FPL	Florida Power & Light
GHB	General-Head Boundary Package (MODFLOW)
GMG	Geometric Multigrid (MODFLOW)
HFB	Horizontal Flow Boundary Package (MODFLOW)
Kh	Horizontal Hydraulic Conductivity
Kv	Vertical Hydraulic Conductivity
M_d	Mass Balance Discrepancy
MNW	Multi-Node Well Package (MODFLOW)
MODFLOW	Modular Groundwater Flow Model
MRGIS	Marine Resources Geographic Information System
MSE	Mechanically Stabilized Earth (Retaining Wall)
MWR	Makeup Water Reservoir
NED	National Elevation Database
NAVD 88	North American Vertical Datum of 1988
NOAA	National Oceanic and Atmospheric Administration
NRMS	Normalized Root Mean Square
OCS	Office of Coast Survey
RCW	Radial Collector Well
RMS	Root Mean Squared
RIV	River Cell Package (MODFLOW)

SEE	Standard Error of the Estimate
SEGS	Southeastern Geological Society
SFWMD	South Florida Water Management District
USGS	United States Geological Survey
US	United States
WEL	Well Package (MODFLOW)

EXECUTIVE SUMMARY

A groundwater flow model of the Florida Power & Light (FPL) Turkey Point site has been developed for Units 6 & 7. The model is a steady-state, constant-density, three-dimensional representation of the surficial aquifer system developed using the numerical code MODFLOW 2000 developed by the United States Geological Survey (USGS), as it is implemented in the user-interface software Visual MODFLOW developed by Schlumberger Water Services.

The groundwater model was developed in two phases. Phase 1 serves two purposes. The first is to evaluate groundwater control options for construction of Units 6 & 7. The second is to simulate the operation of a radial collector well system serving as a temporary source of makeup water. Phase 2 was developed to include several additional post-construction features. These post-construction features include splitting the top model layer into two layers; revision of the top elevation of the diaphragm walls to 2 feet NAVD 88; incorporation of structural backfill in the top model layer; and incorporation of the Makeup Water Reservoir (MWR) as an active feature. Phase 2 consists of four post-construction simulations: a "base-case" simulation, a sensitivity simulation to evaluate the effect of high recharge, a simulation to assess the failure of the MWR north wall, and a simulation to assess the effect of sea-level rise on groundwater elevations.

Hydrostratigraphic layer elevations were developed from geotechnical and geophysical logs for Units 6 & 7, pumping test wells in the Turkey Point Units 6 & 7 plant area and Turkey Point peninsula, pumping wells from the 1975 Turkey Point plant property Upper Floridan Aquifer study, from historical borings and well logs from the Turkey Point plant property, and from logs for wells in the Florida Geological Survey Lithologic database.

Hydraulic conductivity values were based on results from three historical pumping tests in the Biscayne Aquifer on the Turkey Point plant property, regional groundwater models that include the Turkey Point plant property within their domain, recent pumping tests at the plant area and the Turkey Point peninsula, and literature values.

The interaction between surface water and groundwater was simulated by including Biscayne Bay, the cooling canals, L-31E Canal, Card Sound Canal, Florida City Canal, and Model Land Canal (C-107) in the model. Spatially-variable groundwater recharge and evapotranspiration are considered based on land-use classification.

Calibration was approached with a multi-faceted methodology. Initially, the response to three pumping tests (PW-7L, PW-1, and PW-7U) was simulated by adjusting hydraulic conductivities of the various hydrostratigraphic units comprising the Biscayne Aquifer. The conductance values of the various head-dependent boundary conditions were also primary calibration parameters.

Following the calibration, groundwater flow directions were compared to historical data, and a qualitative comparison of calculated groundwater discharge/recharge between cooling water canals and groundwater beneath Biscayne Bay to results from pre-existing surface water modeling was performed. The groundwater model was then validated by simulating an additional pumping test (PW-6U) and comparing the modeled and observed drawdown values.

The conclusion from Phase 1 model simulations of construction dewatering for the Unit 6 and Unit 7 nuclear islands was that by utilizing cut-off walls and implementing a grout blanket between the base of the excavation and the base of the cut-off walls, construction dewatering rates were reduced to approximately 100 gpm for each unit. Phase 1 particle tracking and water balance calculations from the proposed radial collector wells at the Turkey Point peninsula in Biscayne Bay indicate that approximately 97.8 percent of the water pumped from the radial collector wells originates in Biscayne Bay. A suite of sensitivity analyses addressing parameter and water level uncertainty indicate that this percentage remains similar for the tested range of variability.

For Phase 2 model simulations, water table elevations at Units 6 & 7 satisfied the Design Control Document (DCD) criteria. For all simulations, maximum post-construction water table elevations within the nuclear islands, which include the containment, shield, and auxiliary buildings, were estimated to be approximately 2 feet NAVD 88. The maximum increase in water table elevations with high recharge near Units 6 & 7 was estimated to be approximately 0.3 feet higher than the base-case simulation. Maximum post-construction water table elevations, assuming a failure of the MWR north wall, were estimated to be 2.07 feet NAVD 88 at the Units 6 & 7 nuclear islands. The maximum increase in water table elevations at the Units 6 & 7 nuclear islands with sea-level rise was estimated to be approximately 0.03 feet higher than the base-case simulation.

1.0 OBJECTIVE & SCOPE

The objective is to document the development, calibration, and simulation results of a groundwater flow model for the Turkey Point Units 6 & 7 Project at the Turkey Point facility.

A three-dimensional groundwater model was used to simulate steady-state, constant-density groundwater flow in the Biscayne Aquifer to evaluate construction and post-construction activities related to the construction and operation of two new nuclear units (Units 6 & 7).

2.0 AQUIFER DESCRIPTION & AVAILABLE DATA

2.1 Site Overview

Turkey Point plant property is located in Miami-Dade County, Florida, approximately 25 miles south of Miami (Figure 2.4.1-201) and approximately 9 miles southeast of Homestead. It is bordered on the east by Biscayne Bay, on the west by the FPL Everglades Mitigation Bank, and on the northeast by Biscayne National Park. The 5900-acre Industrial Wastewater Facility (approximately 2 miles wide and 5 miles long), of which 4370 acres is water (approximately 75 percent), is a predominant feature within the Turkey Point plant property (Figure 2.4.12-210). Just west of the Industrial Wastewater Facility is the L-31E canal, which is part of the regional drainage system.

The Units 6 & 7 plant area covers an area of approximately 218 acres and is situated south of Units 1 through 5 within the Industrial Wastewater Facility. The units occupy a relatively small portion of the Turkey Point plant property. The preconstruction ground surface in the Units 6 & 7 plant area is generally flat, with elevations ranging from -2.4 to 0.8 feet NAVD 88.

Surface waters are a dominant feature of the Turkey Point plant property and surrounding region given that the plant is located between Biscayne Bay and the Everglades. A network of regional canals surrounds the site boundary and provides drainage for areas west of the Turkey Point plant property. The Units 6 & 7 plant area is within the Industrial Wastewater Facility and is surrounded by cooling canals that return water back to the intake structures for Units 1 through 4.

2.2 Regional Hydrostratigraphy

As discussed in FSAR Subsection 2.4.12, the hydrostratigraphic framework of Florida consists of a thick sequence of Cenozoic sediments that comprise three main units (Reference 1):

- The surficial aquifer system (containing the Biscayne Aquifer and semi-confining Tamiami Formation).
- The intermediate confining unit, referred to as the Hawthorn Group.
- The Floridan aquifer system.

In southern Florida, the surficial aquifer system consists of the Tamiami, Caloosahatchee, Fort Thompson, and Anastasia Formations; the Key Largo and Miami Limestones; and undifferentiated sediments. The thickness of the surficial aquifer system ranges from approximately 20 feet to 400 feet and is approximately 220 feet under the Units 6 & 7 plant area.

The intermediate confining unit separates the Biscayne aquifer from the underlying Floridan aquifer system. It is characterized regionally by a sequence of relatively low hydraulic conductivity, largely clayey deposits, but it can locally contain transmissive units that act as an aquifer system. The Southeastern Geological Society (SEGS) (Reference 1) define the intermediate confining unit as "all rocks that lie between and collectively retard the exchange of water between the overlying surficial aquifer system and the underlying Floridan aquifer system." This unit is also referred to as the Hawthorn Group, with a thickness of approximately 900 feet in southern Florida.

Beneath the intermediate aquifer system/confining unit is the Floridan aquifer system which underlies all of Florida. The system formally consists of three hydrogeologic units: the Upper Floridan aquifer, the middle confining unit, and the Lower Floridan aquifer. The Upper Floridan aquifer is a major source of potable water in Florida, however, in the southeastern portion of the state (including Miami-Dade County) the water is brackish.

Hydrostratigraphic columns are presented in Figures 2.4.12-202 and 2.4.12-204.

2.3 Biscayne Aquifer

The surficial aquifer system within the Turkey Point plant property does not contain all of the regionally identified units. Those units identified within the plant

property as a result of the 1971 (Reference 2), 2008 (Reference 3), and 2009 (Reference 4) subsurface investigations are summarized as:

- Muck — The surface of the site consists of approximately 2 to 6 feet of organic soils called muck. The muck is composed of recent light gray calcareous silts with varying amounts of organic content. This unit does not extend into Biscayne Bay, where exposed rock and sandy material is present in its place.

- Miami Limestone — The Pleistocene Miami Limestone is a white, porous sometimes sandy, fossiliferous, oolitic limestone.

- Upper Higher Flow Zone — At the boundary between the Miami Limestone and Key Largo Limestone is a laterally continuous relatively thin layer of high secondary porosity. The Upper Higher Flow Zone was defined based on a review of geophysical logs and drilling records. The primary identifier was the loss of drilling fluid identified at the boundary of the Key Largo Limestone and Miami Limestone. This observation was also coincident with an increase in the boring diameter as identified by the caliper logging.

- Key Largo Limestone (interpreted as the Fort Thompson Formation elsewhere) — This is a coralline limestone (fossil coral reef) believed to have formed in a complex of shallow-water, shelf-margin reefs and associated deposits along a topographic break during the last interglacial period.

- Freshwater Limestone — At the base of the Key Largo Limestone is a layer of dark-gray fine-grained limestone, referred to as the Freshwater Limestone. Where present, the limestone is generally two feet or more thick and often possesses a sharp color change from light to dark gray at its base marking the transition from the Key Largo Limestone to the Fort Thompson Formation. It is not laterally continuous across the Turkey Point plant property.

- Fort Thompson Formation — The Pleistocene Fort Thompson Formation directly underlies the Key Largo Limestone. The Fort Thompson Formation is generally a sandy limestone with zones of uncemented sand interbeds, some vugs, and zones of moldic porosity after gastropod and/or bivalve shell molds and casts.

- Lower Higher Flow Zone — At the location of Units 6 & 7, a zone of secondary porosity was evident from the drilling and geophysical logs. This occurred at a depth of approximately 15 feet below the top of the Fort Thompson Formation and was assumed to extend across the model domain. The regional drilling

conducted by the USGS (Reference 5) did not identify a laterally persistent layer but rather more isolated zones at varying depths below the Upper Higher Flow Zone. As represented in the model, the Lower Higher Flow Zone represents an aggregation of these observations and is conservative due to the fact it is modeled as laterally extensive.

- Tamiami Formation — The Pliocene Tamiami Formation directly underlies the Fort Thompson Formation. The contact between the Tamiami Formation and the Fort Thompson Formation is an inferred contact picked as the bottom of the last lens of competent limestone encountered. The Tamiami Formation represents a semi-confining unit.

The most permeable portions of the Miami Limestone and Key Largo Limestone are considered to be acting as one hydrogeological unit and designated the "Upper Monitoring Zone." The underlying Fort Thompson is designated the "Lower Monitoring Zone."

The geology is shown in the following cross sections:

- Hydrostratigraphic cross section in the vicinity of the Units 6 & 7 as shown in Figure 2CC-201 and Figure 2CC-202 (Reference 2).

- Geologic cross section across in the vicinity of the Units 6 & 7 as shown in Figure 2CC-203 (Reference 6).

- Boring plan and stratigraphic cross sections parallel to and across Units 6 & 7 as shown in Figure 2CC-204, Figure 2CC-205, and Figure 2CC-206.

- Plan and geologic cross section at the Turkey Point peninsula from exploratory drilling and aquifer testing program as shown in Figure 2CC-207 (Reference 4).

The following list summarizes the stratigraphic picks for the top of each stratum identified above from geotechnical boring logs and well logs:

- Stratigraphic picks from geotechnical boring logs for Units 6 & 7 (Reference 3) B-601 to B-639, B-701 to B-739, and B-802 to B-814.

- Stratigraphic picks from boring logs for the 1971 site investigation (Reference 2), L-1 through L-6, and GH-1 through GH-15.

- Stratigraphic picks from Upper Floridan aquifer study pumping wells (Reference 2), GB-1 and GB-2.

- Geotechnical boring logs from the Feasibility Geological Investigation of Potential Plant Site borings B-1000 through B-1003.

- Additional water well logs available from Florida Geological Survey lithologic database (Reference 7) and the USGS (Reference 8).

- Stratigraphic picks from boring logs for the Turkey Point peninsula (Reference 4) and Units 6 & 7 pumping tests.

In 2010, 14 borings were drilled in and around the Turkey Point plant area as part of the FPL Unit 3 & 4 Uprate Conditions of Certification (Reference 5). Biscayne aquifer monitoring well clusters were subsequently installed at each of the 14 core borings as part of a monitoring plan (Reference 9). The plan was developed and implemented to satisfy Conditions of Certification IX and X of the Turkey Point Units 3 & 4 Uprate Certification. These well clusters were not included in the stratigraphic picks used to develop the model because they were not available at the appropriate time, but downhole logs (caliper and acoustic) performed by the USGS from these borings were qualitatively assessed to confirm zones of secondary porosity.

2.4 Groundwater Levels

During the 2008 subsurface investigation for Units 6 & 7, 22 groundwater monitoring locations were installed within the Units 6 & 7 plant area. Ten observation wells were installed in the Key Largo and Miami Limestone (referred to as the Upper Monitoring Zone) and ten were installed in the Lower Fort Thompson Formation (referred to as the Lower Monitoring Zone). Two piezometers were installed in the Tamiami Formation, one at each proposed reactor site. The 20 observation wells were installed as 10 well pairs, enabling the determination of the vertical gradient between the upper and lower monitoring units. A description of the field activities and groundwater level data evaluation are presented in Reference 3.

Figure 2.4.12-209 shows the 22 monitoring locations within the Units 6 & 7 plant area. The observation wells are named in three series, which represent the location and screened intervals as described below:

- OW-600 series wells are located in the Unit 6 power block area and include "U," "L," and "D" suffix wells monitoring the Miami Limestone, the lower Fort Thompson Formation, and the upper Tamiami Formation.

- OW-700 series wells are located in the Unit 7 power block area and include "U," "L," and "D" suffix wells monitoring the Miami Limestone, the lower Fort Thompson Formation, and the upper Tamiami Formation.

- OW-800 series wells are located outside of the power block areas and include "U" and "L" suffix wells that monitor the Miami Limestone and the lower Fort Thompson Formation.

The U and L observation wells recorded hourly water level measurements between June 2008 and June 2010, after which point the transducers were removed and monitoring ceased. Comparison of well clusters (U and L wells) show an upward gradient during both high and low tides at all monitored locations.

Two regional historic Biscayne Aquifer potentiometric surface maps are also available. They cover the following months:

- May 1993, Figure 2.4.12-219

- November 1993, Figure 2.4.12-220

2.5 Surface Water

Surface water features around the Turkey Point plant property are shown on Figure 2.4.12-210 and include the following:

- Biscayne Bay — This feature is located east of Units 6 & 7 and is a shallow, subtropical lagoon along the southeastern coast of Florida. Biscayne Bay is a fairly recent geological feature and has been modified and dredged with average depths ranging from 6 feet to 10 feet. Surface water flow into Biscayne Bay is primarily controlled by the system of canals, levees, and control structures maintained by the South Florida Water Management District (SFWMD). The National Oceanic and Atmospheric Administration (NOAA) maintains a tidal water level and meteorological data collection station (#8723214) on Virginia Key in Biscayne Bay. The station is located on a pier just to the southwest of the causeway that connects Virginia Key to Key Biscayne (Reference 10). Station #8723214 is the closest active station to the study area. The diurnal range, difference in height between mean higher high

water and mean lower low water for the station is approximately 2.19 feet (Reference 10).

- Cooling Canal System (CCS) (also referred to as the Industrial Wastewater Facility) — The cooling canals are a closed system and do not directly discharge to adjacent surface water, however, the canals are unlined and hence the water interacts with groundwater.

    — After cooling water passes through the Units 1 through 4 condensers and gains heat, the water is released to the northern end of the 32 westernmost canals. These westernmost canals are approximately 4 feet deep and oriented north-south. The warm water flows towards the southern end of the westernmost canals where it then flows eastward across the southern end of the canals to the seven easternmost canals. These easternmost canals provide the cooling water return, and the circulating pumps are located on the return side, in the northeastern corner of the closed loop system. The pumps in the northeastern corner maintain a head difference of four to five feet relative to the release location. This head difference is the driving force for circulation through the system. Blowdown from Unit 5 also contributes to flow in the CCS.

    — The head differential created by the circulating water pumps is maintained despite or in addition to the tidal fluctuations. The head differential is a maximum at the northern end of the system; the highest head is in the northern end of the westernmost canals and the lowest head is in the northern end of the easternmost canals. The release of warm water to the northern end of the cooling canals means that the water level in the westernmost canals is always higher than the water level in Biscayne Bay. The intake of return water from the easternmost canals by the circulating pumps, means that the water level in the easternmost canals is always lower than that of Biscayne Bay. At the southern end of the system, the influence of the enforced head differential is relatively lower and water levels are approximately equal to the water level in Biscayne Bay/Card Sound.

    — Interceptor Ditch — The Interceptor Ditch was constructed in conjunction with the cooling canals to limit inland movement of the water from the cooling canals in the upper portion of the aquifer. This ditch is approximately 30 feet wide, 19 feet deep, and has a total

length of approximately 29,000 feet. The Interceptor Ditch is located approximately 1000 feet to the southeast of the L-31E canal. Operation of the Interceptor Ditch prevents seepage from the industrial wastewater facility from moving landwards towards the L-31E Canal in the upper portion of the aquifer. The Interceptor Ditch is operated (seasonally) only when required to maintain a seaward hydraulic gradient from L-31E.

- L-31E (SFWMD Salinity Structure) — The L-31E Canal (shown in Figure 2.4.12-210) is a stormwater control structure and also provides a salinity barrier that is designed to help prevent saltwater from moving inland. L-31E was constructed prior to the cooling canals being built.

2.6 Recharge and Evapotranspiration

The net infiltration, or groundwater recharge, accounts for the rate of net gain of the groundwater system resulting from surface infiltration. Recharge to the Biscayne Aquifer is controlled by land use, and in southern Florida the recharge occurs mainly through wetland areas. Figure 2CC-208 indicates major land use classifications used by Langevin (Reference 11) for a regional model of the Biscayne Aquifer.

Based on land use and the Turkey Point facility-related surface conditions, three recharge/evapotranspiration zones are considered for the model domain:

- Surface water bodies with continuous head of water, such as Biscayne Bay, the cooling canal system, and regional canals.
- Areas of wetland.
- Buildings and paved areas.

Surface water bodies, buildings, and paved areas in the model are assumed to have zero recharge and zero evapotranspiration. Recharge applied to the wetland areas is determined by using monthly rainfall data from SFWMD Station S20F (Reference 12) located on canal L-31E. Historically, up to four different rainfall data recorders have been used at Station S20F. The NRG recorder (which reports rain gauge data augmented with radar-based rainfall data), is the preferred data source, but is only available for the most recent two years. The TELE (telemetry, i.e. radio network) and OMD (data received from operation/ main, with multiple sources) recorders are considered to be equally reliable secondary sources of data, for years prior to the NRG record. In years when both TELE and OMD data

were available, but NRG data were not, the TELE and OMD records were averaged. Finally, the BELF (Belfort rain gauge) recorder data are used prior to 1992, before the other recorders were available. For the calibration/validation models, a value of 42.6 in/yr is used for the wetlands recharge rate. This value is calculated by summing the total rainfall data for the months during which the on-site 2009 pumping tests were conducted (February to May 2009) and then scaling the total to a year, as shown in Table 2CC-201. For the predictive runs, the long-term average rainfall for the period of record at Station S20F was used, giving a recharge rate of 46.75 in/yr, as shown in Table 2CC-202.

The evapotranspiration rate and extinction depth for the wetland areas is determined using values from Langevin (Reference 11) presented in Table 2CC-203. For the calibration/validation, using maximum evapotranspiration from February to May gives an evapotranspiration rate of 54.52 in/yr. For the predictive runs, maximum evapotranspiration for every month is used to calculate an evapotranspiration rate of 59.50 in/yr. For all models, the extinction depth of 0.69 meters (2.26 feet) for wetlands is used (Table 2CC-203).

2.7 Hydraulic Conductivity

The following sections describe the results from pumping tests and slug tests to evaluate hydraulic conductivity for the Biscayne Aquifer.

2.7.1 Pumping Tests

Pumping tests performed within the footprints of Units 6 & 7 nuclear islands, which consist of the containment, shield, and auxiliary buildings, are summarized as follows:

- PW-6U (Key Largo Limestone) — This pumping test was performed in March 2009, with the test well pumped at an average rate of 5103 gpm for eight hours. The test well is located in the footprint of the Unit 6 reactor building. The hydraulic conductivity was estimated to be 3.3 cm/s.

- PW-7U (Key Largo Limestone) — This pumping test was performed in February 2009, with the test well pumped at an average rate of 4181 gpm for approximately nine hours. The test well is located in the footprint of the Unit 7 reactor building. The hydraulic conductivity was estimated to be 4.3 cm/s.

- PW-6L (Fort Thompson Formation) — This pumping test was performed in March 2009, with the test well pumped at an average rate of 3342 gpm for

eight hours. The test well is located in the footprint of the Unit 6 reactor building. The hydraulic conductivity was estimated to be 0.1 cm/s.

- PW-7L (Fort Thompson Formation) — This pumping test was performed in March 2009, with the test well pumped at an average rate of 3403 gpm for nine hours. The test well is located in the footprint of the Unit 7 reactor building. The hydraulic conductivity was estimated to be 0.2 cm/s.

A pumping test at Turkey Point peninsula to characterize the hydrogeology for a potential radial collector system is summarized as follows (Reference 4):

- PW-1 (Miami Limestone/Cemented Sand/Key Largo Limestone) — This pumping test was performed in April and May 2009, with the test well pumped at an average rate of 7100 gpm for seven days. The hydraulic conductivity of the test zone was estimated to be between 10.3 cm/s and 17.6 cm/s based on a reported range of transmissivity between 700,000 ft^2/day and 1,200,000 ft^2/day.

On the Turkey Point plant property, aquifer pumping tests in the Biscayne Aquifer have been performed in three test wells (Reference 2). Figure 2CC-201 shows locations of test wells GH-11B, GH-14A, and GH-14B. Pumping test results are summarized as follows:

- GH-14A (Miami Limestone) — This pumping test is located to the southeast of L-31E, adjacent to the northwest portion of the cooling canal system. The test was performed in June 1971, with the test well pumped at 1386 gpm for four hours. The hydraulic conductivity was estimated to be 7.9E-02 cm/s.

- GH-11B (Key Largo Limestone) — This pumping test is located between Model Land Canal and L-31E. The test was performed in June 1971, with the test well pumped at 1386 gpm for four hours. The hydraulic conductivity was estimated to be 5.1 cm/s.

- GH-14B (Fort Thompson Formation) — This pumping test is located to the southeast of L-31E adjacent to the northwest portion of the cooling canals. The test was performed in June 1971, with the test well pumped at 1386 gpm for two hours. The hydraulic conductivity was estimated to be 1.6 cm/s.

2.7.2 Literature Values

Several investigations of the Biscayne Aquifer have provided estimates for the hydraulic conductivity of various units of the Biscayne Aquifer. All of these studies have been conducted by either the USGS or SFWMD. Presented in Table 2CC-204 is a summary of hydraulic conductivity values for the Biscayne Aquifer.

2.8 Water Wells

No water supply wells are located in the Biscayne Aquifer within the plant property. Three production wells (PW-1, PW-2, and PW-4) are located in the Upper Floridan aquifer (Figure 2.4.12-211) and provide process water for Units 1 and 2, and process and cooling tower makeup water for Unit 5. The average production of these wells is approximately 170 million gallons per month.

The Biscayne Aquifer at Turkey Point Units 3 & 4 is also used for disposal of domestic wastewater. A single Class V, Group 3 gravity injection well is used to dispose of up to 35,000 gpd of domestic wastewater at the Turkey Point Units 3 & 4 wastewater treatment plant. The well, designated IW-1, is open from 42 to 62 feet bgs and is 8 inches in diameter. Due to the low injection rate (up to 24 gpm) this well is not included in the numerical model.

3.0 MODEL DEVELOPMENT

3.1 Conceptual Hydrogeologic Model

The Biscayne Aquifer is conceptualized as consisting of eight hydrostratigraphic units. The base of the model (bottom of the Tamiami Formation) is designated as a no-flow boundary as leakage through the confining Hawthorn Formation is assumed to be negligible.

Recharge to the Biscayne Aquifer occurs primarily in areas of wetland and along the regional series of canals. Discharge from the Biscayne Aquifer occurs to Biscayne Bay, a portion of the cooling canals, and the regional series of canals. The cooling canals are the dominant stress at the Units 6 & 7 Site. Evapotranspiration is also a dominant stress on the groundwater system.

The model domain was selected to minimize the impact of assumptions regarding boundary conditions at model sides. The boundaries of the model domain were placed where reasonable assumptions regarding local conditions could be made. Figure 2CC-209 shows the model domain. The model area extends several miles

beyond the plant property and covers a total area of 47,500 feet by 37,000 feet (approximately 63 square miles).

The northern and southern model boundaries were extended several miles beyond the plant property, however they do not coincide with any hydrogeologic features. The eastern model boundary extends into Biscayne Bay, and the western boundary was extended beyond the L-31E canal.

3.2 Numerical Model

3.2.1 Numerical Code

The conceptual hydrogeologic model is developed into a three-dimensional numerical groundwater model using the code MODFLOW-2000 (Reference 13) hereafter referred to as MODFLOW. MODFLOW solves the three-dimensional groundwater flow equation using a finite-difference method. This code is widely used in the industry since its development by the USGS (Reference 14 and Reference 15).

MODFLOW has a modular structure that allows the incorporation of additional modules and packages to solve other equations that are often needed to handle specific groundwater problems. Over the years several such modules and packages have been added to the original code. MODFLOW-2000 is major revision of the code that expands upon the modularization approach that was originally included in MODFLOW.

The modeling pre-processor Visual MODFLOW (Reference 16) is used to facilitate the development of the FPL Turkey Point Units 6 & 7 groundwater flow model. Visual MODFLOW is developed by Schlumberger Water Services.

3.2.2 Numerical Solver

The geometric multigrid solver (GMG) in Visual MODFLOW produces converged solutions for the model, and is used for all simulations presented. The GMG solver uses two convergence criteria, the head change between successive outer iterations and the residual criterion, which is based on the change between successive inner iterations. The model uses the default values of 0.01 feet for the head change criterion and 0.01 feet for the residual criterion.

3.2.3 Model Grid

Figure 2CC-210 shows the model grid and site features for the power block vicinity. At its finest, the model grid spacing is approximately three feet by three

feet within the plant area for Units 6 & 7, and expands to 100 feet by 100 feet at the model perimeter. The grid spacing is also refined in the vicinity of the Turkey Point peninsula, to enable simulation of pumping test PW-1 and the radial collector wells. In this area, the grid spacing is reduced to 25 feet by 25 feet.

3.2.4 Model Layers

The model is bounded by the ground surface and bottom of Biscayne Bay on top and the bottom of the Tamiami Formation at the model bottom. A topobathy surface referenced to NAVD 88 was developed for the ground surface topography of the FPL Turkey Point Units 6 & 7 groundwater flow model. A topobathy surface is a surface that combines land elevation and seafloor topography with a uniform vertical datum (Reference 17). Several data sources were reviewed for potential integration into the topobathy surface. The final topobathy surface was developed from the USGS's National Elevation Dataset (NED) Digital Elevation Models (DEMs) (Reference 18) and NOAA's Office of Coast Survey (OCS) harbor soundings (Reference 19). The selection of the final datasets was based primarily on which two datasets produced the smoothest shoreline transition.

Fourteen model layers are included in the Phase 1 model as follows:

- Model Layer 1 — Onshore: organic soils, referred to as muck and marl. Offshore: sand/sediment and Miami Limestone.
- Model Layers 2/3 — Marine limestone, referred to as the Miami Limestone.
- Model Layer 4 — Marine limestone, referred to as the Upper Higher Flow Zone.
- Model Layer 5/6 — Marine limestone, referred to as the Key Largo Limestone (divided into two areal zones based on prior information).
- Model Layer 7 — Freshwater limestone, referred to as the Freshwater Limestone, and where this is absent the Key Largo Limestone.
- Model Layer 8/9 and 11/12/13 — Marine limestone, referred to as the Fort Thompson Formation.
- Model Layer 10 — Marine limestone, referred to as the Lower Higher Flow Zone.

- Model Layer 14 — Marine limestone or sandstone, referred to as the Tamiami Formation.

Elevations are assigned to each model cell based on the results of the interpolation of stratigraphic picks. Figure 2CC-211 and Figure 2CC-212 show cross sections of the model with relevant features highlighted.

3.2.5 Boundary Conditions

The model incorporates several types of boundary conditions, including river cells, recharge cells, evapotranspiration cells, general-head cells, horizontal flow barrier cells, and no-flow cells. A brief description of boundary conditions as they are used in the model is provided below:

- River Boundary — (1) Cooling Canal System, (2) L-31E, (3) C-107, (4) Card Sound Canal, and (5) Florida City Canal: The river boundary condition allows leakage into the model or leakage out of the model based on (a) specified surface water elevation in the canal, (b) simulated groundwater elevations in adjoining grid cells, and (c) sediment conductance at the bottom and sides of the canals. River cells are employed in lieu of constant head cells to allow flexibility to adjust the conductance and hence flow to adjoining cells during calibration.

- Recharge Boundary — Model Layer 1: The recharge boundary condition is applied at the ground surface (top of model layer 1) and simulates the effect of infiltration from precipitation (before evapotranspiration losses). Recharge in the model is only applied to land surfaces (no recharge is applied to surface water features).

- Evapotranspiration Boundary — Model Layer 1: The evapotranspiration boundary condition is applied at the ground surface (top of model layer 1) and simulates the effects of plant transpiration and direct evaporation by removing water from the saturated groundwater regime. Evapotranspiration is applied only over land surfaces in the model.

- General-Head Boundary (GHB):

    — (1) Model Sides: General-head boundary conditions are assigned to the perimeter of all layers. The general-head boundary represents the influence of conditions beyond the model area. Flow through the

onshore general-head boundaries is influenced by aquifer recharge in the Everglades area.

— (2) Biscayne Bay: General-head boundary conditions are assigned to the top of model layer 1 to represent the exchange of water between Biscayne Bay and the underlying aquifer. The specified head in the GHB cell is based on tidal monitoring at Virginia Key. Use of the GHB condition rather than the constant head condition allows for limiting the exchange of water between Biscayne Bay and the underlying aquifer based on the properties of the sea floor sediments.

- Horizontal Flow Barrier Boundary — Mechanically Stabilized Earth (MSE) Retaining Wall and Cut-Off Walls for Units 6 & 7: The horizontal flow barrier boundary is used to simulate the effects of the excavation cut-off walls surrounding the power blocks for Units 6 & 7 for construction dewatering and also the MSE retaining wall surrounding the Units 6 & 7 plant area (excluding the makeup water reservoir). This package was developed to simulate the effects of thin, vertical, low hydraulic conductivity features that restrict the horizontal flow of groundwater.

- No-Flow Boundary — Bottom of Model: The bottom of the model is designated a no-flow boundary because water levels in the Biscayne Aquifer are expected to be negligibly affected by upward leakage through the Lower Tamiami Formation and Hawthorne Group, which is several hundred feet thick and acts as a confining layer.

- No-Flow Boundary — Units 6 & 7 Excavations: The excavations are designated as inactive to flow. Minor seepage will occur through the cut-off walls into the excavations but the quantities will be insignificant.

3.3 Assumptions

The model development includes the assumptions described below.

3.3.1 Equivalent Porous Media

Assumption: The flow regime is simulated using an equivalent porous media (epm).

Rationale: The effects of small-scale heterogeneities become averaged when used in an analysis of this scale. Preferential higher flow zones identified at

the site are relatively thin and are expected to have laminar flow; therefore, they can be represented in the model by assigning higher hydraulic conductivities to these zones using an epm approach (as opposed to conduit flow).

3.3.2 Steady-State Condition

3.3.2.1 Pumping Tests

Assumption: The pumping tests can be modeled by matching the steady-state drawdown values in each observation well rather than a transient simulation matching the entire drawdown curve.

Rationale: Steady-state conditions from the pumping tests are reached after a very short period of time due to 1) the confined nature of the test zones, and 2) the high hydraulic conductivity of the test zones.

3.3.2.2 Groundwater Flow

Assumption: The cooling canals are assumed to be in steady-state.

Rationale: Previous modeling of the cooling canals assumed the system was in equilibrium and hence steady state. Figure 2CC-213 presents the balance of flows as documented in a previous study. This balance assumes that the existing units are operating at capacity. This assumption is conservative for determination of origins of water to the radial collector wells.

3.3.3 Constant-Density

Assumption: The flow regime is simulated with a constant-density groundwater model.

Rationale: The primary purpose of this groundwater model is to estimate quantities for excavation dewatering and to evaluate the influence of the radial collector wells. For these two localized areas of interest the pressure influences of density variation are insignificant relative to the hydraulic gradient imposed by pumping.

Assumption: Seawater is used as the reference fluid.

Rationale: For a constant density model, water levels should be normalized to a reference fluid to satisfy the steady-state, constant-density equation. Water levels in the model are normalized to a saline reference density of 1022.4 kg/

m^3. The hypersaline water of the cooling canal system and the freshwater of the drainage canals are adjusted to seawater using the following equation:

$$h_r = \frac{\rho_w}{\rho_r} h_w - \frac{\rho_w - \rho_r}{\rho_r} z_w$$

Where:

h_r is the head at the reference density

h_w is the observed head at the natural density

z_w is the water (canal) depth at the natural density

ρ_w is the natural density of the water

ρ_r is the reference density

For the calibration cases where the Biscayne Bay level is -1.05 feet NAVD 88, normalized head values at locations around the cooling canals and stormwater management canals are presented in Table 2CC-205.

3.3.4 Hydrostratigraphic Units

Assumption: The Freshwater Limestone is assumed to be absent if the contoured thickness is less than 1.5 feet.

Rationale: It is possible that this layer is laterally continuous and where it is not observed it is due to the method of drilling used. A more likely explanation is that due to the freshwater nature of the deposit it is not laterally continuous and the assumed distribution is a reasonable interpretation. Figure 2CC-214 shows the extent of the Freshwater Limestone in the model.

Assumption: The Upper and Lower Higher Flow Zones are assumed to be laterally continuous. The Upper Higher Flow Zone is assumed to be present on top of the Key Largo Limestone over the model domain. The Lower Higher Flow Zone is assumed to be present 15 feet below the top of the Fort Thompson Formation over the model domain.

Rationale: Review of borings logs indicates mud loss at the contact between the Miami Limestone and Key Largo Limestone. Caliper logs also indicate an enlarged boring diameter at this depth. This layer is identified across the site

and designated the Upper Higher Flow Zone. At Units 6 & 7, where the majority of borings exist, another higher flow zone is identified at approximately 15 feet below the top of the Fort Thompson Formation. Its lateral continuity across the site is not as obvious as the Upper Higher Flow Zone; however, for the purposes of this model it is assumed to be laterally extensive. Uprate monitoring borings, drilled as part of FPL Units 3 & 4 Uprate Conditions of Certification (Reference 5) in 2010 confirm these interpretations

Assumption: The Upper and Lower Higher Flow Zones are assumed to have a thickness of one foot.

Rationale: A study conducted by Renken et al. (Reference 20) suggested a thickness of three feet for an aerially extensive zone of higher hydraulic conductivity. Because the transmissivity of the units needs to be preserved during calibration, selecting a smaller thickness for these units will permit a higher hydraulic conductivity, which will facilitate preferential flow and hence be conservative.

Assumption: Hydrostratigraphic units in layer 1 are assumed to be distributed as shown in Figure 2CC-215.

Rationale: Layer 1 of the model represents the hydrostratigraphic units located at ground surface on land or on the floor of Biscayne Bay. Muck is known to be present on land (Reference 3); however, this unit does not extend into Biscayne Bay, where exposed rock and sandy material is present in its place. Hydrostratigraphic units in Biscayne Bay were assigned using the Marine Resources Geographic Information System (MRGIS) "Benthic Habitats—South Florida" file (Reference 21). Benthic zones designated as "Continuous Seagrass" were designated as sandy material in layer 1 as loose material is necessary to support seagrass. "Patchy (Discontinuous) Seagrass" and "Hardbottom with seagrass" benthic zones were designated as rock in layer 1.

3.3.5 Boundary Conditions

Assumption: Upward leakage through the Hawthorn Group to the Biscayne Aquifer is assumed to be sufficiently small that it will have negligible effect on flow paths within the Biscayne Aquifer, so the bottom of the Tamiami Formation is assumed to be a no-flow boundary for this model.

Rationale: The Hawthorn Group has a relatively low hydraulic conductivity and is hundreds of feet thick in South Florida.

Assumption: The cooling canals and regional canals can be modeled by the MODFLOW River Package (RIV).

Rationale: The River Package is applicable to surface water bodies that can either contribute water to the groundwater system, or act as groundwater discharge zones, depending on the hydraulic gradient between the surface water body and the groundwater system.

Assumption: Biscayne Bay has a surface water elevation of -1.05 feet NAVD 88 in the model for the model calibration and validation phases.

Rationale: This value is the average of the monthly average surface water elevation between February 2009 and May 2009. This time period is when the pumping tests used for calibration and validation occurred.

Assumption: The head difference between release and intake structures of the cooling canals is assumed to be 4.66 feet.

Rationale: Field monitoring during the period of the pumping tests showed an average head difference of 2.33 feet between the barge canal (Biscayne Bay) and the intake basin. Because the southern end of the cooling canal system is assumed to be equal to the water level in Biscayne Bay, and the head difference assumed to be equal between the intake and release sides, the head difference across the circulating water pumps is therefore twice the difference between the barge canal and intake basin, or 4.66 feet. Additional observations to confirm the field monitoring indicate that the water level on the east or intake side of the cooling canal system is drawn down approximately three feet lower than the water level on the west or release side of the cooling canal system. Field observations in 2009 also provide a similar number for the head difference.

Assumption: The 4.66-foot head drop between release and intake structures of the cooling canals can be equally distributed between the south flowing cooling canals and the north flowing cooling canals. Based on the surface water elevation for Biscayne Bay, the following water levels are assigned to the intake and release sides for Units 1 through 4:

— Release side of Units 1 though 4 is 1.28 feet NAVD 88.

— Lake Rosetta (intake structure) is -3.38 feet NAVD 88.

Rationale: The flowpath length for the release side and return canals is approximately equal.

Assumption: Water level at the southern end of the cooling canals is assumed to be equal to the water level in Biscayne Bay/Card Sound.

Rationale: Site information indicated that at the southern end of the cooling canal system the water level is approximately equal to the water level in Biscayne Bay/Card Sound.

Assumption: A thickness of 0.1 feet of sediment is assumed to have built up in the cooling canals.

Rationale: Negligible silt build up is assumed to occur due to the scouring action of the water and the flushing as a result of tide changes and the high hydraulic conductivity of the Miami Limestone.

Assumption: Water level in:

- L-31E is 0.02 feet NAVD 88.
- Interceptor Ditch is -0.28 feet NAVD 88 at the northern end, and remains constant until the point where the water level in L-31E minus the water level in C32 is less than 0.2 feet. At this point, the water level in the Interceptor Ditch reduces linearly to -1.05 feet NAVD 88 at the southern end.
- Westernmost release side cooling canal is 1.08 feet NAVD 88 at northern end dropping linearly to -1.05 feet NAVD 88 at the southern end.

Rationale: Water level in the interceptor ditch is maintained (by pumping) at a certain level to induce a seaward hydraulic gradient, ensuring that water from the cooling canals does not move inland in the upper portion of the aquifer. The Interceptor Ditch is operated (seasonally) only when required to maintain a seaward hydraulic gradient.

3.3.6 Hydraulic Conductivities

Assumption: The anisotropy ratio is determined by calibration and limited to a value between 1:1 and 15:1 for all layers (Kh:Kv).

Rationale: Anisotropy was estimated from Figure 2.4.12-238, which tends to cluster between a value of 1:1 and 10:1. This figure presents the results of USGS studies by Cunningham et al. of horizontal and vertical air permeability measurements on core samples from the Biscayne Aquifer (References 22 and 23). Subsequent work by the same author (Reference 24) indicates similar anisotropy ratios. An upper limit of 15:1 was designated to allow for large-scale features not represented by the core samples.

Assumption: The hydraulic conductivity of material accumulated in the bottom of the cooling canals is assumed to be 1.0E-05 cm/s.

Rationale: This represents a standard value for the hydraulic conductivity of silty sand (Reference 25).

3.3.7 Precipitation and Evapotranspiration

Assumption: Groundwater recharge zones are separated into two zones.

Rationale: Two groundwater recharge zones are used in the model. These zones represent 1) a recharge value of zero applied to: open water and the existing plant area that is paved and impermeable, and 2) wetlands, which have a constant recharge rate. These recharge zones are based on the land use classifications of Langevin as shown in Figure 2CC-208 (Reference 11).

Assumption: Evapotranspiration zones are the same as the groundwater recharge zones.

Rationale: Impermeable areas and open water will also have zero evapotranspiration. Wetland areas will have a constant evapotranspiration rate.

3.3.8 Groundwater Control: Dewatering

Assumption: Figure 2.5.4-222 shows the location of the excavation cut-off walls for constructing Units 6 & 7 structures. The elevation of the base of the excavation is -35 feet NAVD 88 and the cut-off wall depth has been revised from -65 to -60 feet NAVD 88. The thickness of the cut-off walls is 3 feet.

Rationale: The cut-off wall depth has been raised to -60 feet NAVD 88 to avoid setting the toe within the Lower Higher Flow Zone. Borings logs at Units 6 & 7 indicate that the Lower Higher Flow Zone occurs at approximately -65 feet NAVD at this location.

Assumption: The walls are assumed to have a hydraulic conductivity of 1.0E-08 cm/s.

Rationale: The design value for the hydraulic conductivity of the diaphragm (cut-off) walls is 8.3E-10 cm/s (Reference 26). A value of 1.0E-08 cm/s is a conservative estimate that will provide an upper bound on the dewatering rate.

Assumption: Units 6 & 7 are excavated and dewatered sequentially.

Rationale: The construction schedule shows the nuclear island excavations to be excavated sequentially.

Assumption: The rock between the base of the cut-off walls and base of the excavation can be grouted to a hydraulic conductivity of 1.0E-04 cm/s.

Rationale: A value of 1.0E-4 cm/s is an industry standard for this type of formation (Reference 27 and 28).

3.3.9 Radial Collector Wells

Assumption: The three western-most radial collector wells and laterals are modeled as operational for plant operations. Figure 2.4.12-218 shows the general location where all four of the radial collector wells will be located.

Rationale: This simulation will provide a conservative estimate of the quantity of water originating from inland due to the proximity of the radial collector wells to land.

Assumption: Operation of the radial collector wells is simulated using the MODFLOW WEL package.

Rationale: Use of the WEL package is a documented method of simulating horizontal wells (Reference 29). Other methods within MODFLOW of simulating the radial collector wells could include the drain package (DRN) and the multi-node well package (MNW).

Assumption: Operation of the radial collector wells is simulated as steady-state.

Rationale: The radial collector wells are intended to be operated only when the primary source of makeup water is not available. Simulating the radial collector wells on a steady-state basis provides the maximum drawdown from the wells and is therefore a conservative approach.

Assumption: The laterals are assumed to be less than 700 feet in length, with approximately 300 feet of screened casing or open hole at the end of the lateral.

Rationale: A conceptual engineering study (Reference 30) provided an upper estimate of 900 feet for the length of the laterals. This value was adjusted during modeling to remain outside the boundary of the Biscayne National Park. A shorter lateral provides a more conservative estimate. It should also be noted that the layout will go through a formal design process at a later stage.

Assumption: Flow to the radial collector wells is distributed non-linearly along the laterals.

Rationale: The head difference between the water level in the lateral and outside the lateral is greatest closest to the caisson and smallest at the end of the lateral.

4.0 MODEL CALIBRATION

A multi-faceted approach to calibration was taken that included the following:

- Calibration to pumping tests on the Turkey Point plant property.
- Verification using a pumping test on the Turkey Point plant property.
- Performing a qualitative comparison of calculated groundwater flows to and from the cooling canal system with an analytical water balance.
- Qualitatively comparing model wide groundwater flow directions with published potentiometric surface maps.

4.1 Calibration Measures and Statistics

Several parameters providing different measures of the agreement between simulated and observed drawdown levels were used for the calibration of the model. These parameters are defined in terms of the calibration residuals of the drawdown defined as the difference between calculated and observed drawdown. The calibration residual, R_i at a point i is defined as:

$$R_i = {}^{model}X_i - {}^{obs}X_i \quad (1)$$

Where:

$^{model}X_i$ is the calculated drawdown at point i; and

$^{obs}X_i$ is the observed drawdown at point i.

The residual mean, $\bar{R}$ is a measure of the average residual value and is defined by the equation:

$$\bar{R}=\frac{1}{n}\sum_{i=1}^{n}R_i \quad (2)$$

Where n is the number of points where calculated and observed values are compared.

The absolute residual mean (ARM), $\bar{R}$ is a measure of the average absolute residual value and is defined as:

$$\left|\bar{R}\right|=\frac{1}{n}\sum_{i=1}^{n}\left|R_i\right| \quad (3)$$

The Root Mean Squared (RMS) residual is defined by:

$$RMS=\left[\frac{1}{n}\sum_{i=1}^{n}R_i^2\right]^{1/2} \quad (4)$$

The normalized root mean squared (NRMS) is the RMS divided by the maximum difference in the observed drawdown values. It is given by the following equation:

$$NRMS=\frac{RMS}{^{obs}X_{max}-^{obs}X_{min}} \quad (5)$$

A measure of the numerical convergence of each run is the discrepancy between inflows and outflows from the model domain. To satisfy the overall mass balance, this discrepancy should be zero. In practice, however, a mass balance of zero may not be possible. The aim in obtaining a converged numerical solution is to

achieve a mass balance discrepancy as small as possible. The numerical mass balance discrepancy, M_d, is calculated using the following equation:

$$M_d = \frac{V_{in} - V_{out}}{\frac{1}{2}(V_{in} + V_{out})} \quad (6)$$

where

V_{in} is total flow into the model domain; and

V_{out} is total flow out of the model domain.

The final measure of the adequacy of the calibrated model is the discrepancy between the cooling canal system inflows and outflows determined by the groundwater model and the steady-state water balance determined by the site surface water model. Flow values for the groundwater model are determined by assigning flow zones across the discharge and recharge sides of the cooling canal system. Fluxes into and out of these zones are then calculated and compared with the water balance. In a successful calibration, the mass balance discrepancy between the two models will be as small as possible.

4.2 Calibration Criteria

The following criteria for calibration measures and statistics were used for model calibration:

- Root mean squared residual (RMS) < 1 foot.
- Normalized root mean squared residual (NRMS) < 10 percent.
- Absolute residual mean (ARM) < 1 foot.
- Numerical mass balance discrepancy (M_d) < 0.1 percent.
- Physical mass balance in the cooling canal system within an order of magnitude of the water balance from the surface water model.

4.3 Calibration Parameters

The primary calibration parameters were the hydraulic conductivity, and also the conductance for head dependent boundary conditions (cooling canals, regional canals, Biscayne Bay and model sides). These parameters were varied to

achieve satisfactory agreement between simulated and observed pumping test drawdowns, regional flow directions, and flow magnitudes.

4.4 Calibration Results

The original intent was to utilize the steady-state drawdown values from pumping tests PW-7L and PW-1 as the calibration data set and then validate the model using an additional pumping test from the suite conducted in the vicinity of the proposed Units 6 & 7 power blocks. Following calibration to the two tests, the validation case was run (pumping test PW-7U) and the results demonstrated that the model could not replicate the drawdown values observed at the end of this test. As a result, the validation data set subsequently became part of the calibration data set and an additional pumping test (PW-6U) was used for model validation. As the model was able to adequately replicate the drawdown values from the PW-6U pumping test, model validation was achieved.

4.4.1 Simulation of Pumping Tests

Parameter estimation was performed using manual optimization, whereby model parameters were changed on a trial-and-error basis until a satisfactory match was observed between observed and modeled drawdowns. The procedure used to calibrate the model to the drawdown data was to run the model to steady state with no wells operating for an assumed set of model parameters. Following this run, the steady-state head at each of the monitoring well locations was noted and used as the initial head for the simulation with the pumps operating. Following the execution of the model with the pumping well operating, the model drawdown at each well was calculated by subtracting the final head from the starting head values. This model-determined drawdown was then compared to the observed drawdown to calculate calibration statistics. Model parameters were then adjusted to match the observed drawdown values, and the process described above was then repeated. In addition to adjusting the hydraulic conductivity of the hydrogeologic units, the conductance of the general-head boundaries was also adjusted to represent changes in the properties of the layers, thereby tying the conductance of all general-head boundary cells to the hydraulic conductivity of the layer that the boundary cell is contained within.

Initially, the model was calibrated to two pumping tests: PW-7L and PW-1. During the calibration process, the hydraulic conductivity of all layers was allowed to vary within a predefined range, which was determined from the literature and site hydrogeologic parameters given in Table 2CC-204. Following adequate calibration to these two tests, pumping test PW-7U was simulated with the

parameters determined from the prior utilization. This simulation provided a poor match to test PW-7U, and as a result a series of forward runs were conducted where the hydraulic conductivity of the Key Largo Limestone was varied to improve the match. Following an adequate match to PW-7U, it was observed that PW-1 was unacceptably degraded. It was then concluded that a satisfactory match to both the PW-7U and PW-1 drawdown data could not be achieved by treating the hydraulic conductivity of the Key Largo Limestone as a homogeneous property.

The final phase in calibrating involved holding constant parameters below the Freshwater Limestone from the first optimization and further optimizing to the two tests conducted in the Key Largo Limestone. In order to achieve satisfactory calibration, it was necessary to introduce two hydraulic conductivity zones within the Key Largo Limestone, which were delineated based on two pieces of prior information. The first piece of prior information was an observation from the 2010 drilling program that the upper portion of the Fort Thompson Formation (synonymous here with the Key Largo Limestone) exhibited heterogeneity across the model domain. The second was from the type-curve analysis of pumping tests conducted at the nuclear islands (the Units 6 & 7 containment building, shield building, and auxiliary building) and at the Turkey Point peninsula; the tests at the nuclear island consistently demonstrated a lower hydraulic conductivity than the one conducted at the Turkey Point peninsula. The zones were established by drawing a line between PW-1 on the Turkey Point peninsula and the nuclear island, bisecting the line, and then extending another line perpendicular from this point until it intersected the boundaries of the model domain. The two zones are displayed in Figure 2CC-216. The strategy behind this approach was to fix the dominant parameters controlling test PW-7L, hence trying to maintain an optimal calibration and then only allowing parameters above the Freshwater Limestone to vary, which provide primary control on the tests in the Key Largo Limestone. It was important to check this final phase of calibration by simulating all tests separately to ensure that well interference from simulating multiple tests at the same time did not affect the results. In addition, following each round of optimization, the starting heads were updated, and the conductance value for each general head boundary cell was updated to reflect the new hydraulic conductivity value in the direction of flow. These steps were necessary because the optimization runs only updated the hydraulic conductivity of the model layers. The final hydraulic conductivity values determined from the model calibration are presented in Table 2CC-206 and fall within the limits defined by the literature and site review of hydrogeologic parameters.

4.4.1.1 Pumping Test PW-7L

Calibration to pumping test PW-7L results was performed by simulating the steady-state response to pumping from the Fort Thompson Formation within the footprint of the proposed reactor building for Unit 7. This test was one of four conducted in the first quarter of 2009 to assess the feasibility of construction dewatering. Two tests were conducted within the footprint of each of the reactor buildings for Units 6 & 7, one in the Key Largo Limestone (U or upper test zone), and one in the Fort Thompson Formation (L or lower test zone). The layout of the test (test well and monitoring wells) for this phase of calibration is shown in Figure 2CC-217. The notation used for the observation well naming is as follows:

CX-#$

where:

C = Well cluster
X = Reactor building (6 or 7)
# = Number indicating well position
1 = approximately 10 feet east of upper zone test well
2 = approximately 10 feet north of upper zone test well
3 = approximately 25 feet north of upper zone test well
4 = approximately 40 feet north of upper zone test well
5 = approximately 10 feet east of lower zone test well
$ = Alphabetic character designating the well monitoring zone
A = Miami Limestone
B = Freshwater Limestone
C = Tamiami Formation
D = Key Largo Limestone
E = Fort Thompson Formation

The constant rate test of well PW-7L was conducted in March 2009, with an average discharge rate of 3403 gpm for nine hours.

The rationale for selecting test well PW-7L is:

- The hydrogeological units overlying the Fort Thompson formation and within the footprint of the excavation will be contained by a cut-off wall with the implication that the deeper zone tests are more relevant.

- The PW-7L pumping test data were considered more complete than the PW-6L data.

The refined grid in the area of Unit 7 is presented in Figure 2CC-218 along with a close-up showing the test and observation wells in Figure 2CC-219. The model interpolates the numerical results calculated at the grid nodes to the input locations of the observation wells. Because water levels in the Fort Thompson

Formation stabilized within ten minutes of turning on the pump, the test was simulated by matching the drawdown values at the end of the test only. The rationale for this is that the test had reached steady-state and hence a transient simulation was not necessary.

Results of the pumping test simulation are tabulated in Table 2CC-207. This shows simulated and measured drawdown values in each of the monitoring wells that were instrumented. The drawdown response was well matched.

A plot of observed versus simulated drawdown is presented in Figure 2CC-220 for all monitored layers. The normalized root mean square for all layers is 7.9 percent, which is considered acceptable for this model and is within the calibration criteria established in Section 4.2.

4.4.1.2 Pumping Test PW-1

An exploratory drilling and aquifer testing program was performed on the Turkey Point peninsula to assess the hydraulic properties of the Biscayne Aquifer (Reference 4). The program provided data to determine whether a radial collector well system could be implemented at this location to meet the water-supply requirements for Units 6 & 7.

The pumping well, PW-1 was open across the Key Largo Limestone. Five monitoring wells were installed at radial distances of between 75 feet and 2070 feet of the pumping well. Monitoring wells at all radial distances are screened in the Key Largo Limestone to monitor water levels in the test zone. In the case of the closest monitoring well, the zones immediately above (Miami Limestone) and below (Fort Thompson Formation) the test zone are also monitored. The layout of the test (test well and monitoring wells) is shown in Figure 2CC-221. The constant rate test of well PW-1 was conducted in April and May of 2009, with an average discharge rate of 7100 gpm for seven days.

The finite-difference grid in the area of the Turkey Point peninsula and the wells (pumping and observation) is presented in Figure 2CC-223. Results of the pumping test simulation are tabulated in Table 2CC-208. This shows simulated and measured drawdown values in each of the monitoring wells that were instrumented. The drawdown response was well matched.

A plot of observed versus simulated drawdown is presented in Figure 2CC-223 for all monitored layers. The normalized root mean square for all layers is 5.3 percent, which is considered acceptable for this model and is within the calibration criteria established in Section 4.2.

4.4.1.3 Pumping Test PW-7U

Calibration to pumping test PW-7U results was performed by simulating the steady-state response to pumping from the Key Largo Limestone within the footprint of the proposed reactor building for Unit 7. The layout of the test (test well and monitoring wells) for this phase of calibration is shown in Figure 2CC-217 and follows the same notation as test PW-7L described in Subsection 4.4.1.1.

The constant rate test of well PW-7U was conducted in March 2009, with an average discharge rate of 4181 gpm for just under nine hours. Observation wells were constructed in the Miami Limestone, Freshwater Limestone, Tamiami Formation, Key Largo Limestone, and Fort Thompson Formation to monitor the water level response to pumping.

PW-7U was selected as part of the calibration data following its unsuccessful use to validate the model after calibration to PW-7L and PW-1 alone. The grid refinement presented for PW-7L also covers the same area for PW-7U and is presented in Figure 2CC-218 along with a close-up showing the test and observation wells in Figure 2CC-224.

Because water levels in the Key Largo Limestone stabilized within ten minutes of initiating pumping, the test was simulated by matching the drawdown values at the end of the test only. The rationale for this is that the test had reached steady-state and hence a transient simulation was not necessary.

Results of the pumping test simulation are tabulated in Table 2CC-209, which shows simulated and measured drawdown values in each of the monitoring wells that were instrumented. The drawdown response was well matched with the exception of monitoring well C7-1D, which shows greater drawdown compared to C7-2D, both of which are equidistant from the test well. The difference in drawdown between the observation wells could suggest localized heterogeneity and/or well construction issues or instrument malfunction. Review of the well construction information and both the raw data and processed data files did not indicate any obvious well construction or data collection issues that would cause the difference in drawdown. The difference in drawdown between these two wells is likely attributable to small-scale heterogeneities that are not captured in the model. A plot of observed versus simulated drawdown is presented in Figure 2CC-225 for all monitored layers.

The normalized root mean square for all layers is 11.3 percent. Although the NRMS is marginally outside the criterion established in Section 4.2, the RMS,

ARM, and Md are all within limits. This result is considered adequate because the model is also calibrated to two other pumping tests, compared to the regional flow regime, and additionally calibrated to a water balance for the cooling canal system.

4.4.2 Comparison to Regional Flow Regime

For matching of regional flow direction and patterns, simulated groundwater contours and levels were compared to potentiometric surface maps for the Biscayne Aquifer from May and November 1993 (Figure 2.4.12-219 and Figure 2.4.12-220).

The intention of this is to qualitatively capture the overall flow paths and direction. Figure 2CC-226 through Figure 2CC-233 show the simulated heads for each of the hydrostratigraphic units, indicating a predominant flow direction from west to east, which is in agreement with Figure 2.4.12-219 and Figure 2.4.12-220. Flows are more complex in the vicinity of the cooling canals due to the exchange of water between the canals and groundwater. These nuances are not captured in the larger flow picture shown in Figure 2.4.12-219 and Figure 2.4.12-220.

4.4.3 Comparison with Cooling Canal System

The interaction of groundwater with the surface water comprising the cooling canal system was assessed by comparing model results against estimates obtained from an independent water balance model on a steady-state basis. The water balance model for the cooling canal system is displayed schematically in Figure 2CC-213. The model accounts for flow from the release side of the cooling canals downward to the groundwater beneath the canal system and flow from underneath Biscayne Bay inward and upward to the return canals. This figure has been updated to include the simulated flow rates from the groundwater model and is shown in Figure 2CC-234. The area outlined in blue shows that part of the surface water model that is replicated in the current groundwater model. The top figure for each parameter (net blowdown and net makeup) represents that from the surface water model while the lower figure is the calculated value from the groundwater model. Values for comparison were determined from the groundwater model by assigning flow zones across the release and return sides of the cooling canal system. Fluxes into and out of these zones were then calculated for comparison with the water balance. A comparison of the values indicates that the groundwater model shows up to 31 percent higher cooling canal system makeup and blowdown values than the surface water. This is considered

an acceptable match given that the cooling canal system water balance is a simple analytical model.

4.5 Model Validation

The PW-6U test, conducted in the Key Largo Limestone at the location of the proposed site of the Unit 6 nuclear island, was used for model validation. The test and monitoring well layout is depicted in Figure 2CC-235 and uses the same numbering system as described in Subsection 4.4.1.1.

The constant rate test of well PW-6U used an average discharge rate of 5103 gpm for eight hours. Observation wells were constructed in the Miami Limestone, Freshwater Limestone, Tamiami Formation, Key Largo Limestone, and Fort Thompson Formation to monitor the water level response to pumping.

Results of the pumping test simulation are tabulated in Table 2CC-210. This shows simulated and measured drawdown values in each of the monitoring wells that were instrumented. The drawdown response was well matched.

A plot of observed versus simulated drawdown is presented in Figure 2CC-236 for all monitored layers. Although the NRMS of 11.4 percent is marginally outside the criterion established in Section 4.2, the RMS, ARM, and M_d are all within limits. These results are considered acceptable for model validation, considering that PW-6U data are completely independent.

4.6 Conclusions

The model is calibrated based on the following observations:

- Calibration to pumping tests at PW-7L, PW-1, and PW-7U indicate a good match between observed and modeled drawdown values.
- Matching of regional flow patterns.
- Comparison with an independent cooling canal system water model shows similar flow exchanges between the cooling canals and the groundwater beneath them.
- Validation of the model to pumping test PW-6U indicates a good match between observed and modeled drawdown values.
- Hydraulic conductivity values obtained by model calibration are within the range of values reported in the literature.

5.0 PHASE 1 CONSTRUCTION & POST-CONSTRUCTION SIMULATIONS

Predictive simulations are used for two purposes: evaluating groundwater control options during construction of Units 6 & 7, and operation of the radial collector well system and its influence of the existing groundwater regime.

A concrete cut-off wall for construction groundwater dewatering control will be installed around the excavations for Units 6 & 7. It is estimated that the cut-off wall will extend to an elevation of -60 feet NAVD 88 with the base of the excavation at an elevation of -35 feet NAVD 88. The top of the cut-off wall will extend up to an elevation of 2 feet NAVD 88. In addition, the rock between the base of the excavation and the base of the cut-off walls will be grouted. The purpose of modeling the construction dewatering is to estimate discharge rates required to maintain the water table below the base of the excavation.

Radial collector wells will be installed on Turkey Point peninsula in order to provide backup cooling tower makeup water for the proposed AP1000 units at Units 6 & 7 when the primary supply of makeup water is not available. These simulations are performed to determine the origins of water that supply the RCW system, using MODPATH (Reference 31) and ZoneBudget (Reference 32).

5.1 Groundwater Control During Construction

Groundwater flow simulations for dewatering of the nuclear island excavations were performed with the calibrated base model. For these simulations, the muck is left in place in the model. It is likely that during earthworks, the muck will be stripped and replaced with backfill to provide a stable working platform. This simplification is expected to have no impact on the dewatering rates.

Several refinements were made to the Phase 1, base model to represent the excavations:

- The interior of the excavation (ground surface to -35 feet NAVD 88) was defined as inactive to flow.
- The Horizontal Flow Boundary (HFB) package (Reference 33) was used to simulate the cut-off walls from the base of the excavation down to an elevation of -60 feet NAVD 88.
- Constant head cells were added to the layer below the excavation to represent the sump pumps in the base of the excavation used to maintain dry working conditions. The constant head level was set to -35 feet NAVD 88 (the floor of

the excavation), and pumping rates were calculated from the simulated inflows to the constant head cells. The grid elevations of the cells immediately below the base of the excavation were adjusted to provide a uniform, thin layer within which the constant head cells could be placed.

- A new hydraulic conductivity zone was added from the base of the excavation to the base of the cut-off walls to simulate grouting.

- The water level in Biscayne Bay was set to the long-term average of -0.81 feet NAVD 88.

- Water levels in the cooling canal system, L-31E Canal, Card Sound Canal, and the Model Land Canal (C-107) were adjusted based on the long-term average Biscayne Bay water level.

Figure 2.5.4-222 shows an excavation profile at the power block while Figure 2CC-237 illustrates the implementation of the excavation in the model. Figure 2CC-237 shows the model grid, excavation walls, and sump pumps. A cross section through the model illustrating the depth of the excavation and cut-off walls is presented in Figure 2CC-238.

The two excavations were dewatered sequentially to represent the construction schedule. For each unit, the model was run to steady-state, starting with previously derived steady-state heads under no pumping conditions. ZoneBudget was used along with the simulation to determine the quantity of water being extracted from the interior dewatering wells.

To aid in construction-related groundwater control, grout plugging will be performed between the bottom of the excavation and the bottom of the cut-off wall. The rationale behind this methodology is to reduce the hydraulic conductivity by injecting grout into a pattern of holes within the excavation between the bottom of the excavation and the bottom of the cut-off wall. By reducing the hydraulic conductivity of the rock, lower discharge rates are achieved, such that sump pumps in the floor of the excavation rather than active dewatering wells can be used to keep the excavation dry during construction. Additional dewatering methods may be implemented during excavation to assist in the removal of groundwater storage within the area to be excavated.

Figure 2CC-239 shows the proposed methodology whereby grout is injected in a series of "Primary" borings until refusal is achieved. Subsequent borings are then drilled in between the borings of the prior step. Three series of borings are

possible after the "Primary" set: a "Secondary," "Tertiary," and "Quarternary" set. Each set is drilled and grout injected until refusal occurs. "Quarternary" borings may not be required at all locations; only where excessive seepage is observed as the excavation progresses.

In the base case, a hydraulic conductivity of 1.0E-04 cm/s is used for the grouted formations. Discharge rates obtained from this model yield a value of 96 gpm for each unit. A series of runs evaluating different values for the hydraulic conductivity of the grouted formations were performed to determine a feasible range of discharge rates that may be achievable with grouting. In addition to the run described above, values of 1.0E-03 cm/s, 1.0E-05 cm/s, and 1.0E-06 cm/s were simulated. The results are displayed graphically in Figure 2CC-240.

5.2 Post-Construction Radial Collector Well Simulation

Groundwater flow simulations for the radial collector wells were performed with the calibrated base model. Several refinements were made to represent the conditions at the site post-construction:

- Cut-off walls installed during construction (and represented in dewatering simulations) are left in place.
- Concrete fill added within the cut-off walls between -35 feet NAVD 88 (base of excavation) and -16 feet NAVD 88 with a hydraulic conductivity of 1.0E-08 cm/s.
- Concrete mud mat for reactor building added within cut-off walls between -16 feet NAVD 88 and -14 feet NAVD 88 with a hydraulic conductivity of 1.0E-08 cm/s.
- Reactor building included as inactive to flow.
- Redefined new zones of recharge at the Units 6 & 7 plant area as represented in Figure 2CC-241. The values of recharge for grass and gravel of 2 in/yr and 10 in/yr, respectively, were selected to represent the land surface and also the relatively lower recharge expected compared to the wetlands, which dominates a large majority of the model area beyond the plant area.
- Backfill added between reactor building and cut-off walls with a hydraulic conductivity of 0.01 cm/s.

- Muck removed from area in immediate vicinity of reactor buildings and replaced with backfill (hydraulic conductivity of 0.01 cm/s).

- The water level in Biscayne Bay set to the long-term average of -0.81 feet NAVD 88.

- Recharge and evaportranspiration set to long-term average values.

- Water levels in the cooling canal system shifted to account for the change in Biscayne Bay water level.

- Mechanically Stabilized Earth (MSE) retaining walls, as shown in Figure 2.5.4-201 installed around the perimeter of the Turkey Point Units 6 & 7 plant area down to 0 feet NAVD 88. The MSE retaining wall is also shown as implemented in the numerical model in Figure 2CC-261.

To simulate the radial collector wells and laterals, other changes were made to the model:

- Four pumping wells placed on approximately the last 300 feet of each lateral to represent the screened intervals. Flows were distributed along the laterals based on head loss calculations. The flows are as follows: 872 gpm at the end, 881 gpm at 100 feet from the end, 909 gpm at 200 feet from the end, and 956 gpm at 300 feet from the end of the lateral. Total flows are 3618 gpm per lateral or 28,944 gpm per radial collector well (8 laterals per radial collector well x 3618 gpm per lateral). In the model, the pumping wells are located at approximately 100-foot intervals.

- Three of the four radial collector wells are operational, resulting in a total system pumping rate of 86,832 gpm (3 radial collector wells x 28,944 gpm per radial collector well). To maximize the allocation of water from inland areas to the radial collector wells, the three wells closest to the shore were modeled as operational.

- Zones defined around the model domain to estimate the volume of water coming from land or Biscayne Bay.

- The radial collector wells pumped from the Upper Higher Flow Zone. An alternate scenario was also modeled in which the radial collector wells are pumped from the Key Largo Limestone.

- The top of the cut-off walls truncated at the boundary of the Miami Limestone and muck (approximate elevation -4 feet NAVD 88). The actual elevation will be 2 feet NAVD 88, however this simplification is expected to have no effect on the RCW calculations of approach velocity and origin of flow to the RCW. (Post-construction groundwater levels at Units 6 & 7 are discussed in Section 6.0.)

Figure 2CC-242 shows the modeled location of the radial collector wells on the Turkey Point peninsula with the finite-difference grid overlaid and also the location of the pumping wells (light blue) representing the screened portion of the laterals. Figure 2CC-243 shows the potentiometric surface after model execution in the Upper Higher Flow Zone. Figure 2CC-244 shows the head contours in layer 1. Figure 2CC-245 is a section across the most centrally located radial collector well showing groundwater contours for all modeled layers. Figure 2CC-246 and Figure 2CC-247 show the drawdown in the vicinity of the Turkey Point peninsula in layer 1 and the Upper Higher Flow Zone (pumped zone) respectively. In the alternate case where the radial collector wells are instead placed in the Key Largo Limestone, the water table, groundwater contours, and drawdown plots are virtually identical to those produced when the radial collector wells are pumped from the Upper Higher Flow Zone.

5.2.1 Origins of Water Supplying Radial Collector Wells

To determine the origins of water supplying the radial collector wells a multi-step process is followed. The first step is to place a particle in each boundary condition cell representing a source of water (River, General-Head, and Recharge). Particles are not placed in other cells because the model is steady-state and therefore all water discharging from the RCWs has to originate from a boundary condition. MODPATH is then run in forward tracking mode and the endpoint file reviewed to identify only those particles that end up in the pumping cells representing the RCWs. Once those particles have been identified their starting locations are set up as a separate zone within ZoneBudget for tracking purposes. Following execution of ZoneBudget, the separate fluxes from each of the boundaries (River, General-Head, and Recharge minus Evapotranspiration) are summed and compared to the discharge from the RCW system as a check. For both the base case with the laterals in the Upper Higher Flow Zone and the alternate case with the laterals in the Key Largo Limestone, 99.9 percent of the expected flow to the RCW system is accounted for by the ZoneBudget boundary fluxes. The results presenting the origins of the water to the RCW are presented in Table 2CC-211 and broken down into two main components. The first of these is flow from Biscayne Bay, which includes vertical flow down through the Bay floor

and lateral flow from the sides of the model in the Bay. The second component is flow from inland, which is further broken down into water originating from the CCS, and that originating from recharge by precipitation.

Figure 2CC-248 and Figure 2CC-249 present the output for layers 1 and 2 for the base case where the laterals are placed in the Upper Higher Flow Zone. The blue colored clusters on these figures show the starting location of particles that ultimately discharge to the RCW. In the alternate case where the radial collector wells are pumped from the Key Largo Limestone, the flow distribution is the same as the base case, as is shown in Table 2CC-211.

The cumulative induced flow quantities of the radial collector wells were examined by comparing the difference in flow into the model across the western, northwestern, and southeastern boundaries when the radial collector wells are operating at steady-state, versus the steady-state case when no wells are running. Eastward flow is defined as the flow across the western boundary and the flow across the northern boundary from the western edge of the model to L-31E. Flow quantities were determined using ZoneBudget. In both cases, 26 gpm of additional flow into the model domain is induced across the model boundaries as compared to the case with no pumps operating. When compared to the total RCW system pumping rate of 86,832 gpm (Section 5.2), an induced flow across the model domain of 26 gpm is relatively small.

5.2.2 Approach Velocity at Bay/Aquifer Interface

In order to provide a range of expected approach velocities through the floor of Biscayne Bay, three separate velocities were calculated while simulating the operation of the radial collector wells. Using the Biscayne Bay capture zone identified in Figure 2CC-248 and the additional zones identified in Figure 2CC-250, three values for the approach velocity were calculated representing the following:

1. Average approach velocity for entire control volume (blue in NE corner of Figure 2CC-248).

2. Average approach velocity for immediate area defined by the radial collector wells (green in Figure 2CC-250).

3. Average approach velocity for the laterals (colored zones along laterals in Figure 2CC-250).

The volumetric flow rate for each of these zones was calculated using ZoneBudget and then divided by the area of the zone to calculate an approach

velocity. The following values were obtained for the three zones for the base case with the radial collector wells pumping from the Upper Higher Flow Zone:

- Entire RCW Catchment: 3.3E-05 cm/s (1.1E-06 ft/s)
- Immediate RCW Area: 5.2E-04 cm/s (1.7E-05 ft/s)
- Average of all RCW Laterals: 6.2E-04 cm/s (2.0E-05 ft/s)

To further illustrate these results, a plot of the Darcy velocities in the top layer of the model showing the spatial variation in approach velocity (ft/day) through the floor of Biscayne Bay is given in Figure 2CC-251. Irregularities in the contours of the Darcy velocity are related to the hydraulic conductivity distribution for layer 1 (Figure 2CC-215). When the radial collector wells are instead located in the Key Largo Limestone, the approach velocities are only slightly different compared to the base case (Table 2CC-212).

5.2.3 Sensitivity Analysis

A suite of sensitivity analyses was performed on the radial collector well simulations to address parameter uncertainty and water level variation. The radial collector wells pump from the Upper Higher Flow Zone in all sensitivity runs. The Upper Higher Flow Zone is used because it is the shallowest zone of higher hydraulic conductivity.

Two sensitivity runs were performed to address the variation in Biscayne Bay water levels. These runs considered that Biscayne Bay water levels vary seasonally. One case was run with Biscayne Bay set at the seasonal high water level, and another case was run with Biscayne Bay set at the seasonal low level. The seasonal extreme values were determined by taking the highest and lowest monthly mean sea level measurements at NOAA's tidal water level and meteorological data collection station (#8723214) on Virginia Key in Biscayne Bay. Based on data from February 1994 to March 2010, the seasonal low level of Biscayne Bay is -1.40 feet NAVD 88 while the seasonal high level of Biscayne Bay is 0.09 feet NAVD 88 (Reference 10). Using the equation given in Subsection 3.3.3, water levels in the cooling canals, L-31E Canal, Card Sound Canal, and Model Land Canal (C-107) were adjusted based on the water level in Biscayne Bay. The areal extent of the GHB cells representing Biscayne Bay was not adjusted for this sensitivity analysis. Results of the seasonal water level runs indicate that either increasing or decreasing the Biscayne Bay water level has no observable effect on the approach velocities for the RCW. Increasing the Biscayne Bay water level slightly increases the percent contribution to the radial collector wells from Biscayne Bay, while lowering the Biscayne Bay water level

slightly decreases the percent contribution to the radial collector wells. Changing the Biscayne Bay level induces an additional flow into the model domain of 23 gpm for the high water level case and 27 gpm for the low water level case when compared to the case with no pumps operating.

Two additional sensitivity runs were performed to assess the impact of the anisotropy ratio in Biscayne Bay on the radial collector well simulations. In the base model, an anisotropy ratio of 15:1 (Kh:Kv) is used. In the sensitivity runs, the vertical hydraulic conductivity (Kv) is either doubled or halved, producing anisotropy ratios of 7.5:1 and 30:1, respectively. This change is only made offshore to the first three layers of the model, which represent the Miami Limestone (and a small area of sediment in layer 1). Results of the anisotropy sensitivity runs indicate that for the RCW laterals and the immediate RCW area, the approach velocities increase as the Kv increases, and decrease as the Kv decreases. Doubling the Kv slightly increases the percent contribution to the radial collector wells from Biscayne Bay, while halving the Kv slightly decreases the percent contribution to the radial collector wells. Changing the anisotropy ratio in Biscayne Bay induces an additional flow into the model domain of 7 gpm for the double Kv case and 82 gpm for the half Kv case, when compared to the case with no pumps operating.

A final set of sensitivity runs were performed to evaluate the impact of the hydraulic conductivity of the Key Largo Limestone on the radial collector well simulations. The reason for this additional suite is because the Key Largo Limestone is divided into two zones of hydraulic conductivity based on information identified in Subsection 4.4.1. These zones were defined to improve the calibration and these sensitivity runs are intended to determine if the difference in hydraulic conductivity between the zones results in any change in the induced flow across the western boundary. The results indicate that an additional 11 gpm of flow is induced across the model boundaries when the horizontal hydraulic conductivity is 5.9 cm/s and 34 gpm when the horizontal hydraulic conductivity is 10 cm/s when compared to the case with no pumps operating.

A compilation of the results for the base case and sensitivity cases can be found in Table 2CC-211 for the origin of water to the radial collector wells and Table 2CC-212 for the approach velocities of each zone. As was done with the base case, a comparison of the RCW discharge was made with the ZoneBudget boundary fluxes as a check. For these sensitivity cases, between 99.8 percent and 100.4 percent of the expected flow to the RCW system is accounted for by the ZoneBudget boundary fluxes. For both the base case with the laterals in the Upper Higher Flow Zone and the alternate case with the laterals in the Key Largo

Limestone, 99.9 percent of the expected flow to the RCW system is accounted for by the ZoneBudget boundary fluxes. In addition to the tabulated summary a graphical representation of the sensitivity of these parameters to the 0.1 foot drawdown contour is presented in Figures 2CC-252, 2CC-253, and 2CC-254 for the aforementioned cases.

6.0 PHASE 2 REVISIONS TO THE GROUNDWATER MODEL

The post-construction simulations for the Phase 1 groundwater model were developed to evaluate the impact on the groundwater system from RCW pumping. The Phase 2 simulations were developed to estimate maximum water table elevations at Units 6 & 7 and do not include pumping of the RCW system. Phase 2 revisions to the model are documented in Sections 6.1 to 6.3. Assumptions corresponding with these changes are described in Section 7.0.

The Phase 2 simulations include four post-construction simulations (Cases 1 through 4). Each case is described below.

Case 1: Base-case model with the hydraulic conductivities of the structural backfill and the non-structural backfill as shown in Figure 2CC-256 and further explained in Section 7.1. Recharge rates for the uppermost active layer at Units 6 & 7 are shown in Figure 2CC-257. The same recharge assumption is applied for Cases 3 and 4.

Case 2: Sensitivity case for high recharge rates for grass and gravel (46.75 in/yr for each surface type, respectively).

Case 3: Simulation of a catastrophic failure of the MWR north wall. The north wall is selected as a limiting case with respect to the potential impact on Units 6 & 7.

Case 4: Simulation assuming sea-level rise at the Units 6 & 7 site. The assumptions for this simulation are discussed in Section 7.3.

6.1 New Model Layer to Incorporate a Revised Top Elevation of the Diaphragm Walls

The post-construction simulations developed for Phase 1 were revised to include new features in the top model layer, which was split into two layers. A new model layer was added to represent the top of the diaphragm walls for Units 6 & 7 (Figure 2CC-255). The locations of the diaphragm walls in plan view are shown in Figure 2.5.4-201. The top of the diaphragm walls was placed at elevation 2 feet

NAVD 88. With the addition of a new layer, the model is a fifteen-layer model. The model developed in Phase 1 was a fourteen-layer model. General head and river boundary conditions affected by splitting the top layer were adjusted to approximate their volumetric flux rates from the fourteen-layer, post-construction model. Based on a comparison of the volumetric flux rates of general head and river leakage boundary conditions, the fourteen-layer model and the fifteen-layer model were verified to be equivalent; the flux rates for the two models matched within 1 percent.

6.2 Modifications to the Structural Fill in the Top Model Layer

Structural fill was added to the top model layer for the nuclear island areas (Figure 2CC-258). In Phase 1, the structural backfill and non-structural backfill were included as one zone in the top model layer. For Phase 2, structural fill is located within the diaphragm walls, as shown in Figure 2CC-255. Structural fill will be used within the nuclear island areas and beneath nonsafety-related power block structures. The hydraulic conductivity for the structural fill is 1.0E-02 cm/s. Assumptions regarding this zone are discussed further in Subsection 7.1.1.

6.3 Modifications to the Makeup Water Reservoir Simulated in the Model

Located approximately a quarter-mile south of Units 6 & 7, the MWR supplies makeup water to replace water lost as evaporation, drift and blowdown due to operation of the wet cooling towers that are part of the circulating water system used for normal plant cooling. The MWR is located approximately 700 feet south of the Units 6 & 7 nuclear island areas. The west, south, and east sides of the MWR lie approximately 50 feet to 100 feet from the bordering cooling water canals as shown in Figure 2.4.2-202. The MWR is roughly a right-angled trapezoid in plan view with a footprint of approximately 37 acres.

In Phase 1, the MWR was represented as inactive cells. For Phase 2, however, the representation of the MWR was revised to simulate operational water losses and to reflect the water stored in the MWR. The water level in the MWR was set at a constant elevation of 24 feet NAVD 88 and the sidewalls were represented with HFB boundary conditions. Assumptions for the MWR are documented in Sections 7.2 and 7.4.

7.0 PHASE 2 MODEL ASSUMPTIONS

In addition to the assumptions presented in Section 3.3, assumptions used for Phase 2 are presented below. Note that some of the assumptions are case specific.

7.1 Backfill

Two types of backfill are proposed for the Units 6 & 7 site: Category I Engineered Fill ("structural backfill") and Category II Engineered Fill ("non-structural backfill") (FSAR Subsection 2.5.4.5.3). The hydraulic conductivity of structural fill is referred to as "K_{95}" since structural fill will be compacted to a minimum of 95 percent of maximum dry density (FSAR Subsection 2.5.4.5.3). The hydraulic conductivity of non-structural fill is referred to as "K_{92}," since non-structural fill will be compacted to a minimum of 92 percent of maximum dry density (FSAR Subsection 2.5.4.5.3).

7.1.1 Structural Fill

Assumption: Structural backfill is included in the model at and within the location of the diaphragm walls (Figure 2CC-258). Structural fill will be used from an elevation of approximately -16 feet NAVD 88 to the finish grade elevation of 25.5 feet NAVD 88. Structural backfill on the excavation slope outside of the diaphragm walls was not included in the model.

Rationale: FSAR Subsection 2.5.4.5.3 states that structural fill will be used within the nuclear island areas and beneath nonsafety-related power block structures.

Assumption: Assuming a d_{10} (percent fraction that is finer than 10 percent) of approximately 0.02 cm for a typical compacted Florida limerock, the hydraulic conductivity of the structural fill (K_{95}) is estimated as 1.0E-02 cm/s for the base-case simulation (Case 1).

Rationale: Grain size distributions for a typical compacted Florida limerock are provided in Figure 3.1 of Reference 34. Based on a d_{10} grain size of 0.02 cm, K_{95} can be estimated using the following approximation developed by Hazen (Reference 35, p. 350):

$$K(\text{cm/s}) = C_H d_{10}^2 \qquad (7)$$

where K is hydraulic conductivity (cm/s); C_H is the Hazen empirical coefficient (assumed to be 100); and d_{10} is in units of centimeters. K_{95} is estimated to be 4.0E-02 cm/s. The value assumed for K_{95} was rounded to 1.0E-02 cm/s.

7.1.2 Non-Structural Fill

Non-structural fill will be used at non-structural areas of the Units 6 & 7 power blocks and as needed to build up the Units 6 & 7 plant area to post-construction grade. Non-structural fill will be used from an elevation of approximately -5 feet NAVD 88 to the finish grade elevation of 25.5 feet NAVD 88.

Assumption: For all cases, K_{92}=1.35E-02 cm/s.

Rationale: The relationship of permeability to porosity can be estimated from the Kozeny-Carman equation (Reference 36, p. 67):

$$K = C_0\left[\frac{n^3}{(1-n)^2}\right]/M_s^2 \tag{8}$$

where C_0 is a coefficient, M_s is the specific surface area of the porous matrix (defined per unit volume of solid), and n is porosity. C_0 is assumed a constant (Reference 37) and M_s is assumed to be independent of the packing arrangement. Furthermore, porosity can be related to bulk density and mineral density as follows (Reference 38, p. 30):

$$n = 1 - \frac{\rho_b}{\rho_m} \tag{9}$$

where ρ_b is bulk density and ρ_m is mineral density. Thus, Eq. (8), in combination with the definition of porosity (Reference 38, p. 29) and Eq. (9), K_{95} can be related to the hydraulic conductivity of any other compaction percentile, p:

$$\frac{K_{95}}{K_p} = \left(\frac{n_{95}}{n_p}\right)^3\left(\frac{\rho_p}{\rho_{95}}\right)^2 \tag{10}$$

Assuming that the maximum bulk density of the structural backfill is 2.10 g/cm^3 (131 pcf) (see Figure 4.13 of Reference 34) and that the mineral density for a typical Florida limerock is 2.73 g/cm^3 based on the specific gravity of Miami Limestone (Table 2.5.4-205), Eq. (9) and Eq. (10) can be used to estimate the ratio of K_{95}/K_{92}. With K_{92}/K_{95} equal to 0.73, K_{92}= 1.35E-02 cm/s.

7.2 Makeup Water Reservoir

As discussed in Section 6.3, the Makeup Water Reservoir (MWR) supplies makeup water to replace water lost as evaporation, drift and blowdown due to operation of the wet cooling towers that are part of the circulating water system used for normal plant cooling. Several model characteristics were used to represent the MWR. The use of inactive cells is discussed in Subsection 7.2.1, constant head boundary conditions in Subsection 7.2.2, horizontal flow barriers in Subsection 7.2.3, and hydraulic conductivity in Subsection 7.2.4. Assumptions regarding the MWR leakage are documented in Subsection 7.2.4. The use of ZoneBudget to assess vertical and lateral leakage from the MWR is discussed in Section 7.4.

In the model, the top elevation of the MWR sidewalls was set to 24 feet NAVD 88. The top elevation of the reservoir bottom slab was set to -2 feet NAVD 88 and the bottom of the slab was set to an elevation of -4 feet NAVD 88.

7.2.1 Inactive Cells

Assumption: The Mechanical Draft Cooling Towers and Circulating Water Pumphouse were set as inactive cells.

> Rationale: The Mechanical Draft Cooling Towers and Circulating Water Pumphouse associated with the MWR are concrete/solid structures.

7.2.2 Constant Head

Assumption: The water level inside the MWR was simulated by a constant head boundary condition, with a head elevation of 24 feet NAVD 88 (Figure 2CC-261).

> Rationale: The head elevation is equal to the top elevation of the reservoir. As stated in FSAR Subsection 2.4.8, the maximum operating water level in the MWR basin is assumed to be 22.5 feet NAVD 88. However, there are extreme conditions when the water level could be higher, such as during extreme rainfall events. For example, for a one-half probable maximum precipitation storm event, a maximum water level of elevation 24.2 feet NAVD 88 (FSAR Subsection 2.4.4) was considered, which is 0.2 feet above the top elevation of the MWR wall at elevation 24.0 feet NAVD 88. As this event would occur for only a few hours, a water surface elevation of 24 feet NAVD 88 was assumed for the MWR.

7.2.3 Horizontal Flow Barriers

Assumption: The MWR sidewalls were simulated as horizontal flow barrier (HFB) boundary conditions to account for operational leakage (Figure 2CC-259). The walls were assumed to be 2 feet thick, with a hydraulic conductivity of 1.0E-08 cm/s.

Rationale: The MWR sidewall thickness of 2 feet is based on preliminary design. As discussed in Subsection 3.3.8, the design value for the diaphragm (cut-off) walls is 8.3E-10 (Reference 26). A value of 1.0E-08 cm/s will provide a conservative estimate for operational leakage.

Assumption: For Case 3, HFBs along the north wall of the MWR were removed. The HFB boundary conditions along the west, south, and east edges of the MWR sidewalls and bottom reservoir slab were included in the simulation.

Rationale: HFB boundary conditions were removed along the north wall of the MWR to simulate the impact on water table elevations near Units 6 & 7 from a catastrophic failure of the MWR north wall. The failure was restricted to the north wall as a limiting case.

7.2.4 Hydraulic Conductivity

Assumption: A new hydraulic conductivity zone was introduced for the concrete slab below the MWR to allow for a fixed 0.1 percent leakage from the MWR (Figure 2CC-259). For all cases but Case 4, which simulates the effect of sea-level rise, the hydraulic conductivity of the MWR bottom reservoir slab was assumed to be 1.46E-06 cm/s. For Case 4, the hydraulic conductivity of the MWR bottom reservoir slab was assumed to be 1.58E-06 cm/s.

Rationale: The assumption of a 0.1 percent leakage is based on a general recommendation of no more than a 1/10th of one-percent volume loss per day for concrete-lined reservoirs (Reference 39). Therefore, assuming the MWR volume is approximately 300,000,000 gallons, the allowable leakage to the surrounding area is 300,000 gpd. In order to reflect a leakage of 300,000 gpd, a reservoir bottom slab hydraulic conductivity of 1.46E-06 cm/s was implemented in the model. Lateral leakage and vertical leakage from the MWR were assessed using ZoneBudget (Reference 32), which is discussed in Section 7.4.

7.3 Sea-Level Rise Boundary Conditions

In Case 4, general head and river boundary conditions were revised to evaluate the impact of expected long-term sea-level rise on groundwater levels in the nuclear island areas.

Assumption: For the simulation that considers sea-level rise (Case 4), a sea-level rise of 1 foot over the seasonal high water value of 0.09 feet (1 foot + 0.09 feet NAVD 88 = 1.09 feet NAVD 88) was assumed for general head boundary conditions in Biscayne Bay.

> Rationale: As discussed in FSAR Subsection 2.4.5.2.2.1, the long-term sea-level rise trend is 0.78 feet in 100 years. Therefore, a conservative sea-level rise estimate of 1 foot was assumed for this analysis. The seasonal high water level of elevation 0.09 feet NAVD 88 for Biscayne Bay is documented in Reference 10.

Assumption: For Case 4, general head and river boundary conditions were based on a sea level elevation of 1.09 feet NAVD 88.

> Rationale: For the FPL site, head values for general head boundary conditions and river boundary conditions vary with sea level fluctuations. Water levels in the cooling water canals, L-31E Canal, Card Sound Canal, and Model Land Canal (C-107) were adjusted based on the water level in Biscayne Bay. The general head and river boundary conditions for the sea-level rise case were 1.9 feet higher than those for the base-case simulation.

For this case, a sea-level rise of 1 foot is added to the seasonal high sea level of 0.09 feet NAVD 88, whereas the long-term average value is -0.81 feet NAVD 88 (Sections 5.1 and 5.2).

7.4 ZoneBudget

ZoneBudget (Reference 32) was used to assess lateral and vertical leakage from the MWR. ZoneBudget was used in conjunction with the MWR leakage and sidewall assumptions that are discussed in Section 7.2.

Assumption: Three zones were introduced into the model to assess leakage from the MWR. A zone was created to represent the MWR. A separate zone was created to represent the area beyond the MWR sidewalls. A zone was also created below the MWR bottom reservoir slab.

Rationale: As discussed in Section 7.2, a target vertical leakage of 0.1 percent of the reservoir capacity (300,000 gpd) was assumed for the predictive model simulations. ZoneBudget values indicate negligible (<0.1 percent) lateral leakage. The ZoneBudget analysis also indicates that the target vertical leakage of 300,000 gpd was achieved for all simulation cases within 1 percent.

8.0 PHASE 2 POST-CONSTRUCTION SIMULATIONS

The Phase 2 simulations include four post-construction simulations (Case 1 through Case 4). Each case is described below. A summary of the simulated maximum water table elevations is provided in Table 2CC-213.

For estimating maximum water table elevations, six observation points were incorporated into Layer 1 of the model at the northwestern corner of each unit, inside the diaphragm wall (Figure 2CC-260). Observation points were placed at these locations due to the northwest to southeast gradient that was observed in Figure 2CC-262. The gradient indicates that higher water table elevations are expected to occur at the northwest corner of each unit.

Case 1: Base-case model with K_{95}=1.0E-02 cm/s (Figure 2CC-258). Recharge rates for the uppermost active layer are provided in Figure 2CC-257. The same recharge assumption is applied for Cases 3 and 4. Post-construction water table elevations for the Units 6 & 7 nuclear islands and surrounding areas assuming K_{95}=1.0E-02 cm/s are shown in Figure 2CC-262. The figure indicates a northwest to southeast hydraulic gradient across the site. Table 2CC-213 and Figure 2CC-262 indicate water table elevations of approximately 2 feet NAVD 88 in the Units 6 & 7 nuclear island areas for the base-case simulation. Model observation points indicate maximum water table elevations of 2.07 feet NAVD 88 within the Units 6 & 7 nuclear islands. The water table mounds within the diaphragm walls because recharge occurring within the perimeter of these walls (Figure 2CC-256) is constrained laterally on all sides by the diaphragm walls and vertically by the underlying concrete fill. Outside the nuclear island areas, however, water table elevations range from approximately -0.4 to -0.9 feet NAVD 88. As shown in Figure 2CC-262, the simulation does not indicate water table mounding in the area between the Units 6 & 7 nuclear islands. Mounding does not occur in this region because recharge entering the groundwater system between the two nuclear islands is constrained to the east and west by the Units 6 & 7 diaphragm walls, respectively, but is not constrained to the north, south or vertically downward by any low hydraulic conductivity material. Therefore,

groundwater recharged in this area can flow to the north, south or downward through the relatively high hydraulic conductivity fill and native materials.

Case 2: Sensitivity case for high recharge rates for grass and gravel (46.75 in/yr for each surface type) (Figure 2CC-257). Maximum post-construction water table elevations with a higher rate of non-paved recharge (46.75 in/yr) were estimated to be 2.34 feet NAVD 88 within the Units 6 & 7 nuclear islands (Table 2CC-213).

Case 3: Simulation of a catastrophic failure of the MWR north wall. The collapse was limited to the north wall as a limiting case with respect to the potential impact on Units 6 & 7. Maximum post-construction water table elevations assuming a failure of the MWR north wall were estimated to be 2.07 feet NAVD 88 within the Units 6 & 7 nuclear islands (Table 2CC-213). Because of its high hydraulic conductivity, the Miami Limestone acts as a sink for water released from the location of the north wall. Consequently, the effects of a catastrophic failure only extend a couple of hundred feet from the MWR and do not influence water levels in the nuclear island areas. Simulated groundwater contours for Case 3 are provided in Figure 2CC-263.

Case 4: Simulation assuming sea-level rise at the Units 6 & 7 site. The assumptions for this simulation are discussed in Section 7.3. Maximum post-construction water table elevations assuming sea-level rise were estimated to be approximately 2.10 feet NAVD 88 at the Units 6 & 7 nuclear islands (Table 2CC-213). Outside of the Units 6 & 7 plant area, some areas of inland flooding occurred for this case for land elevations below 1.09 feet NAVD 88. Simulated groundwater contours on the Units 6 & 7 plant area are provided in Figure 2CC-264.

9.0 CONCLUSIONS

A steady-state, constant-density, three-dimensional model was developed to simulate groundwater flow at the Turkey Point Units 6 & 7 Site. The model was developed and calibrated using available historic data and data collected in support of the Combined License Application (COLA).

The groundwater model was developed in two phases. Phase 1 evaluates groundwater control options for construction of Units 6 & 7 and also simulates the operation of a radial collector well system to serving as a temporary source of makeup water. The Phase 2 model simulates operational MWR leakage, the failure of the MWR north wall and the effect of sea-level rise on groundwater

elevations at Units 6 & 7. Phase 2 simulations include post-construction features not represented in Phase 1.

The Phase 1 calibrated model was used to simulate construction dewatering for the Unit 6 and Unit 7 nuclear islands. Calculated pumping rates to enable dry working conditions are 96 gpm for each excavation, when each unit is constructed separately. These simulations for groundwater control involve injecting grout between the bottom of the excavation and the bottom of the cut-off wall and using sump pumps in the base of the excavation to remove seepage through the grout plug into the excavation.

The Phase 1 model was also used to determine the origin of water supplying the radial collector wells by a combination of particle tracking and evaluating flows through different parts of the model. These simulations indicate that approximately 97.8 percent of the pumped water will originate from Biscayne Bay while the remainder will originate from inland.

For Phase 2 simulations, water table elevations satisfied the Design Control Document (DCD) criteria for normal water level elevation of up to 2 feet below plant elevation for the Westinghouse Advanced Passive 1000 (AP1000). For all simulations, maximum post-construction water table elevations within the nuclear islands were estimated to be approximately 2 feet NAVD 88 (Table 2CC-213). The maximum increase in water table elevations under Units 6 & 7 with high recharge near Units 6 & 7 was estimated to be approximately 0.3 feet higher than the base-case simulation. The maximum increase in water table elevations at Units 6 & 7 with sea-level rise was estimated to be approximately 0.03 feet higher than the base-case simulation.

10.0 REFERENCES

1. Southeastern Geological Society, *Hydrogeological Units of Florida*, Special Publication 28, Ad Hoc Committee on Florida Hydrostratigraphic Unit Definition, 1986.

2. Dames & Moore, *Geohydrologic Conditions Related to the Construction of Cooling Ponds*, *Florida Power & Light Company, Steam Generating Station, Turkey Point, Florida*, prepared for Brown and Root, Inc., 1971.

3. MACTEC Engineering and Consulting, Inc., *Final Data Report—Geotechnical Exploration and Testing: Turkey Point COL Project Florida City, Florida*, Rev. 2, included in COL Application Part 11, October 6, 2008.

4. HDR Engineering, Inc., *Turkey Point Exploratory Drilling and Aquifer Performance Test Program*, prepared for Florida Power & Light Company, August 2009. Available at http://publicfiles.dep.state.fl.us/Siting/Outgoing/FPL_Turkey_Point/Units_6_7/Completeness/Plant_Associated_Facilities/1st_round_Completeness/FPL_Response_1st_Incompleteness/Attached%20Reports/HDR/Aquifer%20Performance%20Test_August-2009Report_HDR%20APT_FPL_081909.pdf, accessed October 17, 2011.

5. JLA Geosciences Inc., *Geology and Hydrogeology Report for FPL Turkey Point Plant Groundwater, Surface Water, & Ecological Monitoring Plan,* 2010. Available at http://www.sfwmd.gov/portal/page/portal/xrepository/sfwmd_repository_pdf/fpl_tp_geo_and_h2ogeo_rept.pdf, accessed October 17, 2011.

6. Dames & Moore, *Florida Aquifer Water Supply Investigation, Turkey Point Area, Dade County, Florida*, prepared for Florida Power & Light Company, 1975.

7. Florida Geological Survey, Lithologic Database, 2008. Available at http://www.dep.state.fl.us/geology/gisdatamaps/litholog.htm, accessed September 6, 2008.

8. Reich, C., R. Halley, T. Hickey, and P. Swarzenski, *Groundwater Characterization and Assessment of Contaminants in Marine Areas of Biscayne National Park*, Technical Report/NPS/NRWRD/NRTR-2006/356, 2006. Available at http://sofia.usgs.gov/publications/reports/bisc_gw_char/Bisc_gw_char.pdf, accessed May 17, 2012.

9. Florida Power & Light Company, *FPL Turkey Point Power Plant Groundwater, Surface Water, and Ecological Monitoring Plan,* Exhibit B. October 2009. Available at http://publicfiles.dep.state.fl.us/siting/Outgoing/FPL_Turkey_Point/Units_6_7/Completeness/Plant_Associated_Facilities/2nd_round_Completeness/FPL_Response_Part_A_Information/Attachments/2nd%20Round%20Attachments/101409%20Final%20Turkey%20Point%20Monitoring%20Plan.pdf, accessed November 10, 2010.

10. National Oceanic and Atmospheric Administration,*Tides & Currents Virginia Key, FL #8723214 web page* 2010. Available at http://

tidesandcurrents.noaa.gov/station_info.shtml?stn=8723214%20Virginia%20Key,%20FL, accessed October 13, 2010.

11. Langevin, C., *Simulation of Ground-Water Discharge to Biscayne Bay, Southeastern Florida*, U.S. Geological Survey, Water-Resources Investigations Report 00-4251, 2001.

12. South Florida Water Management District. *South Florida Water Management District DBHYDRO database query, Station S20F,* 2010. Available at http://www.sfwmd.gov/dbhydroplsql/show_dbkey_info.date_selection?v_js_flag=Y&v_db_request_id=2802506&v_parameter_string=&v_dbkey=05816%2FVN225%2FK8666%2F16692&v_frequency=&v_sdate=19680522&v_edate=20101025, accessed October 14, 2010.

13. Harbaugh, A., E. Banta, M. Hill, and M. McDonald, MODFLOW-2000, The U.S. Geological Survey Modular Ground-Water Model — User Guide to Modularization Concepts and the Ground-Water Flow Process, U.S. Geological Survey, Open-File Report 00-92, 2000. Available at http://pubs.er.usgs.gov/usgspubs/ofr/ofr200092, accessed September 30, 2008.

14. McDonald, M, and A. Harbaugh. *A Modular Three-Dimensional Finite-Difference Ground-Water Flow Model,* U.S. Geological Survey, Open-File Report 83-875, 1984. Available at http://pubs.er.usgs.gov/usgspubs/ofr/ofr83875, accessed September 29, 2008.

15. McDonald, M. and A. Harbaugh,. *Chapter A1 — A Modular Three-Dimensional Finite-Difference Ground-Water Flow Model,* Techniques of Water-Resources Investigations of the U.S. Geological Survey, Book 6, Modeling Techniques, 1988. Available at http://pubs.er.usgs.gov/usgspubs/twri/twri06A1, accessed September 29, 2008.

16. Schlumberger Water Services. *Visual MODFLOW Professional Ver. 4.3*, User's Manual, 2008.

17. National Oceanic and Atmospheric Administration, Coastal Services Center, *Topographic and Bathymetric Data Considerations: Datums, Datum Conversion Techniques and Data Integration, Part II: A Roadmap to a Seamless Topobathy Surface*, Technical Report NOAA/CSC/20718-PUB, 2008.

18. National Oceanic and Atmospheric Administration, *VDatum — Online User's Guide*. Available at http://vdatum.noaa.gov/docs/usersguide.html, accessed October 13, 2010.

19. National Oceanic and Atmospheric Administration, *FME SpatialDirect*, Office of Coast Survey Harbor Sounding2010. Available at http://ocs-spatial.ncd.noaa.gov/SpatialDirect/translationServlet?SSFunction=prepareFetch, accessed May 13, 2010.

20. Renken, R., K. Cunningham, A. Shapiro, R. Harvey, M. Zygnerski, D. Metge, and M. Wacker, *Pathogen and Chemical Transport in the Karst Limestone of the Biscayne Aquifer: 1. Revised Conceptualization of Groundwater Flow*, Water Resources Research, Vol. 44, 2008.

21. Fish and Wildlife Research Institute, Marine Resources Geographic Information System GIS Data, Benthic Habitats — South Florida. Available at http://ocean.floridamarine.org/mrgis_ims/Description_Layers_Marine.htm, accessed June 25, 2010.

22. Cunningham, K., J. Carlson, G. Wingard, E. Robinson, and M. Wacker,*Characterization of Aquifer Heterogeneity Using Cyclostratigraphy and Geophysical Methods in the Upper Part of the Karstic Biscayne Aquifer, Southeastern Florida*, U.S. Geological Survey, Water-Resources Investigations Report 03-4208, 2004.

23. Cunningham, K., M. Wacker, E. Robinson, J. Dixon, and G. Wingard, *A Cyclostratigraphic and Borehole-Geophysical Approach to the Development of a Three-Dimensional Conceptual Hydrogeologic Model of the Karstic Biscayne Aquifer, Southeastern Florida*. U.S. Geological Survey, Scientific Investigations Report 2005-5235, 2006.

24. Cunningham, K., M. Sukop, H. Huang, P. Alvarez, H. Curran, R. Renken, and J. Dixon, *Prominence of Ichnologically Influenced Macroporosity in the Karst Biscayne Aquifer: Stratiform "Super-K" Zones,* Geological Society of America Bulletin, Vol. 121, No. 1/2, pp. 164–180, 2009.

25. Fetter, C., *Applied Hydrogeology*, 3d ed., Prentice Hall, 1994.

26. Rice, R. and J. Walton, *Design Factors Affecting the Flow of Water through Below-Ground Concrete Vaults*, Journal of Environmental Engineering Vol. 132, No. 10, pp. 1346–1354, October 2006,

27. Warner, J., *Practical Handbook of Grouting: Soil, Rock, and Structures,* John Wiley and Sons, 2004.

28. Weaver, K. and D. Bruce, *Dam Foundation Grouting, Revised and Expanded Edition*, American Society of Civil Engineers, Subsection 14.2.1 Permeability Criteria, 2007.

29. Gamble, B. and S. Stowe, *Approaches to Modeling Collector Wells and Horizontal Wells with MODFLOW,* MODFLOW and More 2008: Groundwater and Public Policy, Conference proceedings, pp. 489–493, 2008.

30. HDR Engineering Inc., *Cooling Water Supply and Disposal Conceptual Design Report — Florida Power & Light Proposed Units 6 & 7 at Turkey Point — March 2009*. Available at http://publicfiles.dep.state.fl.us/Siting/Outgoing/FPL_Turkey_Point/Units_6_7/Completeness/Plant_Associated_Facilities/1st_round_Completeness/FPL_Response_1st_Incompleteness/Attached%20Reports/HDR/Cooling%20Water_%20March-2009/Report_HDR_CoolingWater_ConceptualDesign.pdf, accessed October 17, 2011.

31. Pollock, D., User's Guide for MODPATH/MODPATH-PLOT, *Version 3: A Particle Tracking Post-Processing Package for MODFLOW, the U.S. Geological Survey Finite-Difference Ground-Water Flow Model* U.S. Geological Survey, Open-File Report 94-464, 1994. Available at http://water.usgs.gov/software/MODPATH/code/doc/ofr94464.pdf, accessed January 31, 2011.

32. Harbaugh, A., *A Computer Program for Calculating Subregional Water Budgets Using Results from the U.S. Geological Survey Modular Three-Dimensional Ground-Water Flow Model*, U.S. Geological Survey, Open-File Report 90-392, 1990.

33. Hsieh, P., and J. Freckleton, *Documentation of Computer Program to Simulate Horizontal-Flow Barriers Using the United States Geological Survey's Modular Three-Dimensional Finite-Difference Ground-Water Flow Model,* U.S. Geological Survey, Open-File Report 92-477, 1993. Available at http://water.usgs.gov/nrp/gwsoftware/modflow2005/ofr92_477_HFB.pdf, accessed May 27, 2009.

34. McVay, M., and J. Ko, *Evaluating Thick Lift Limerock-Base Course SR-826*, Miami, Florida, FDOT No. C-7984, April 2005.

35. Freeze, R., and J. Cherry, *Groundwater*, Prentice Hall, Englewood Cliffs, New Jersey, 1979.

36. Bear, J., *Hydraulics of Groundwater*, originally published by McGraw-Hill, Dover edition reprint, published in 2007, Mineola, New York, 1979.

37. Carman, P., *Fluid Flow Through a Granular Bed*, Transactions of the Institution of Chemical Engineers, London, 15, pp. 150–156, 1937.

38. Jury, W., W. Gardner, and W. Gardner, *Soil Physics*, 5th ed., John Wiley and Sons, Inc., New York, 1991.

39. American Concrete Institute, *Tightness Testing of Environmental Concrete Structures* (ACI 350.1/350.1R-7), Chap., Hydrostatic Test, HST, For Open or Covered Tanks, 2010.

40. Krupa, A., and M. Mullen, *Literature Review And Assessment Of Geologic Logs To Determine The Extent Of A Dense Limestone Layer In The Upper Portion Of The Biscayne Aquifer In The Pennsuco Wetlands, Miami-Dade County, Florida,* 2005.

41. Sonenshein, R., *Methods to Quantify Seepage Beneath Levee 30, Miami-Dade County, Florida*, U.S. Geological Survey, Water-Resources Investigations Report 2001-4074, 2001.

42. Merritt, M., *Simulation of the Water-Table Altitude in the Biscayne Aquifer, Southern Dade County, Florida, Water Years 1945-89*, U.S. Geological Survey, Water Supply Paper 2458, 1996.

43. Swain, E., B. Howie, and J. Dixon, *Description and Field Analysis of a Coupled Ground-Water/Surface-Water Flow Model (MODFLOW/ BRANCH) with Modifications for Structures and Wetlands in Southern Dade County, Florida*, U.S. Geological Survey, Water-Resources Investigations Report 1996-4118, 1996.

44. Fish, J. and M. Stewart, *Hydrogeology of the Surficial Aquifer System, Dade County, Florida*, U.S. Geological Survey, Water-Resources Investigations Report 90-4108, 1991.

Table 2CC-201
Station S20F: Rainfall Data for February to May 2009

2009		Total Precipitation (inches)
Month	**Days**	**VN225**
Feb	28	0.34
Mar	31	3.72
Apr	30	0.27
May	31	9.63
Total	120	13.96
Rounded to nearest tenth		14.0
Scaled to Year		**42.6** **in/yr**

Source: Based on Reference 12.

Table 2CC-202
Station S20F: Annual Rainfall Data

Water Year	Precipitation (inches)					Combined Series (inches)
	BELF 5618	OMD 16692	TELE K866	NRG VN225	Recorder Selected	
1969	67.52				BELF	67.52
1970	40.67				BELF	40.67
1971	32.16				BELF	32.16
1972	54.38				BELF	54.38
1973	40.60				BELF	40.60
1974	35.48				BELF	35.48
1975	43.08				BELF	43.08
1976	43.68				BELF	43.68
1977	43.89				BELF	43.89
1978	38.06				BELF	38.06
1979	33.89				BELF	33.89
1980	41.17				BELF	41.17
1981	45.46				BELF	45.46
1982	46.19				BELF	46.19
1983	59.62				BELF	59.62
1984	36.92				BELF	36.92
1985	37.37				BELF	37.37
1986	38.75				BELF	38.75
1987	41.54				BELF	41.54
1988	73.31				BELF	73.31
1989	46.84				BELF	46.84
1990	39.89				BELF	39.89
1991	40.41				BELF	40.41
1992	46.26	60.38			OMD	60.38
1993	38.59	36.18			OMD	36.18
1994	55.10	60.06			OMD	60.06
1995	74.75	86.11			OMD	86.11
1996	49.55	49.56			OMD	49.56
1997	53.25	49.98			OMD	49.98
1998	48.01	57.41	64.32		OMD/TELE	60.87
1999	36.46	44.62	44.90		OMD/TELE	44.76
2000	38.87	41.23	41.64		OMD/TELE	41.44
2001	57.35	47.41	47.66		OMD/TELE	47.54
2002		48.91	48.48		OMD/TELE	48.70
2003		43.75	43.48		OMD/TELE	43.62
2004		32.60	32.90		OMD/TELE	32.75
2005		47.91	44.98		OMD/TELE	46.45
2006		44.54	44.97		OMD/TELE	44.76
2007		51.14	51.42		OMD/TELE	51.28
2008		44.11	45.47	45.61	NRG	45.61
2009		44.89	44.00	45.86	NRG	45.86
					Average	46.75 in/yr

Source: Based on Reference 12.

Table 2CC-203
Extinction Depth and Maximum Evapotranspiration Rate

Land-use category	Runoff Coefficient	Extinction depth (m)
Urban	0.5	0.3
Agriculture	0.5	0.43
Rangelend	0.2	0.7
Upland forests	0.2	0.7
Water	0	0.183
Wetlands	0	0.69
Barren land	0	0.15
Transportation	0.5	0.3

	January	February	March	April	May	June–October	November	December
Maximum evapotanspiration rate (cm/d)	0.20	0.28	0.36	0.43	0.46	0.53	0.30	0.28

Source: Based on Reference 11.

Table 2CC-204
Regional Hydraulic Conductivity Values Based on Onsite Tests and Literature Review

	FPL Onsite Tests				Literature Review							
HG Unit	Kh min	Kh max	Kv min	Kv max	Kh min	Ref	Kh max	Ref	Kv min	Ref	Kv max	Ref
Offshore Sediment												
Onshore Muck			*2.5E-04*	*2.5E-04*	3.5E-05	40	1.8E-02	41	3.5E-04	11	1.8E-03	41
Miami Limestone	7.9E-02	7.9E-02	5.0E-03	8.0E-03	3.5E-05	40	1.1E+01	42	3.5E-02	41	1.1E+00	43
Upper Higher Flow Zone												
Key Largo	3.3E+00	1.8E+01			1.1E+00	41	3.5E+01	44	1.1E-01	41		
Freshwater Limestone			7.0E-05	3.0E-03	3.5E-05	40	3.5E-04	41	3.5E-05	41	3.0E-03	40
Lower Higher Flow Zone												
Fort Thompson	1.0E.-01	1.6E+00			1.8E-01	42	1.1E+01	42	1.8E-02	43	1.1E+00	43
Tamiami Formation			3.0E-02	4.0E-01	3.5E-05	43	7.1E-01	44	3.5E-06	43	7.1E-03	41

Notes: Hydraulic conductivity values are in cm/s.
Italicized values indicate instances where only one hydraulic conductivity value was available and thus the maximum and minimum values are equal.

Table 2CC-205
Surface Water Levels Corrected to Reference Density

Surface Water Feature	Location	Base of Canal (ft NAVD 88)	Canal Stage (ft NAVD 88)	Water Type	Water Density (kg/m^3)	Reference Head (ft NAVD 88)
Interceptor Ditch	CHD of -0.28	-19.2	-0.28	FW	996.70	-0.76
Interceptor Ditch	Start of variable H	-19.2	-0.18	FW	996.70	-0.66
Interceptor Ditch	End of variable H	-19.2	-1.05	FW	996.70	-1.51
L-31E	All	-22.8	0.02	FW	996.70	-0.55
Southern Portion of Grand Canal Outside the CCS	All	-21.2	-1.05	SALINE	1022.40	-1.05
C-106	All	-14	-1.05	SALINE	1022.40	-1.05
E-W Release Canal	H = 1.28	-21.2	1.28	CCS	1048.00	1.84
E-W Release Canal	H = 1.08	-21.2	1.08	CCS	1048.00	1.64
N-S Shallow Canal	H = 1.08	-3.02	1.08	CCS	1048.00	1.18
N-S Shallow Canal	H = -1.05	-3.02	-1.05	CCS	1048.00	-1.00
E-W Collector	All	-21.2	-1.05	CCS	1048.00	-0.55
Grand Canal	Top	-21.2	-3.18	CCS	1048.00	-2.73
Grand Canal	Bottom	-21.2	-1.05	CCS	1048.00	-0.55
E. Return Canal	Top	-19.2	-3.18	CCS	1048.00	-2.78
E. Return Canal	Bottom	-19.2	-1.05	CCS	1048.00	-0.60
Units 6 & 7 plant area	SW	-21.2	-3.18	CCS	1048.00	-2.73
Units 6 & 7 plant area	NE	-21.2	-3.28	CCS	1048.00	2.83
Intake Basin	NE Units 6 & 7 plant area	-21.2	-3.28	CCS	1048.00	-2.83
Intake Basin	Pumps	-21.2	-3.38	CCS	1048.00	-2.93

FW — Freshwater
CCS — Hypersaline

FW ρ	996.7	kg/m^3
Ref ρ (Bisc. Bay)	1022.4	kg/m^3
CCS ρ	1048.0	kg/m^3

Table 2CC-206
Model Calibration — Hydraulic Conductivity

	Hydraulic Conductivity (cm/s)		
HG Unit	**Kh**	**Kv**	**Anisotropy Ratio**
Offshore Sediment	3.53E-02	2.4E-03	15:1
Onshore Muck	4.4E-03	4.4E-04	10:1
Miami Limestone	8.8E-02	5.9E-03	15:1
Upper Higher Flow Zone	3.0E+01	3.7E+00	8:1
Key Largo SW	5.9E+00	7.4E-01	8:1
Key Largo NE	1.0E+01	1.3E+00	8:1
Freshwater Limestone	3.4E-05	2.3E-06	15:1
Lower Higher Flow Zone	1.7E+00	1.7E-01	10:1
Fort Thompson	3.3E-01	3.3E-02	10:1
Tamiami Formation	2.8E-04	2.8E-05	10:1

Table 2CC-207
Model Calibration PW-7L — Measured Versus Simulated Drawdowns (at end of test)

Well	HG Unit	Easting	Northing	DRAWDOWN (ft) Observed	DRAWDOWN (ft) Calculated	Ri (Obs-Calc)	|Ri|	|Ri|^2
C7-2A	**Miami Limestone**	875822.2	396944.9	0.31	0.48	-0.18	0.18	0.03
C7-2C	**Tamiami Formation**	875822.2	396944.9	1.54	1.19	0.35	0.35	0.12
C7-2D	**Key Largo Limestone**	875817.3	396944.9	0.34	0.49	-0.15	0.15	0.02
C7-2E	**Fort Thompson Formation**	875817.3	396944.9	3.56	4.44	-0.87	0.87	0.76
C7-3A	**Miami Limestone**	875922.4	396960.2	0.32	0.48	-0.16	0.16	0.03
C7-3C	**Tamiami Formation**	875822.4	396960.2	2.91	1.21	1.70	1.70	2.89
C7-3D	**Key Largo Limestone**	875817.2	396959.9	0.35	0.49	-0.14	0.14	0.02
C7-3E	**Fort Thompson Formation**	875817.2	396959.9	4.96	6.10	-1.15	1.15	1.32
C7-4A	**Miami Limestone**	875822.3	396975.2	0.32	0.48	-0.16	0.16	0.03
C7-4C	**Tamiami Formation**	875822.3	396975.2	2.03	1.22	0.81	0.81	0.66
C7-4E	**Fort Thompson Formation**	875817.3	396974.3	11.40	9.37	2.03	2.03	4.13
C7-5A	**Miami Limestone**	875829.5	396984.1	0.32	0.48	-0.16	0.16	0.02
C7-5D	**Key Largo Limestone**	875828.1	396989.3	0.38	0.48	-0.10	0.10	0.01
C7-5E	**Fort Thompson Formation**	875828.1	396989.3	12.61	10.85	1.77	1.77	3.12
PW-7L	**Fort Thompson Formation**	875819.4	396985.1					

Difference	**12.30**	**10.37**	Number	**14**	**14**
Maximum	**12.61**	**10.85**	Total	**9.72**	**13.16**
Minimum	**0.31**	**0.48**	ARM	**0.69**	
			RMS		**0.97**
			NRMS (%)		**7.9**
			M_d (%)		**0.00**

Note: Easting and Northing in State Plane Coordinates, North American Datum of 1983/Adjustment of 1990, Florida East, Zone 0901, US ft.

Table 2CC-208
Model Calibration PW-1 — Measured Versus Simulated Drawdowns (at the end of test)

Well	HG Unit	Easting	Northing	DRAWDOWN (ft) Observed	DRAWDOWN (ft) Calculated	Ri (Obs-Calc)	|Ri|	|Ri|^2
MW-1A	Miami Limestone	880083.2	401545.1	0.78	0.74	0.04	0.04	0.00
MW-1B	Key Largo Limestone	880083.2	401545.1	0.71	0.78	-0.07	0.07	0.00
MW-1D	Fort Thompson Formation	880083.2	401545.1	0.63	0.63	0.00	0.00	0.00
MW-2B	Key Largo Limestone	880967.2	402023.5	0.19	0.17	0.02	0.02	0.00
MW-3B	Key Largo Limestone	878292.6	401339.6	0.08	0.07	0.01	0.01	0.00
MW-4B	Key Largo Limestone	878331.1	400609.9	0.09	0.06	0.03	0.03	0.00
PW-1	Key Largo Limestone	880146.6	401595.4					

Difference	**0.70**	**0.72**	Number	**6**	**6**
Maximum	**0.78**	**0.78**	Total	**0.18**	**0.01**
Minimum	**0.08**	**0.06**	ARM	**0.03**	
			RMS		**0.04**
			NRMS (%)		**5.3**
			M_d (%)		**0.00**

Note: Easting and Northing in State Plane Coordinates, North American Datum of 1983/Adjustment of 1990, Florida East, Zone 0901, US ft.

Table 2CC-209
Model Calibration PW-7U — Measured Versus Simulated Drawdowns (at end of test)

Well	HG Unit	Easting	Northing	DRAWDOWN (ft) Observed	DRAWDOWN (ft) Calculated	Ri (Obs-Calc)	|Ri|	|Ri|^2
C7-1A	Miami Limestone	875829.5	396932.8	0.88	1.03	-0.15	0.15	0.02
C7-1C	Tamiami Formation	875829.5	396932.8	0.42	0.52	-0.10	0.10	0.01
C71D	Key Largo Limestone	875829.6	396937.7	2.07	1.50	0.57	0.57	0.33
C7-1E	Fort Thompson Formation	875829.6	396937.7	0.50	0.62	-0.12	0.12	0.01
C7-2A	Miami Limestone	875822.2	396944.9	0.89	1.04	-0.15	0.15	0.02
C7-2C	Tamiami Formation	875822.2	396944.9	0.42	0.52	-0.10	0.10	0.01
C7-2D	Key Largo Limestone	875817.3	396944.9	1.48	1.55	-0.07	0.07	0.01
C7-2E	Fort Thompson Formation	875817.3	396944.9	0.54	0.62	-0.08	0.08	0.01
C7-3A	Miami Limestone	875822.4	396960.2	0.75	1.02	-0.27	0.27	0.07
C7-3C	Tamiami Formation	875822.4	396960.2	0.35	0.52	-0.17	0.17	0.03
C7-3D	Key Largo Limestone	875817.2	396959.9	1.27	1.30	-0.03	0.03	0.00
C7-3E	Fort Thompson Formation	875817.2	396959.9	0.42	0.61	-0.19	0.19	0.04
C7-4A	Miami Limestone	875822.3	396975.2	0.82	1.00	-0.18	0.18	0.03
C7-4C	Tamiami Formation	875822.3	396975.2	0.44	0.52	-0.08	0.08	0.01
C7-4D	Key Largo Limestone	875817.3	396974.3	1.13	1.18	-0.06	0.06	0.00
C7-4E	Fort Thompson Formation	875817.3	396974.3	0.52	0.61	-0.09	0.09	0.01
PW--7U	Key Largo Limestone	875819.3	396935.3					

Difference	**1.72**	**1.03**	Number	**16**	**16**
Maximum	**2.07**	**1.55**	Total	**2.41**	**0.60**
Minimum	**0.35**	**0.52**	ARM	**0.15**	
			RMS		**0.19**
			NRMS (%)		**11.3**
			M_d (%)		**0.00**

Note: Easting and Northing in State Plane Coordinates, North American Datum of 1983/Adjustment of 1990, Florida East, Zone 0901, US ft.

Table 2CC-210
Model Validation PW-6U — Measured Versus Simulated Drawdowns (at end of test)

Well	HG Unit	Easting	Northing	DRAWDOWN (ft) Observed	DRAWDOWN (ft) Calculated	Ri (Obs-Calc)	|Ri|	|Ri|^2
C6-1A	Miami Limestone	876678.1	396935.4	1.46	1.37	0.08	0.08	0.01
C6-1C	Tamiami Formation	876678.1	396935.4	0.53	0.53	0.01	0.01	0.00
C6-1D	Key Largo Limestone	876677.9	396940.4	1.66	1.86	-0.20	0.20	0.04
C6-1E	Fort Thompson Formation	876677.9	396940.4	0.57	0.58	-0.01	0.01	0.00
C6-2A	Miami Limestone	876670.8	396947.3	1.34	1.39	-0.05	0.05	0.00
C6-2C	Tamiami Formation	876670.8	396947.3	0.53	0.53	0.00	0.00	0.00
C6-2D	Key Largo Limestone	876665.5	396947.4	2.08	1.95	0.13	0.13	0.02
C6-2E	Fort Thompson Formation	876665.5	396947.4	0.58	0.58	0.00	0.00	0.00
C6-3A	Miami Limestone	876670.5	396962.6	1.09	1.36	-0.27	0.27	0.07
C6-3C	Tamiami Formation	876670.5	396962.6	0.51	0.53	-0.01	0.01	0.00
C6-3D	Key Largo Limestone	876665.7	396962.5	1.30	1.60	-0.30	0.30	0.09
C6-3E	Fort Thompson Formation	876665.7	396962.5	0.50	0.58	-0.07	0.07	0.01
C6-4A	Miami Limestone	876670.9	396978.1	0.98	1.30	-0.32	0.32	0.10
C6-4C	Tamiami Formation	876670.9	396978.1	0.56	0.52	0.04	0.04	0.00
C6-4D	Key Largo Limestone	876666.0	396977.9	1.01	1.43	-0.42	0.42	0.17
C6-4E	Fort Thompson Formation	876666.0	396977.9	0.52	0.57	-0.05	0.05	0.00
PW--6U	Key Largo Limestone	876668.7	396938.0					

Difference	**1.58**	**1.43**	Number	**16**	**16**
Maximum	**2.08**	**1.95**	Total	**1.96**	**0.51**
Minimum	**0.50**	**0.52**	ARM	**0.12**	
			RMS		**0.18**
			NRMS (%)		**11.4**
			M_d (%)		**0.00**

Note: Easting and Northing in State Plane Coordinates, North American Datum of 1983/Adjustment of 1990, Florida East, Zone 0901, US ft.

Table 2CC-211
Phase 1 — Radial Collector Wells — Origin of Water (including sensitivity analysis)

	Percent Contribution to Radial Collector Wells							
Zone	**RCW in Upper High Flow Zone (Base Case)**	**RCW in Key Largo Limestone**	**Seasonal High Water Level**	**Seasonal Low Water Level**	**Double Vertical Hyd. Cond.**	**Half Vertical Hyd. Cond.**	**Key Largo All High K (Blue)**	**Key Largo All Low K (Red)**
Biscayne Bay	97.8%	97.8%	98.1%	97.6%	99.1%	95.4%	97.6%	98.5%
Flow from inland	2.2%	2.2%	1.9%	2.4%	0.9%	4.6%	2.4%	1.5%
– Via Cooling Canal System	2.0%	2.0%	1.8%	2.1%	0.8%	3.2%	2.1%	1.4%
– Regional Eastward Flow	0.2%	0.2%	0.1%	0.3%	0.1%	1.4%	0.3%	0.2%

Note: The top two rows contribute to the total flow and sum to 100 percent. The bottom two rows are components of inland flow. Not all component flows sum to the total inland flow due to rounding. (Blue) and (Red) in final two columns refer to the colors shown for the Key Largo hydraulic conductivity distribution shown in Figure 2CC-216.

Table 2CC-212
Phase 1 — Radial Collector Wells — Approach Velocity (including sensitivity analysis)

	Approach Velocity (cm/s)							
Zone	**RCW in Upper High Flow Zone (Base Case)**	**RCW in Key Largo Limestone**	**Seasonal High Water Level**	**Seasonal Low Water Level**	**Double Vertical Hyd. Cond.**	**Half Vertical Hyd. Cond.**	**Key Largo All High K (Blue)**	**Key Largo All Low K (Red)**
Entire RCW Catchment	3.3E-05	3.3E-05	3.2E-05	3.3E-05	3.7E-05	2.9E-05	3.2E-05	3.5E-05
Immediate RCW Area	5.2E-04	5.1E-04	5.2E-04	5.2E-04	7.3E-04	3.5E-04	5.2E-04	6.3E-04
Average of all RCW Laterals	6.2E-04	6.1E-04	6.2E-04	6.2E-04	9.2E-04	4.0E-04	6.1E-04	7.7E-04

Note: (Blue) and (Red) in final two columns refer to the colors shown for the Key Largo hydraulic conductivity distribution shown in Figure 2CC-216.

Table 2CC-213
Phase 2 — Simulated Heads Observation Points in Model Layer 1 Near Units 6 & 7

SIMULATION	Head for Obs Point #1 (ft NAVD 88)	Head for Obs Point #2 (ft NAVD 88)	Head for Obs Point #3 (ft NAVD 88)	Head for Obs Point #4 (ft NAVD 88)	Head for Obs Point #5 (ft NAVD 88)	Head for Obs Point #6 (ft NAVD 88)	Maximum Head Obs. (ft NAVD 88)
Case 1: Base Case	2.01	2.05	2.07	2.01	2.05	2.07	**2.07**
Case 2: K_{95}=1.0E-02; Recharge=46.75	2.04	2.23	2.34	2.04	2.23	2.34	**2.34**
Case 3: MWR North Wall Failure	2.01	2.05	2.07	2.01	2.05	2.07	**2.07**
Case 4: Sea Level Rise	2.03	2.08	2.10	2.03	2.07	2.10	**2.10**

Note: Maximum water table elevations below 23.5 ft NAVD 88 satisfy the Design Control Doument (DCD) criteria. Observation points shown in Figure 2CC-260.

Figure 2CC-201 Cross Section Location

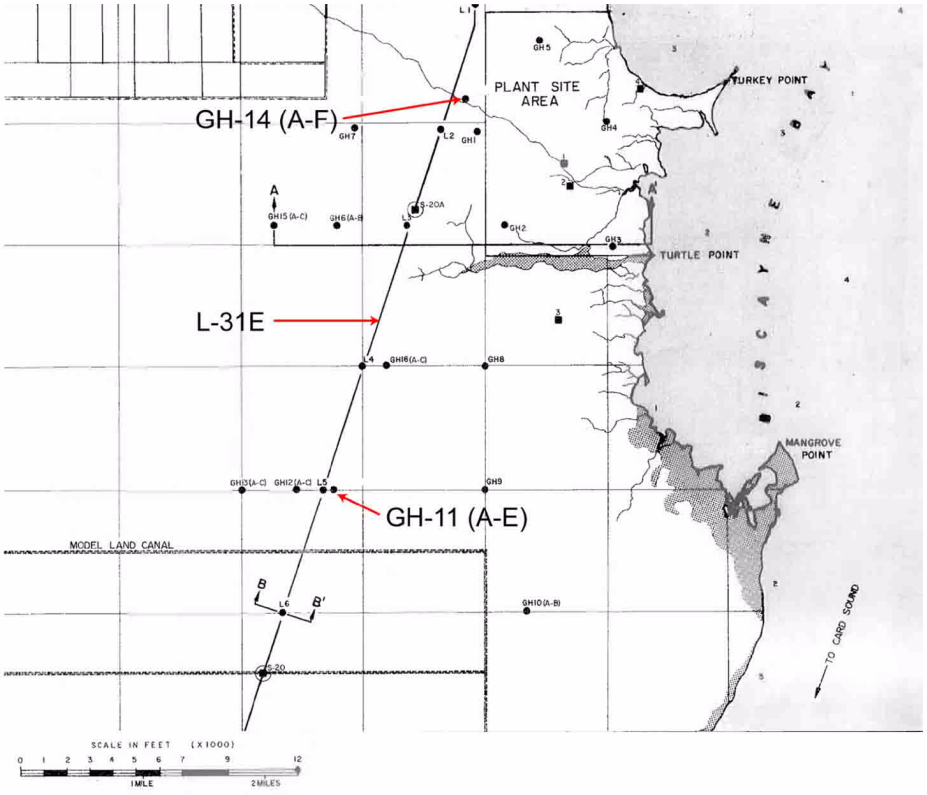

Source: Adapted from Reference 2
Note: Best available scan from original document

Figure 2CC-202 Hydrostratigraphic Cross Section A-A'

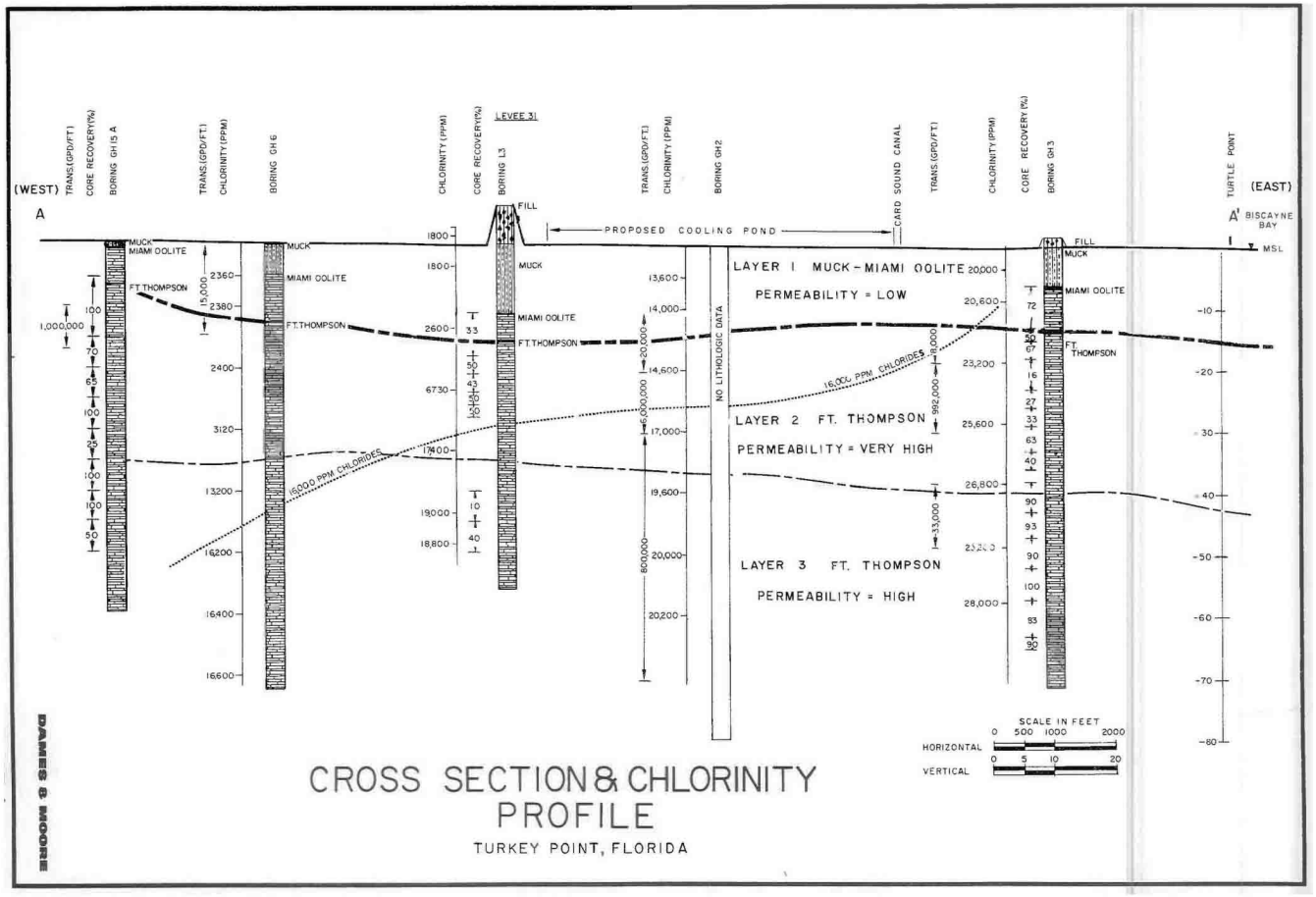

Source: Reference 2
Note: Best available scan from original document

Figure 2CC-203 West-East Cross Section in the Vicinity of the Southern End of the Turkey Point Plant Property

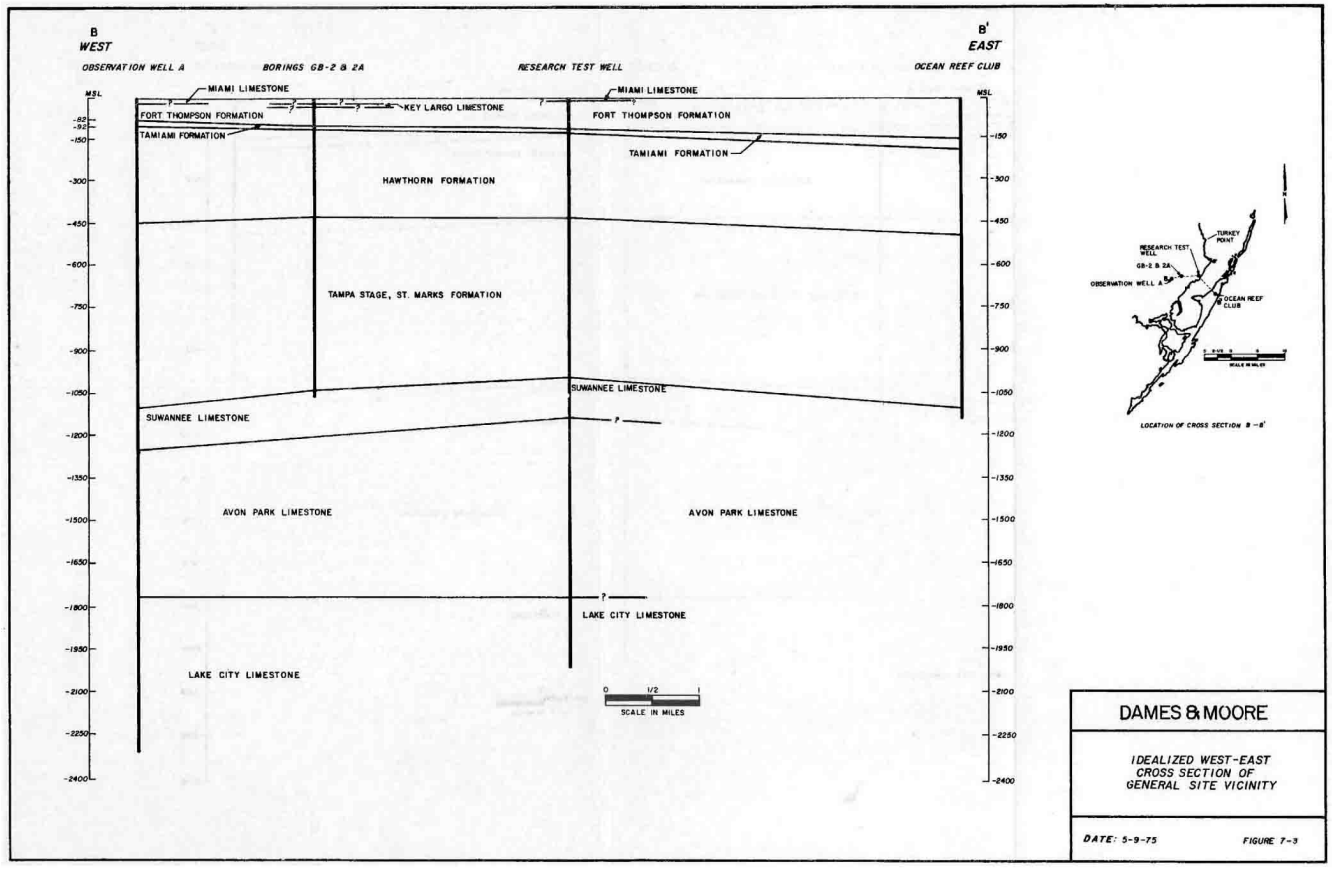

Source: Reference 6
Note: Best available scan from original document

Figure 2CC-204 Feasibility Geological Investigation of Potential Plant Site (2006) — Boring and Stratigraphic Cross Section Locations

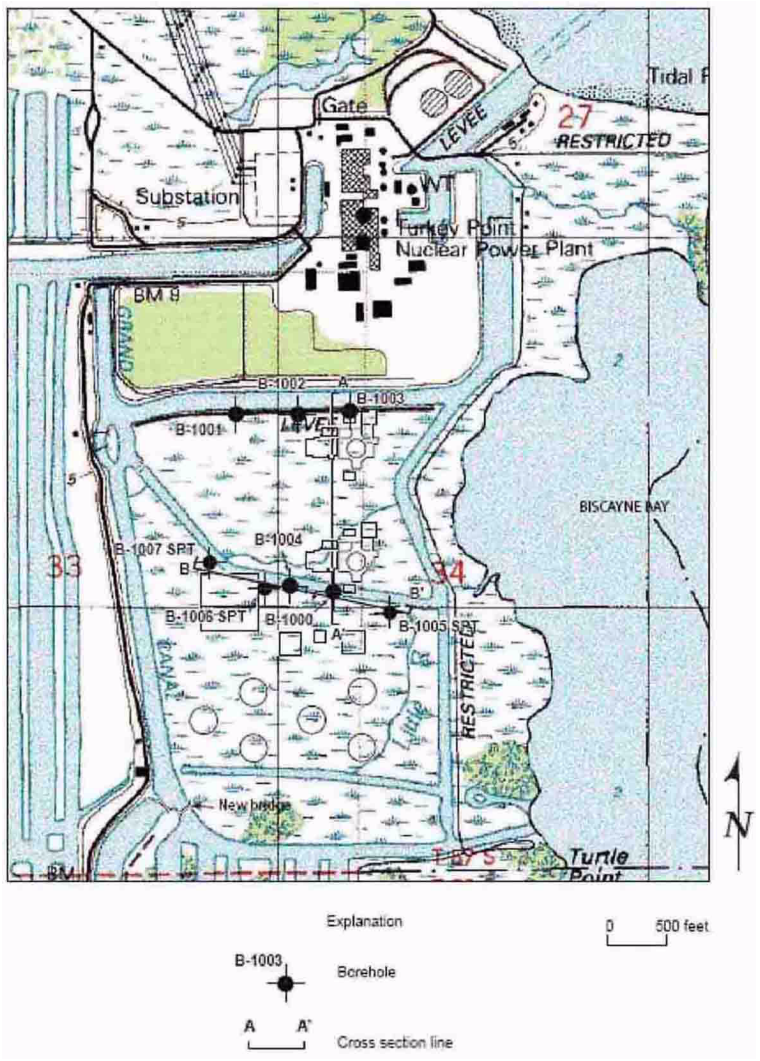

Figure 2CC-205 Feasibility Geological Investigation of Potential Plant Site (2006) — Stratigraphic Cross Section A-A'

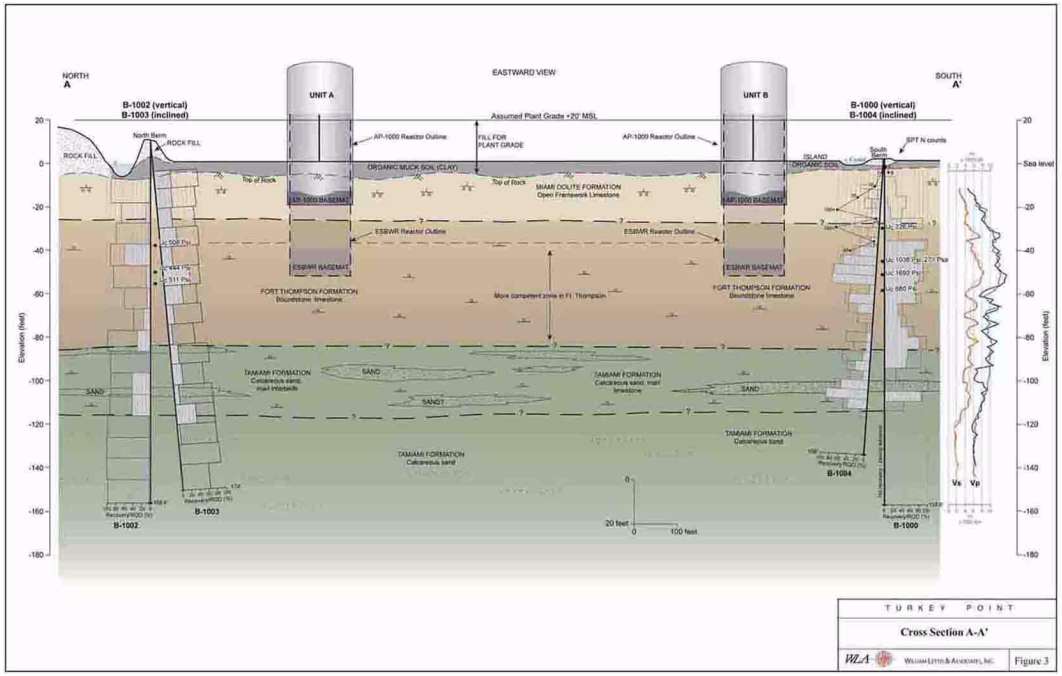

Figure 2CC-206 Feasibility Geological Investigation of Potential Plant Site (2006) — Stratigraphic Cross Section B-B'

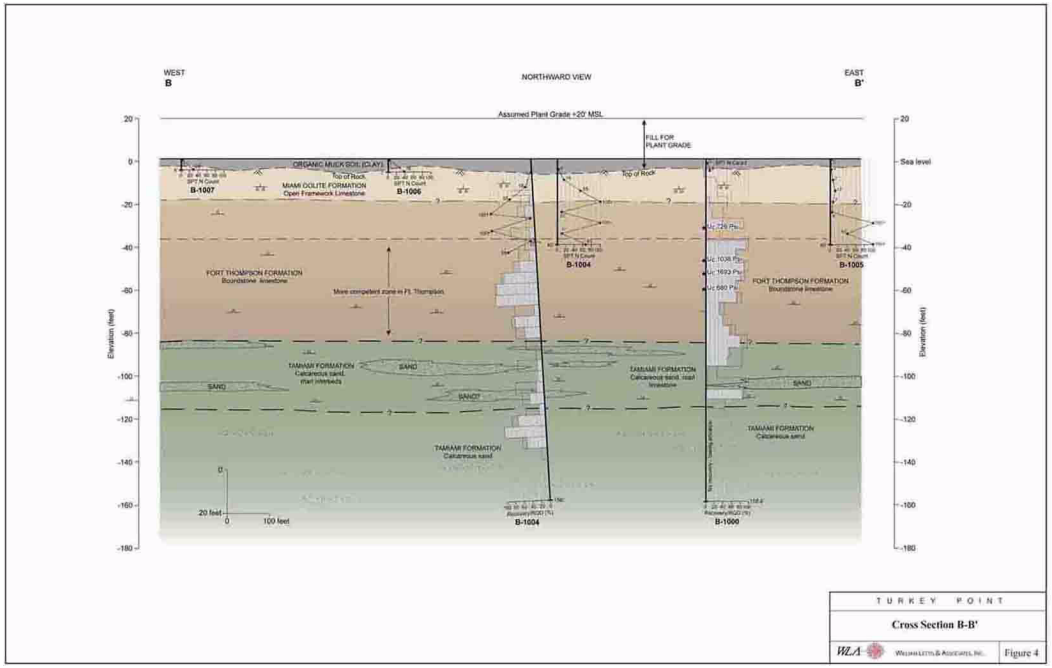

Figure 2CC-207 Stratigraphic Cross Section from Wells Drilled for Turkey Point Peninsula Aquifer Performance Test

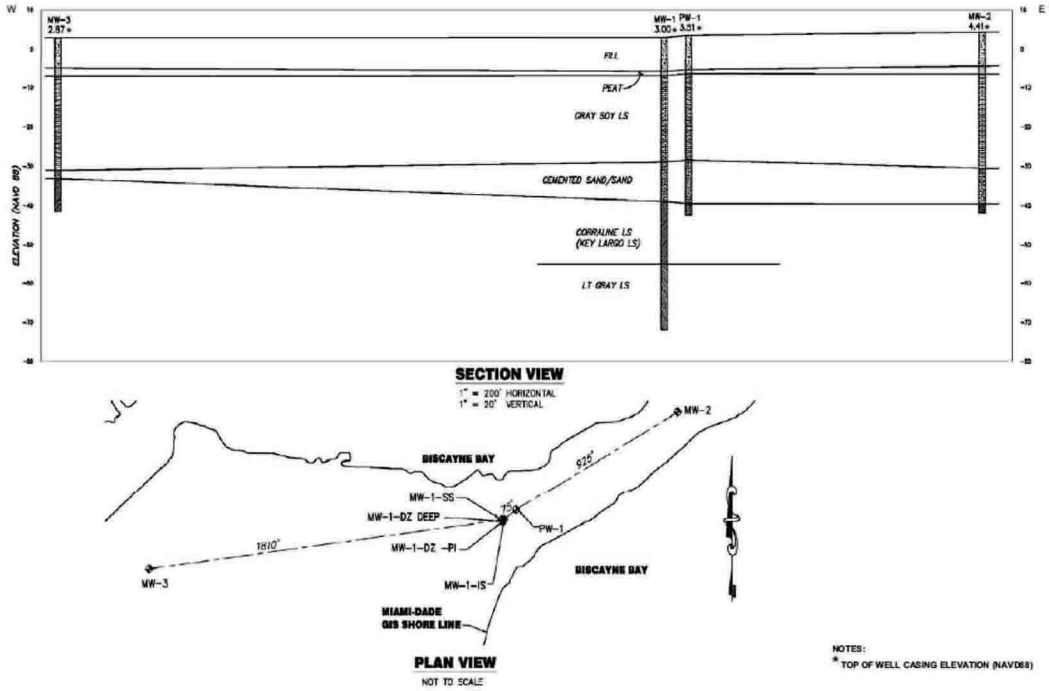

Figure 2CC-208 Land Use for Southern Florida

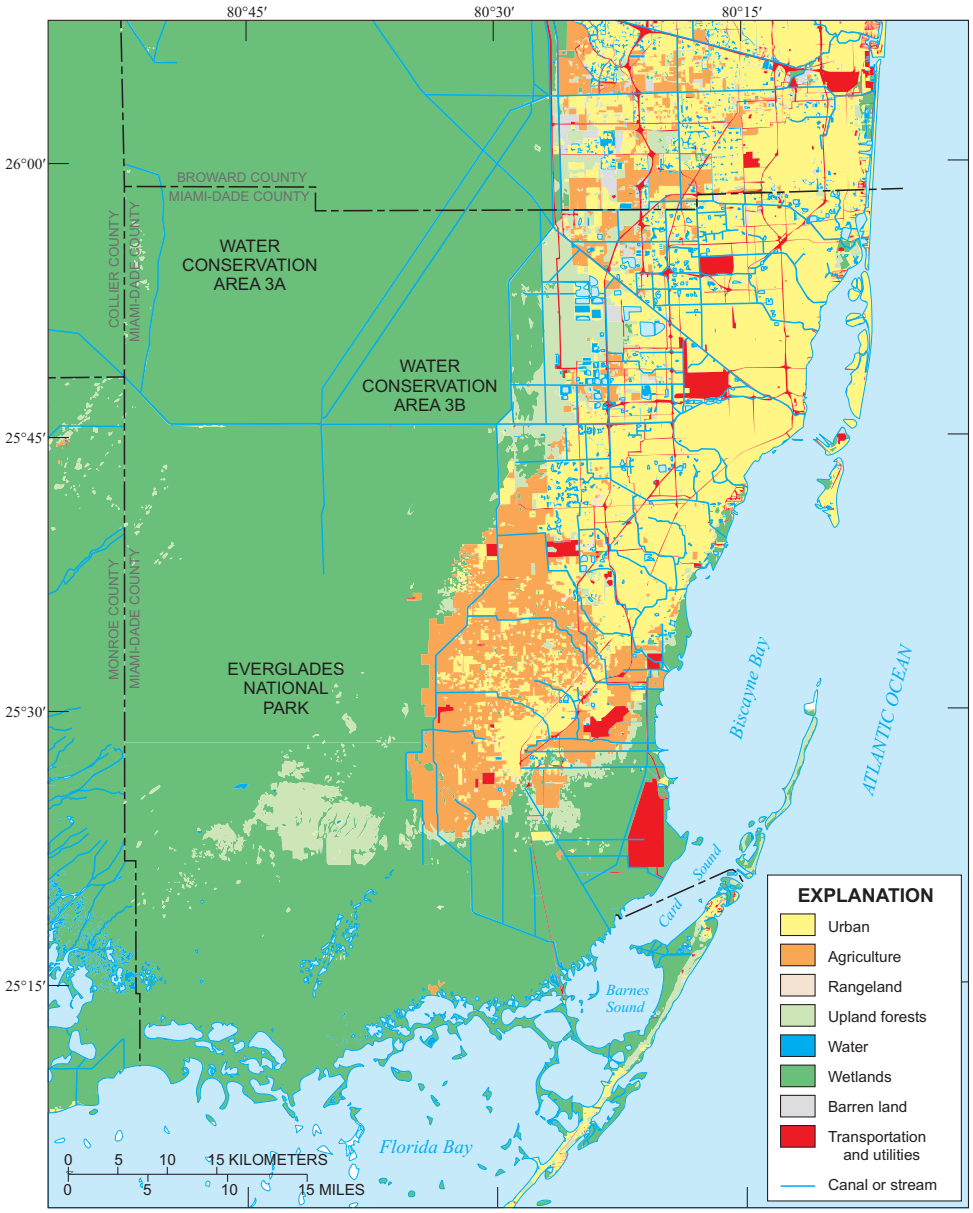

Source: Reference 11

Figure 2CC-209 Numerical Model Domain

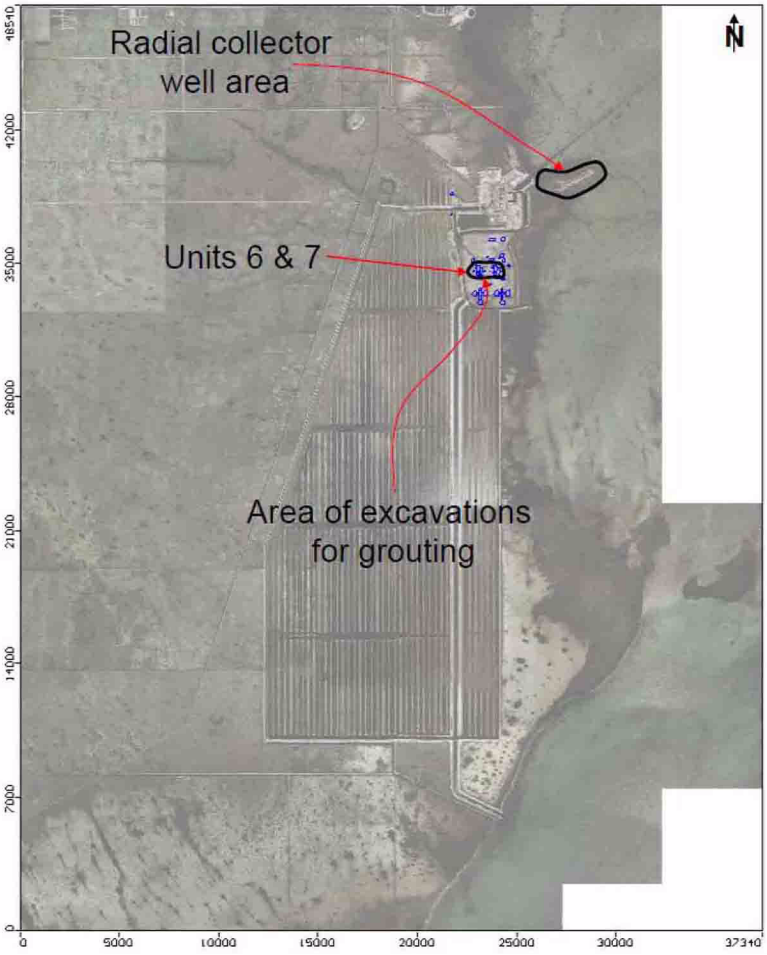

Notes: Model domain identified by extents of axes, not extents of image. While portions on right side are where aerial imagery is not available.
Vertical and horizontal axes represent model coordinates in ft. Model origin at easting 852766, northing 862512 (in State Plane Coordinates, North American Datum of 1983/Adjustment of 1990, Florida East, Zone 0901, US ft.)

Figure 2CC-210 Model Grid and Site Features for the Units 6 & 7 Power Block

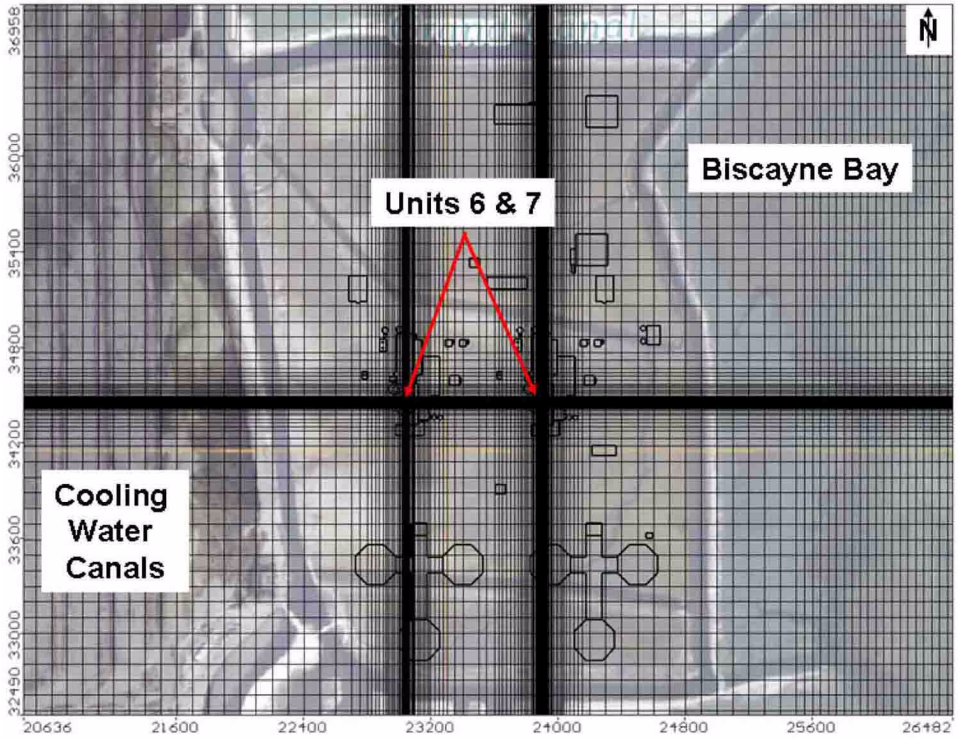

Note:Vertical and horizontal axes represent model coordinates in ft. Model origin at easting 852766, northing 362512 (in State Plane Coordinates, North American Datum of 1983/Adjustment of 1990, Florida East, Zone 0901, US ft).

Figure 2CC-211 East-West Model Cross Section towards southern End of the Turkey Point Cooling Canals

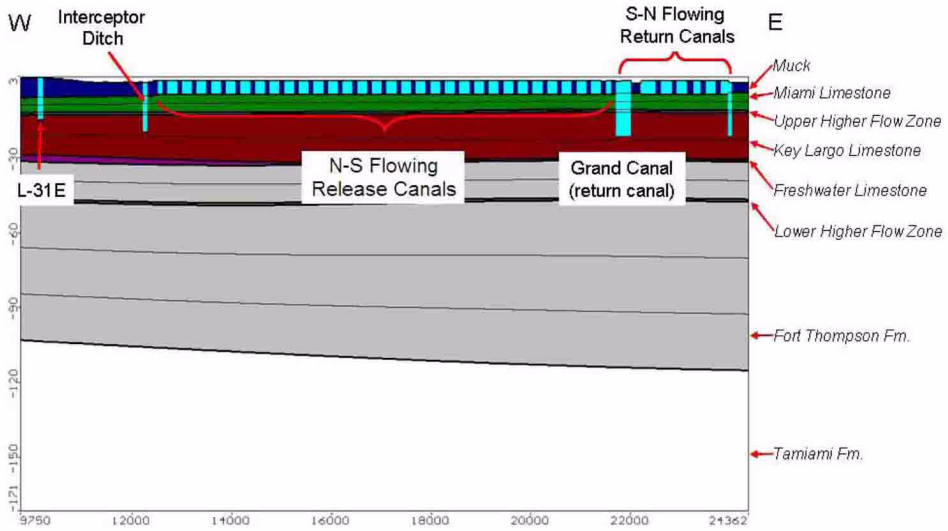

Notes: Section along Row 420, vertical exaggeration 50:1
Vertical axis represents elevation in ft NAVD 88. Horizontal axis represents model coordinates in ft. Model origin at easting 852766, northing 362512 (in State Plant Coordinates, North American Datum of 1983/Adjustment of 1990, Florida East, Zone 0901, US ft).

Figure 2CC-212 South-North Model Cross Section along Return Canal of Turkey Point Cooling Canals

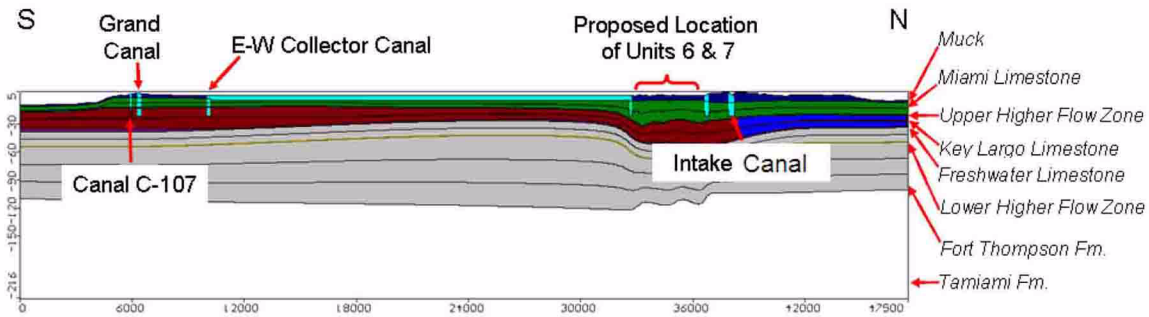

Notes: Section along Column 280, vertical exaggeration 50:1.
Vertical axis represents elevation in ft NAVD 88. Horizontal axis represents model coordinates in ft. Model origin at easting 852766, northing 362512 (in State plane Coordinates, North American Datum of 1983/Adjustment of 1990, Florida East, Zone 0901, US ft).

Figure 2CC-213 Cooling Canals Water Balance

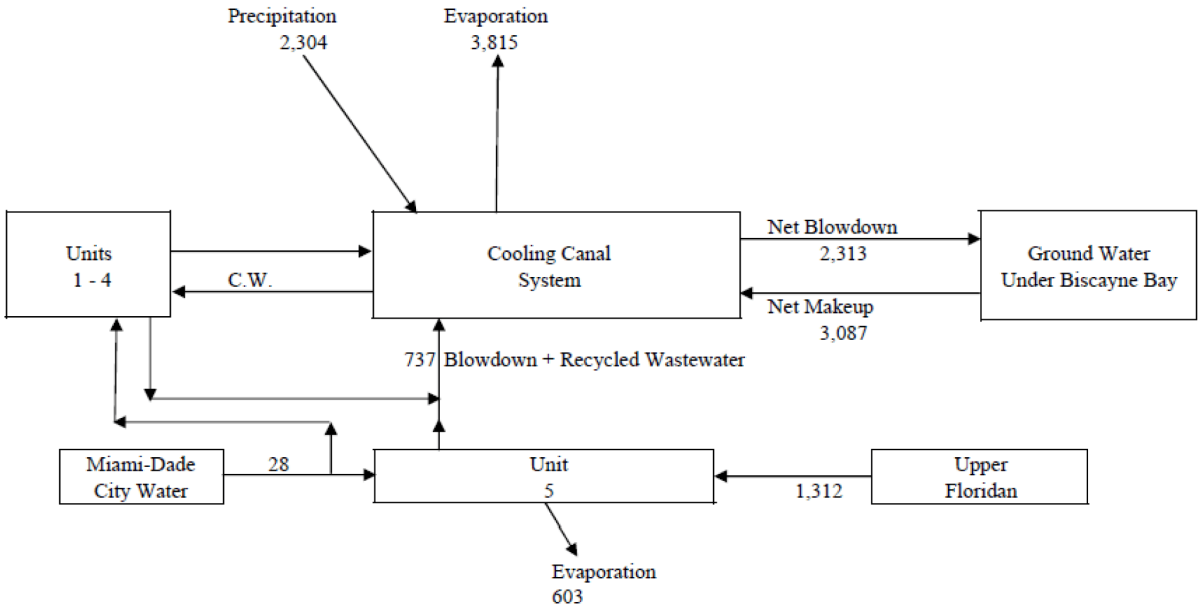

Note: Units in acre-ft/month

Figure 2CC-214 Extent of Freshwater Limestone and Key Largo Limestone in Model Layer 7

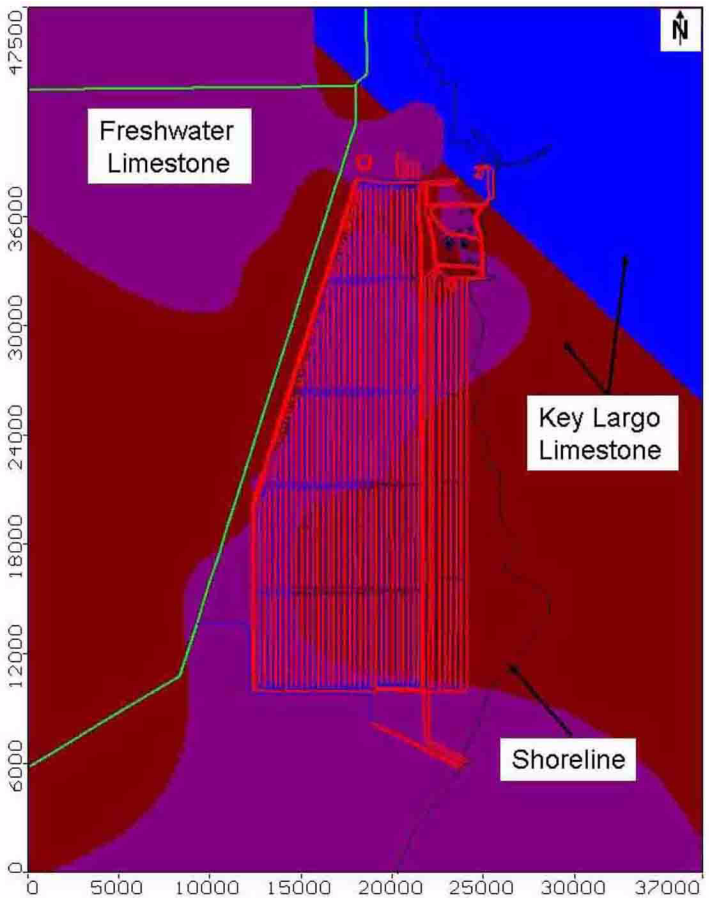

Note: Vertical and horizontal axes represent model coordinates in ft. Model origin at easting 852766, northing 362512 (in State Plane Coordinates, North American Datum of 1983/Adjustment of 1990, Florida East, Zone 0901, US ft).

Figure 2CC-215 Material Distribution in Biscayne Bay

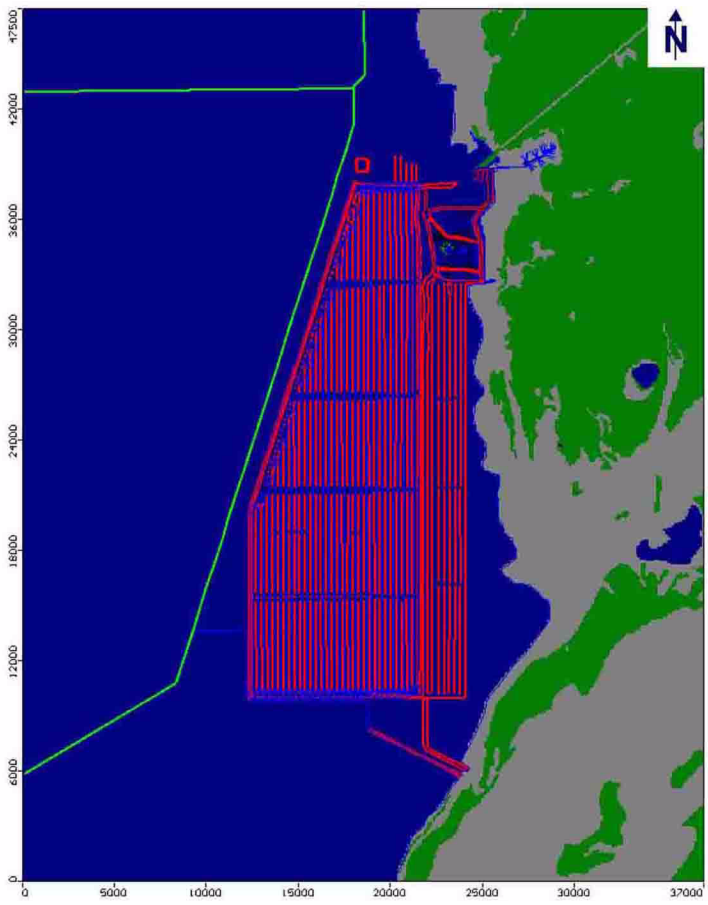

Notes: Blue = Muck. Green = Miami Limestone. Grey = Offshore Sediment.
Vertical and horizontal axes represent model coordinates in ft. Model origin at easting 852766, northing 362512 (in State Plane Coordinates, North American Datum of 1983/Adjustment of 1990, Florida East, Zone 0901, US ft).

Figure 2CC-216 Model Calibration — Delineation of Hydraulic Conductivity Zones in the Key Largo Limestone

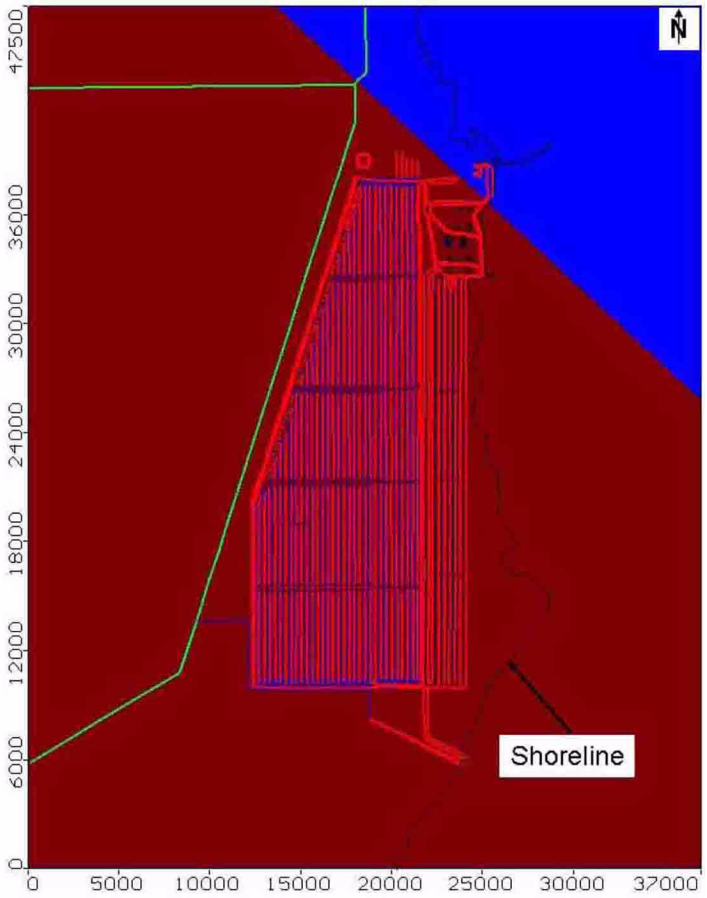

Legend: Dark Red = Key Largo Limestone Southwest. Blue = Key Largo Limestone Northeast. Green Lines = SFWMD Canals.

Note: Vertical and horizontal axes represent model coordinates in ft. Model origin at easting 852766, northing 362512 (in State Plane Coordinates, North American Datum of 1983/Adjustment of 1990, Florida East, Zone 0901, US ft)

Figure 2CC-217 Model Calibration — Layout of Pumping Well and Observation Well Clusters for Pumping Tests PW-7L and PW-7U

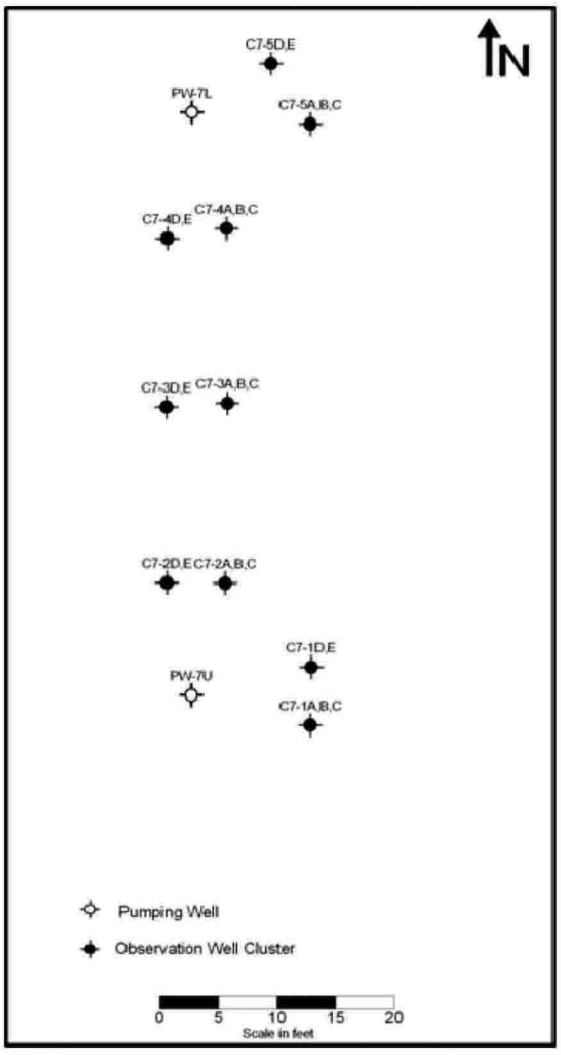

Figure 2CC-218 Grid Refinement in Vicinity of Unit 7 Reactor Footprint

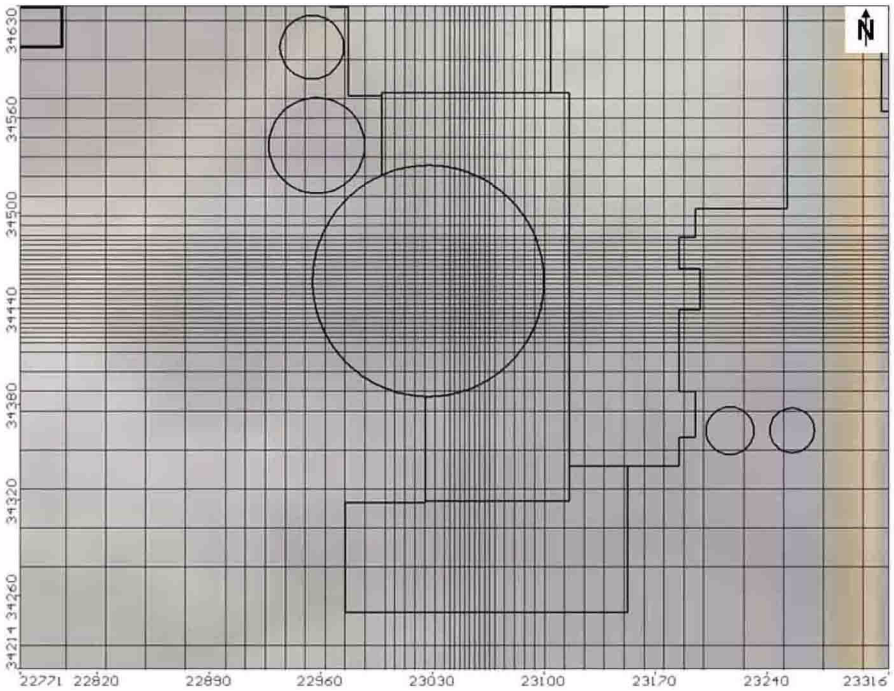

Notes: Black lines represent Unit 7 reactor building and associated structures.
Vertical and horizontal axes represent model coordinates in ft. Model origin at easting 852766, northing 362512 (in State Plane Coordinates, North American Datum of 1983/Adjustment of 1990, Florida East, Zone 0901, US ft).

Figure 2CC-219 Test Well PW-7L and Related Observation Wells

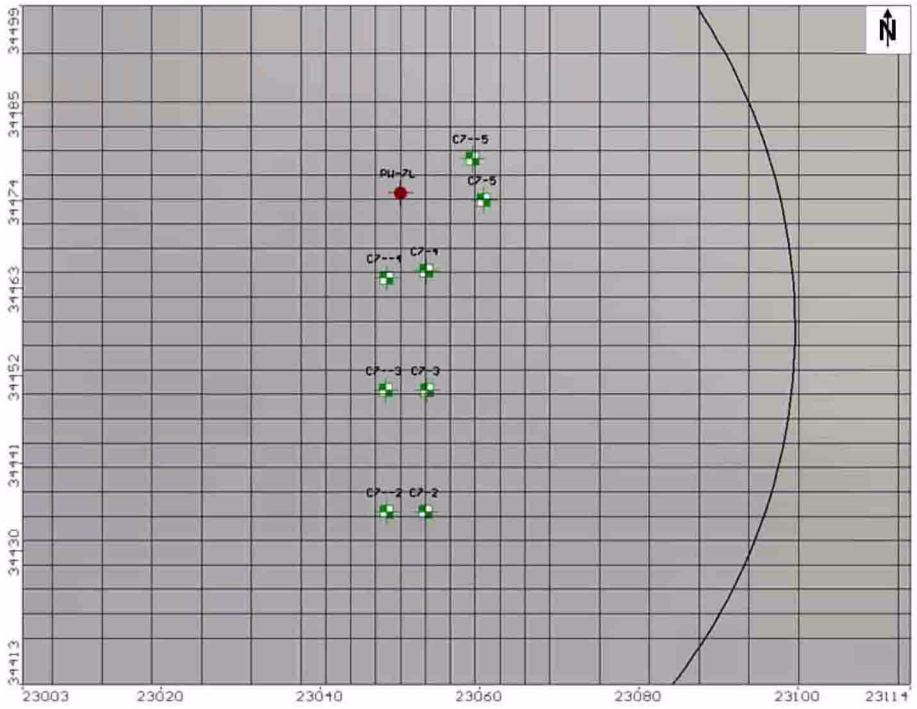

Notes: Red symbol = pumping well. Green symbol = observation well. Black line represents eastern edge of Unit 7 reactor building.
Vertical and horizontal axes represent model coordinates in ft. Model origin at easting 852766, northing 362512 (in State Plane Coordinates, North American Datum of 1983/Adjustment of 1990, Florida East, Zone 0901, US ft).

Figure 2CC-220 Test Well PW-7L: Observed Versus Calculated Drawdowns

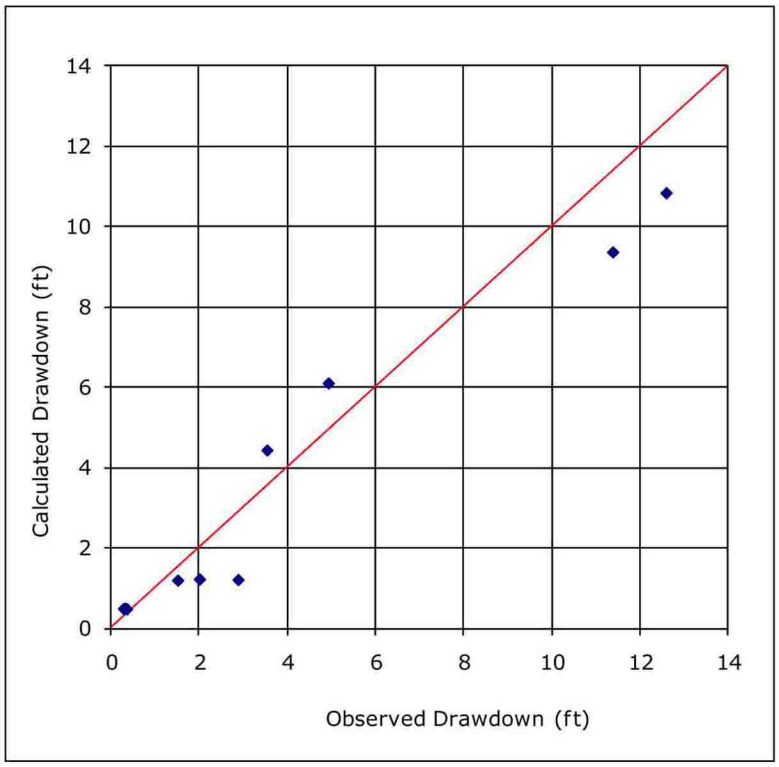

Figure 2CC-221 Model Calibration — Pumping and Monitoring Wells Layout for Pumping Test PW-1

Figure 2CC-222 Model Calibration — Finite Difference Grid and Well Layout for Pumping Test PW-1

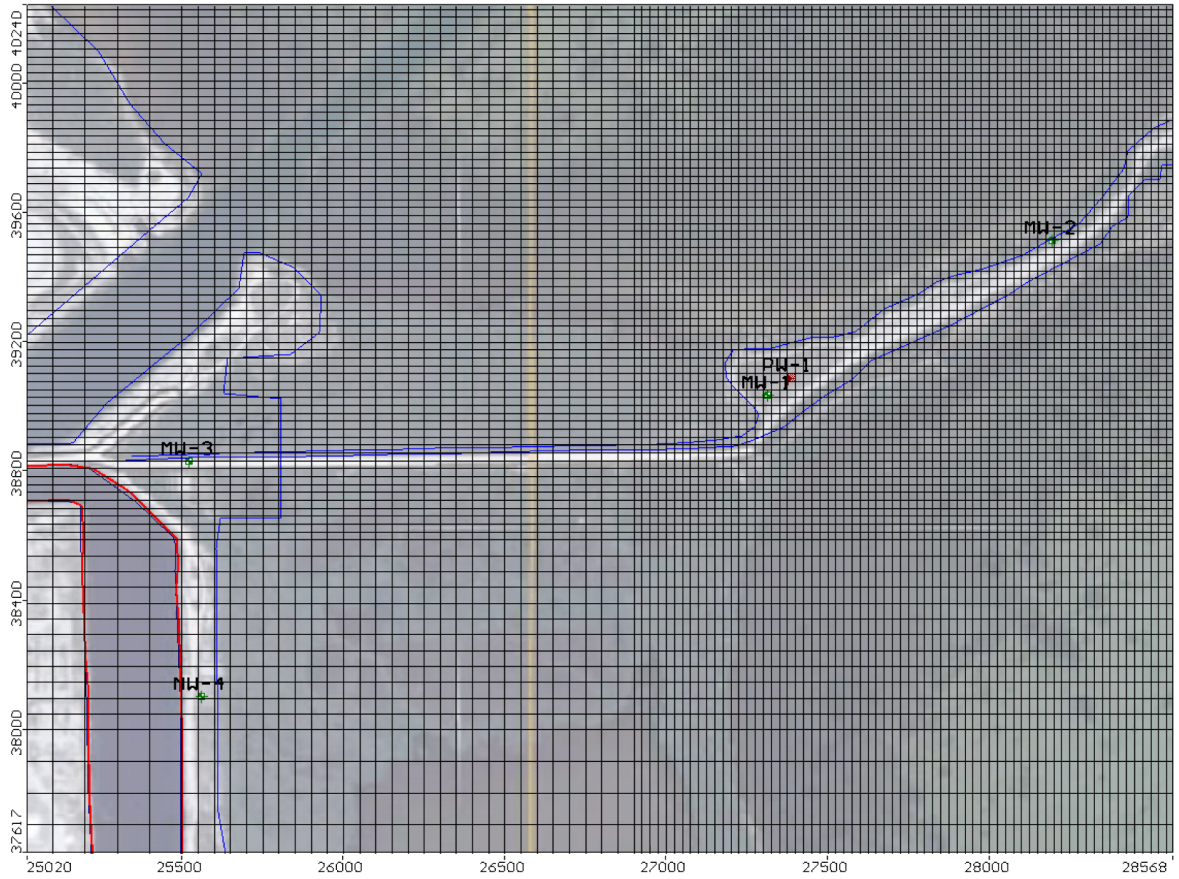

Note: Blue line = shoreline. Red line = CCS outline. Red symbol = pumping well. Green symbol = observation well. Radial collector well locations shown on Figure 2CC-242.
Vertical and horizontal axes represent model coordinates in ft. Model origin of easting 852766, northing 362512 (in State Plane Coordinates, North American Datum of 1983/Adjustment of 1990. Florida East, Zone 0901. US ft.)

Figure 2CC-223 Test Well PW-1: Observed versus Calculated Drawdowns

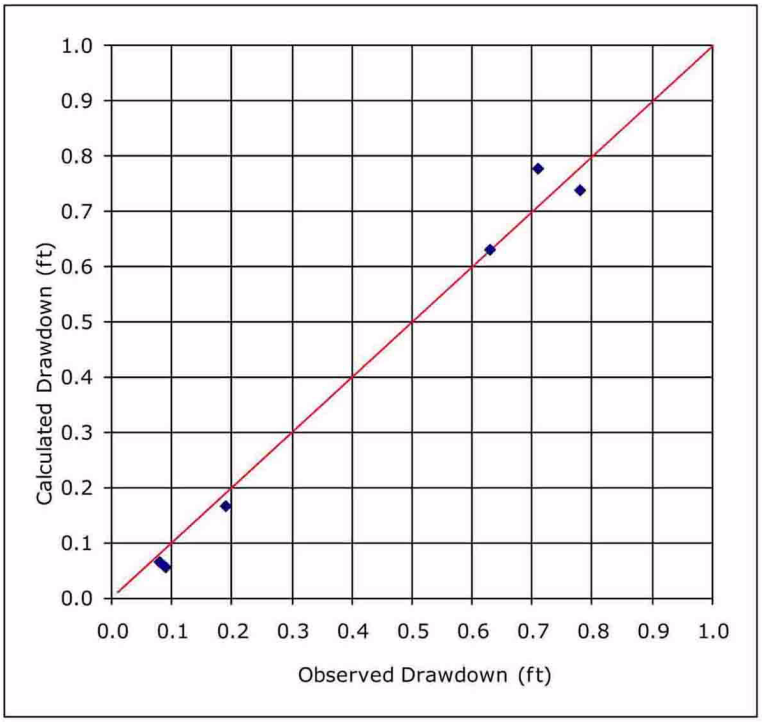

Figure 2CC-224 Model Calibration — Finite Difference Grid and Well Layout for Test PW-7U

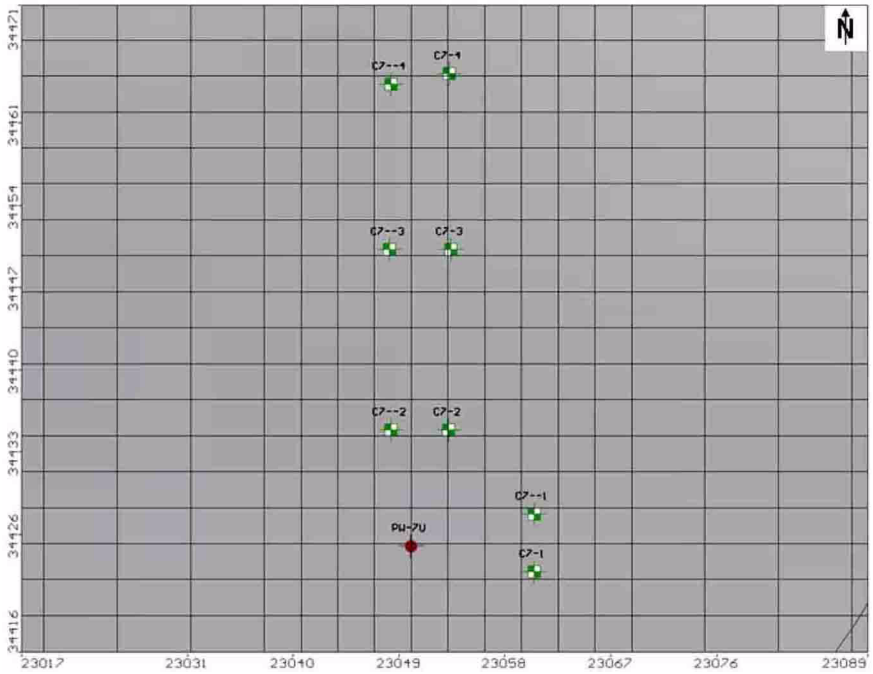

Notes: Red symbol = pumping well. Green symbol = observation well.
Vertical and horizontal axes represent model coordinates in ft. Model origin at easting 852766, northing 362512 (in State Plane Coordinates, North American Datum of 1983/Adjustment of 1990, Florida East, Zone 0901, US ft).

Figure 2CC-225 Test Well PW-7U: Observed versus Calculated Drawdowns

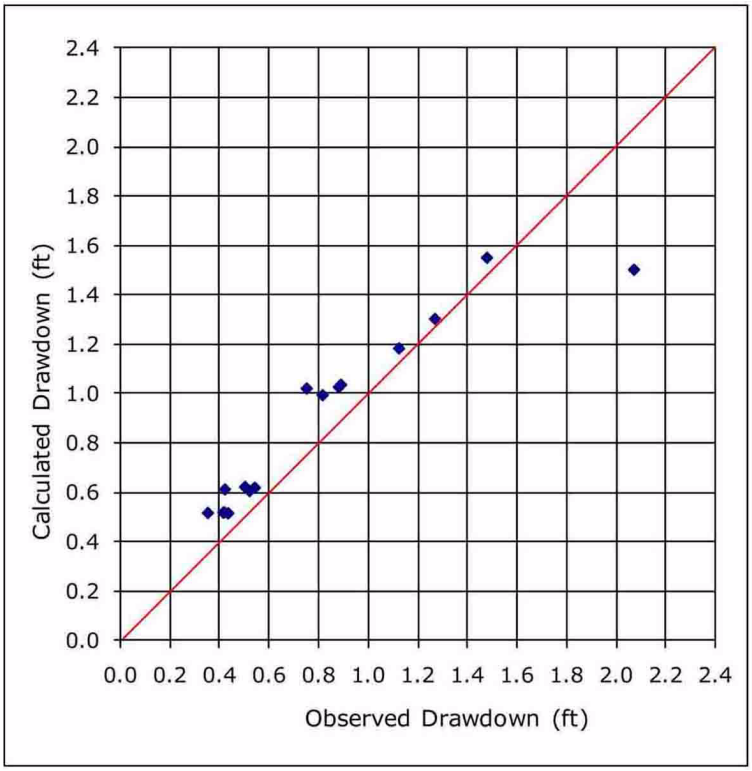

Figure 2CC-226 Simulated Groundwater Contours — Model Layer 1 — Onshore Muck and Offshore Sand/Sediments and Miami Limestone

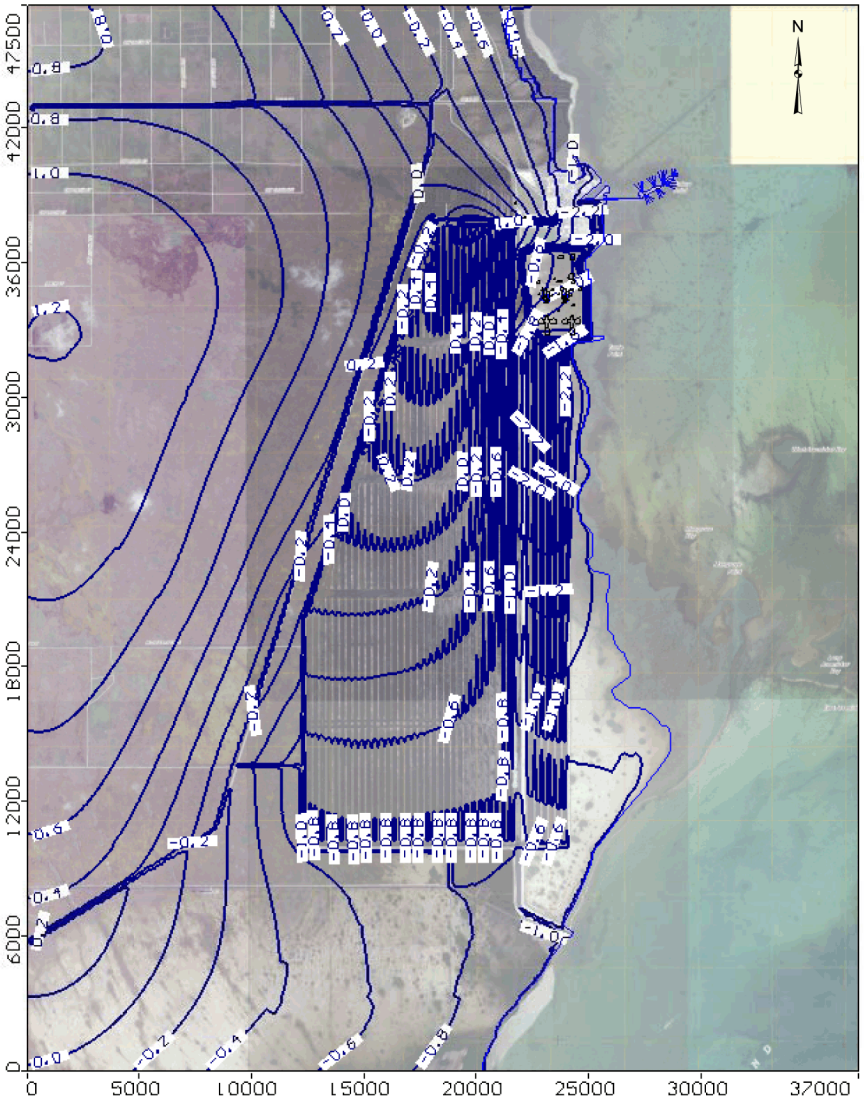

Legend: Contour interval is 0.2 ft NAVD 88.
Notes: Light yellow portion in top right is where aerial imagery is not available. Vertical and horizontal axes represent model coordinates in ft. Model origin at easting 852766, northing 362512 (in State Plane Coordinates, North American Datum of 1983/Adjustment of 1990, Florida East, Zone 0901, US ft).

Figure 2CC-227 Simulated Groundwater Contours — Model Layer 3 — Miami Limestone

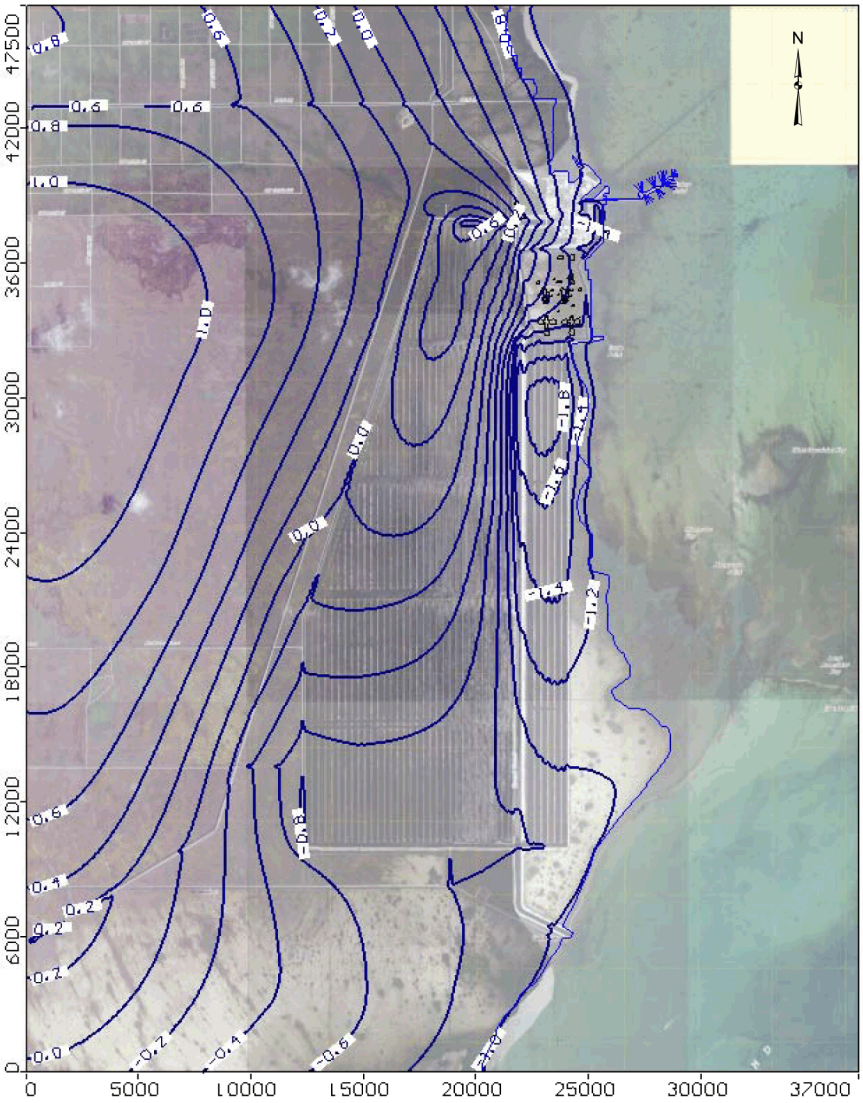

Legend: Contour interval is 0.2 ft NAVD 88
Notes: Light yellow portion in top right is where aerial imagery is not available. Vertical and horizontal axes represent model coordinates in ft. Model origin at easting 852766, northing 362512 (in State Plane Coordinates, North American Datum of 1983/Adjustment of 1990, Florida East, Zone 0901, US ft).

Figure 2CC-228 Simulated Groundwater Contours — Model Layer 4 — Upper Higher Flow Zone

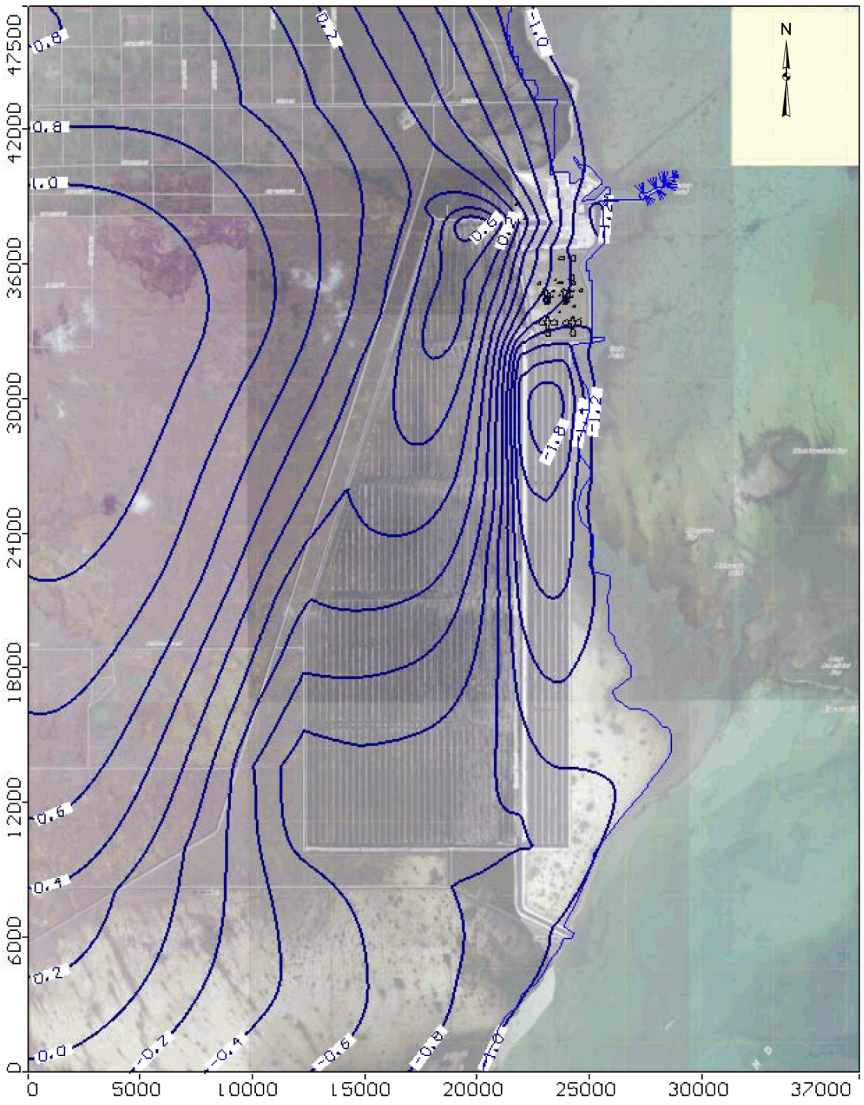

Legend: Contour interval is 0.2 ft NAVD 88
Notes: Light yellow portion in top right is where aerial imagery is not available. Vertical and horizontal axes represent model coordinates in ft. Model origin at easting 852766, northing 362512 (in State Plane Coordinates, North American Datum of 1983/Adjustment of 1990, Florida East, Zone 0901, US ft).

Figure 2CC-229 Simulated Groundwater Contours — Model Layer 5 — Key Largo Limestone

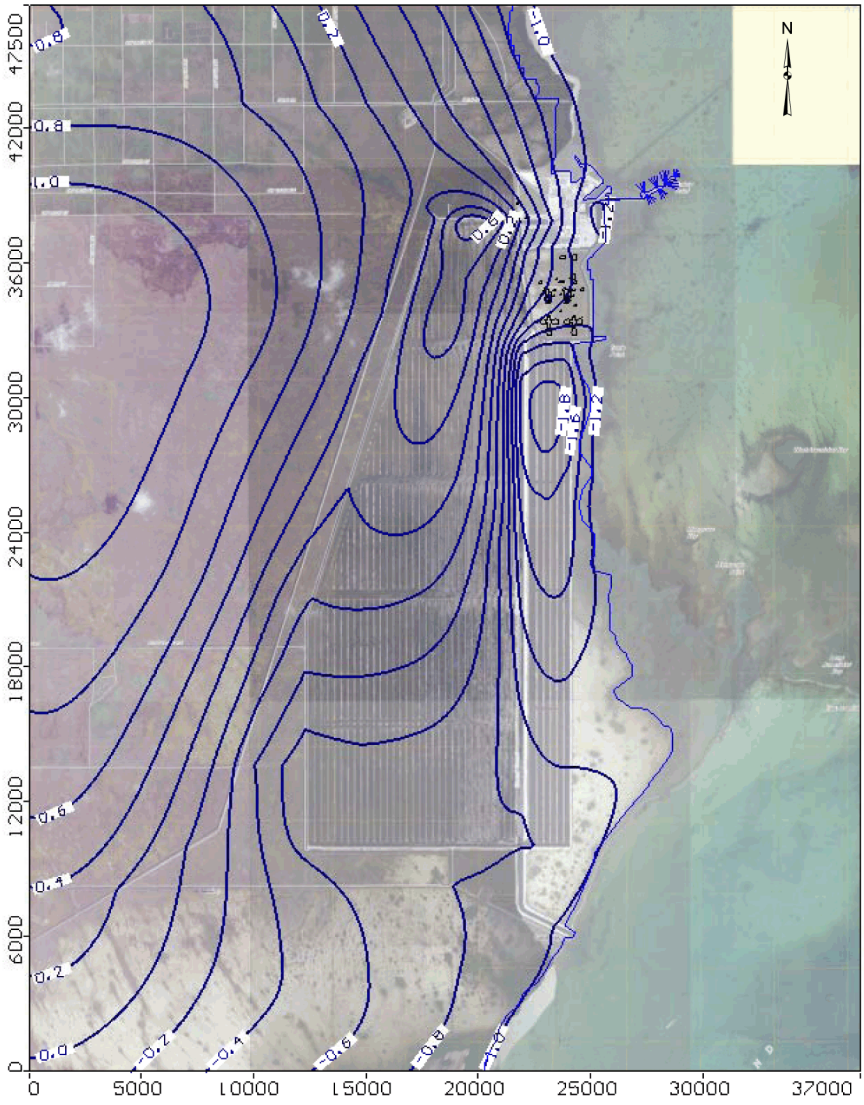

Legend: Contour interval is 0.2 ft NAVD 88
Notes: Light yellow portion in top right is where aerial imagery is not available. Vertical and horizontal axes represent model coordinates in ft. Model origin at easting 852766, northing 362512 (in State Plane Coordinates, North American Datum of 1983/Adjustment of 1990, Florida East, Zone 0901, US ft).

Figure 2CC-230 Simulated Groundwater Contours — Model Layer 7 — Freshwater Limestone

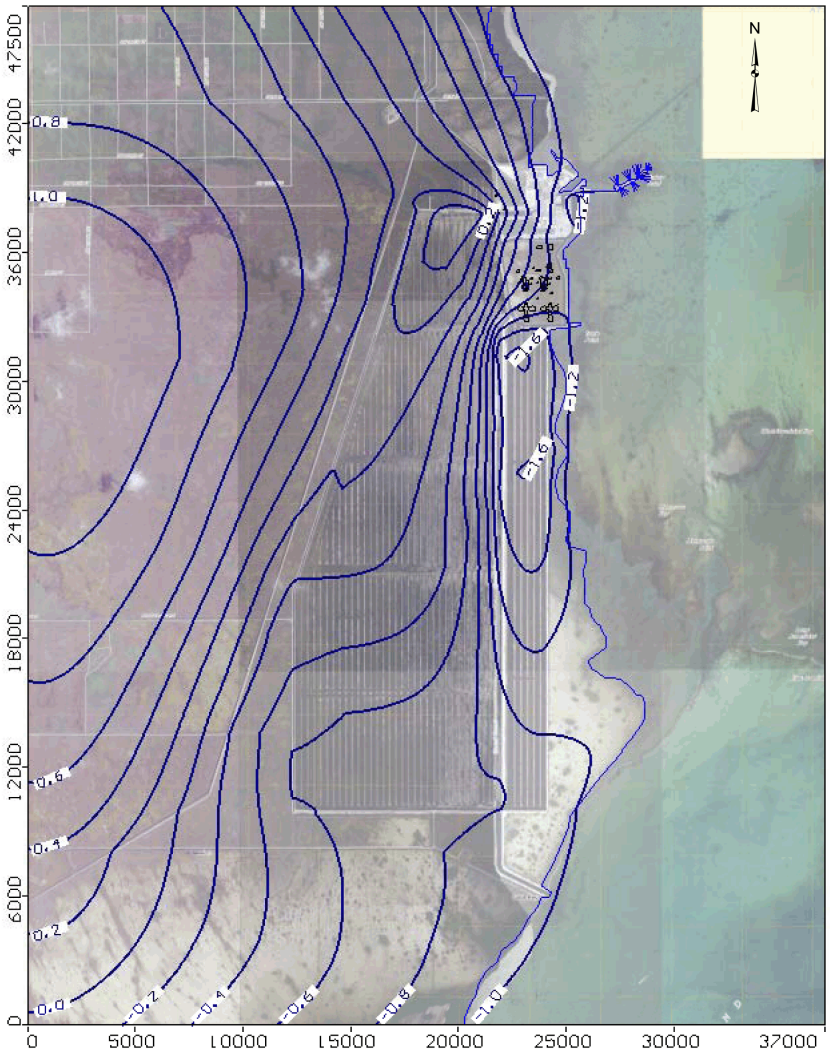

Legend: Contour interval is 0.2 ft NAVD 88
Notes: Light yellow portion in top right is where aerial imagery is not available. Vertical and horizontal axes represent model coordinates in ft. Model origin at easting 852766, northing 362512 (in State Plane Coordinates, North American Datum of 1983/Adjustment of 1990, Florida East, Zone 0901, US ft).

Figure 2CC-231 Simulated Groundwater Contours — Model Layer 9 — Fort Thompson Formation

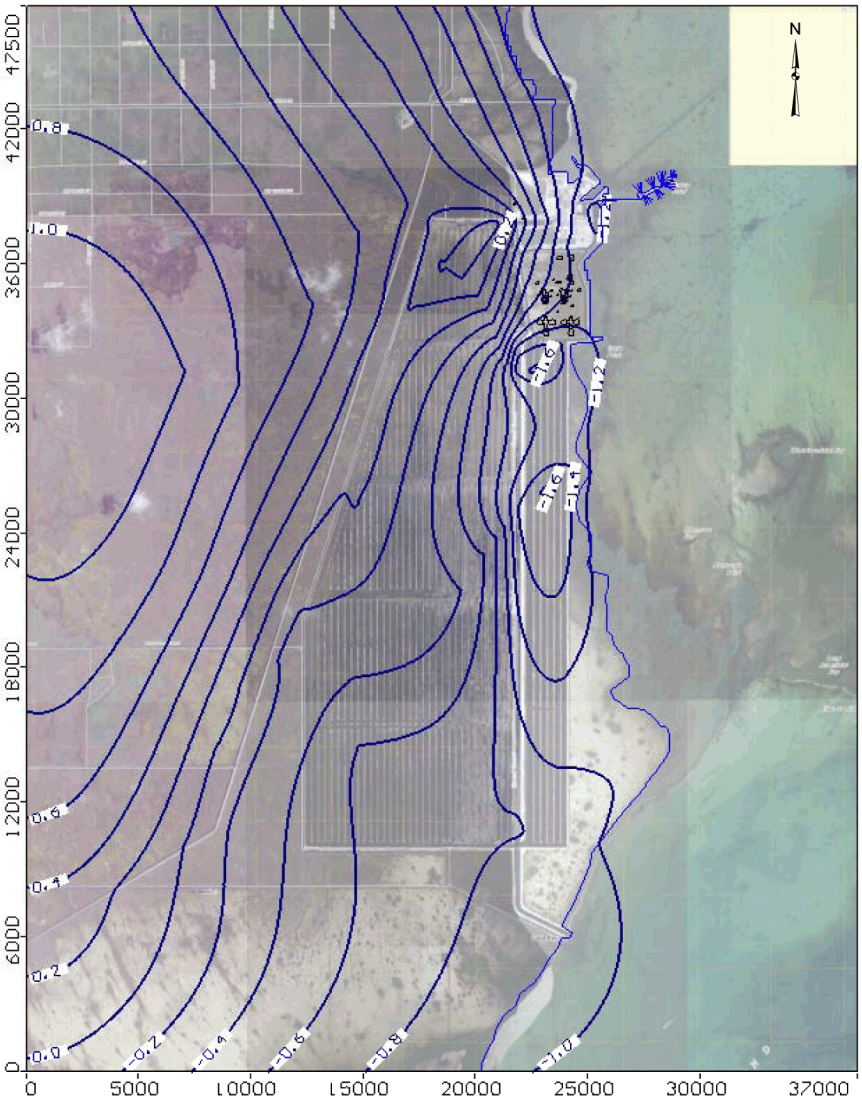

Legend: Contour interval is 0.2 ft NAVD 88
Notes: Light yellow portion in top right is where aerial imagery is not available. Vertical and horizontal axes represent model coordinates in ft. Model origin at easting 852766, northing 362512 (in State Plane Coordinates, North American Datum of 1983/Adjustment of 1990, Florida East, Zone 0901, US ft).

Figure 2CC-232 Simulated Groundwater Contours — Model Layer 10 — Lower Higher Flow Zone

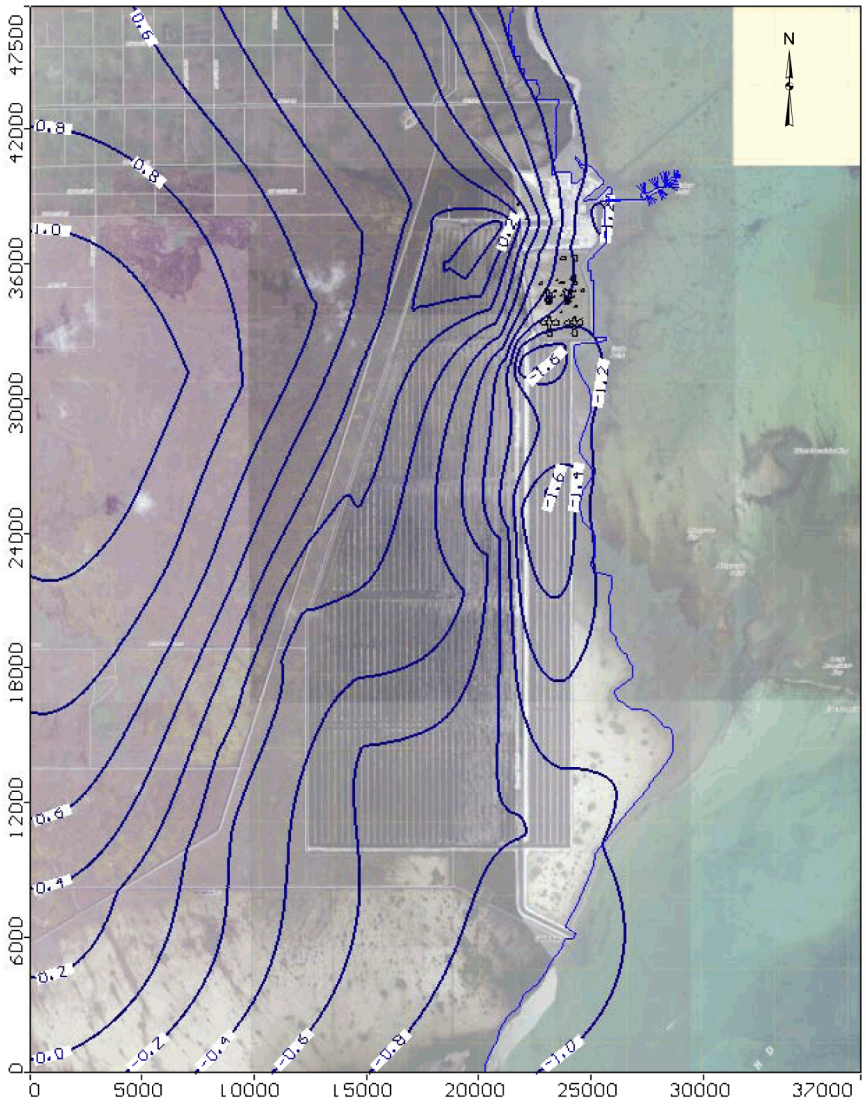

Legend: Contour interval is 0.2 ft NAVD 88
Notes: Light yellow portion in top right is where aerial imagery is not available. Vertical and horizontal axes represent model coordinates in ft. Model origin at easting 852766, northing 362512 (in State Plane Coordinates, North American Datum of 1983/Adjustment of 1990, Florida East, Zone 0901, US ft).

Figure 2CC-233 Simulated Groundwater Contours — Model Layer 14 — Tamiami Formation

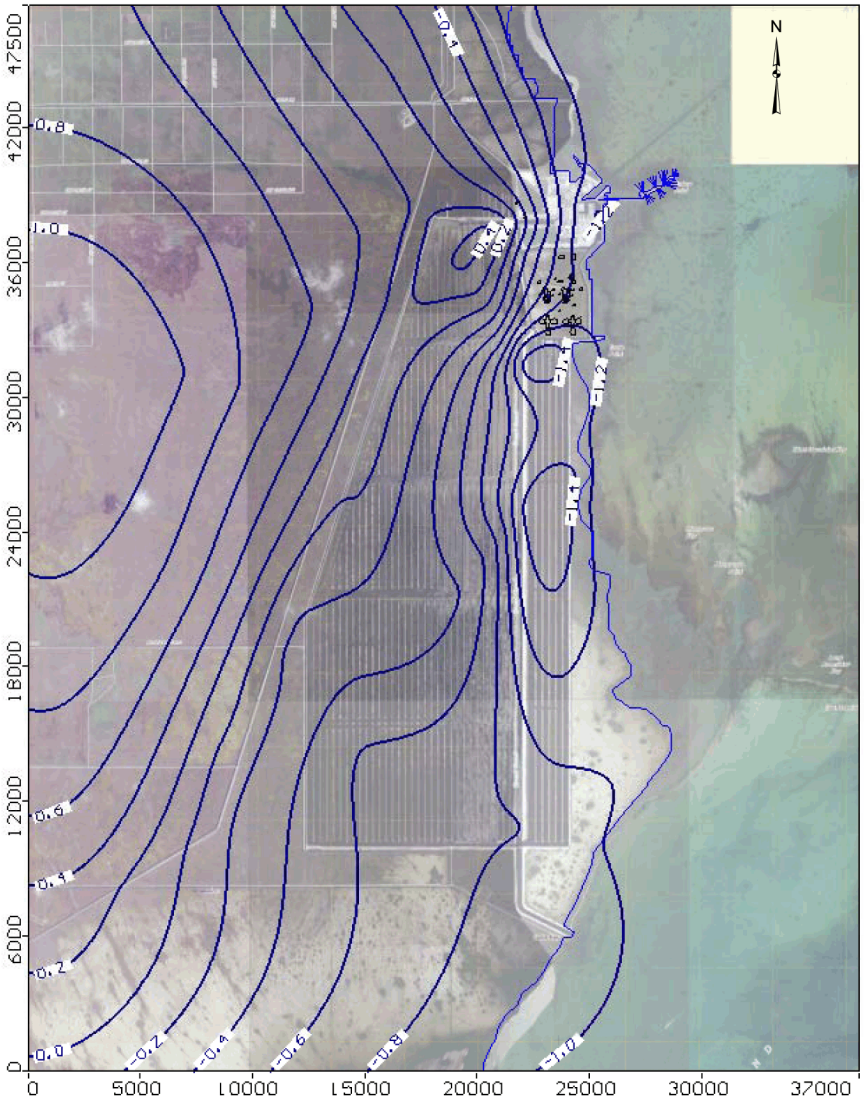

Legend: Contour interval is 0.2 ft NAVD 88
Note: Light yellow portion in top right is where aerial imagery is not available. Vertical and horizontal axes represent model coordinates in ft. Model origin at easting 852766, northing 362512 (in State Plane Coordinates, North American Datum of 1983/Adjustment of 1990, Florida East, Zone 0901, US ft).

Figure 2CC-234 Existing Cooling Canals Water Balance — Comparison with Groundwater Model

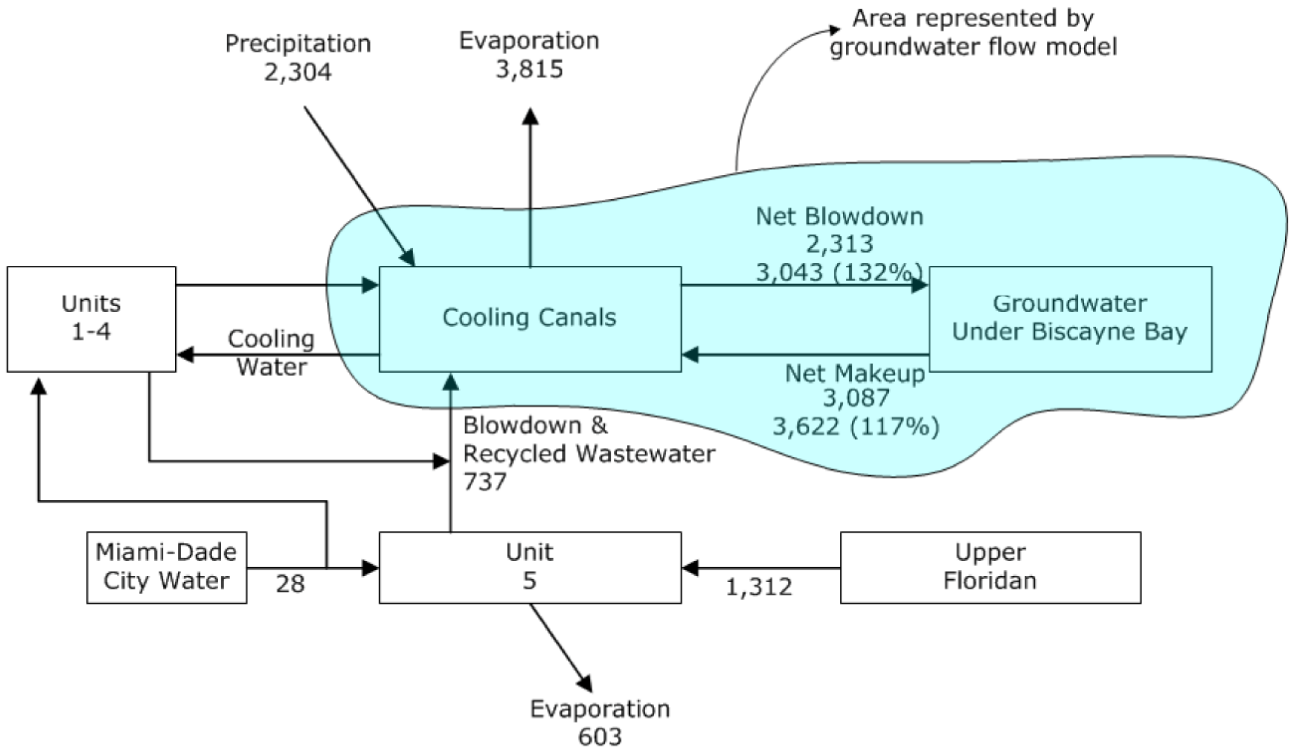

Top value is plant at full capacity from surface water model; lower value is from groundwater model at average plant conditions. Value in parentheses is percentage difference between surface water model and groundwater model.

Note: Units in acre-ft/month.

Figure 2CC-235 Model Validation — Layout of Pumping and Observation Wells for Pumping Test PW-6U

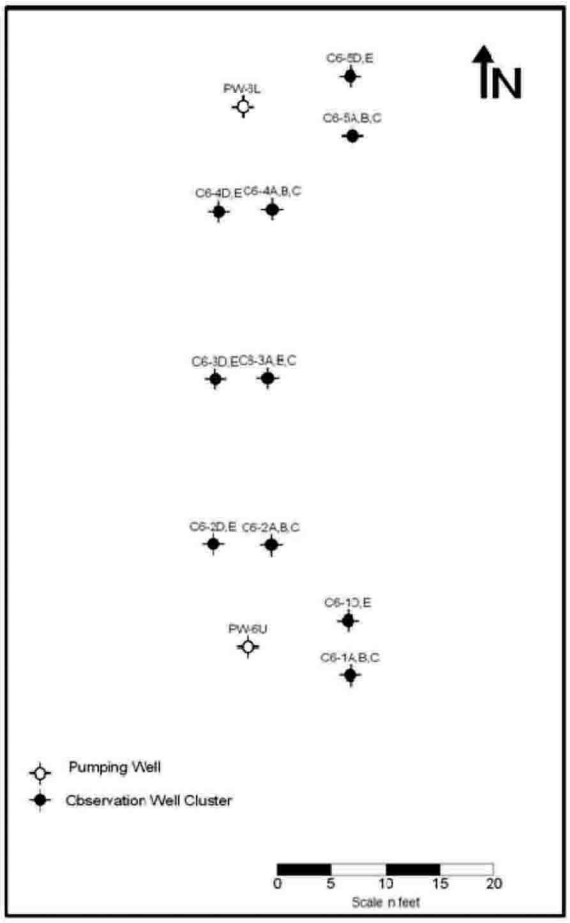

Figure 2CC-236 Test Well PW-6U: Observed versus Calculated Drawdowns

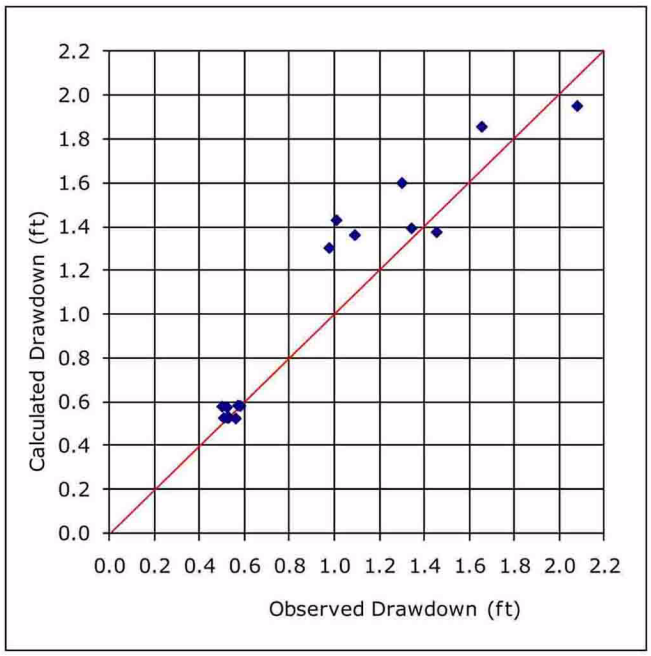

Figure 2CC-237 Location of Units 6 & 7 Construction Cut-Off Walls, Simulated Sump Pumps, and Gridlines

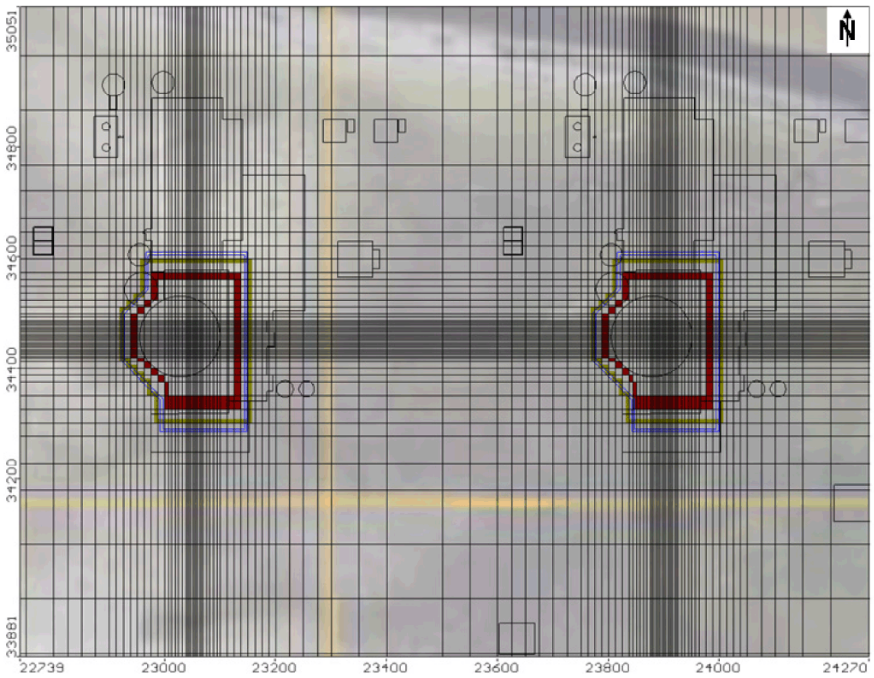

Legend: Blue lines represent reactor building and associated structures. Khaki (green) cells represent implementation of MODFLOW's HFB flow package in model to represent cut-off walls. Red cells represent sump pumps (inside cut-off walls).

Note: Vertical and horizontal axes represent model coordinates in ft. Model origin at easting 852766, northing 362512 (in State Plane Coordinates, North American Datum of 1983/Adjustment of 1990, Florida East, Zone 0901, US ft).

Figure 2CC-238 Cross Section of Model Setup for Unit 7 Excavation

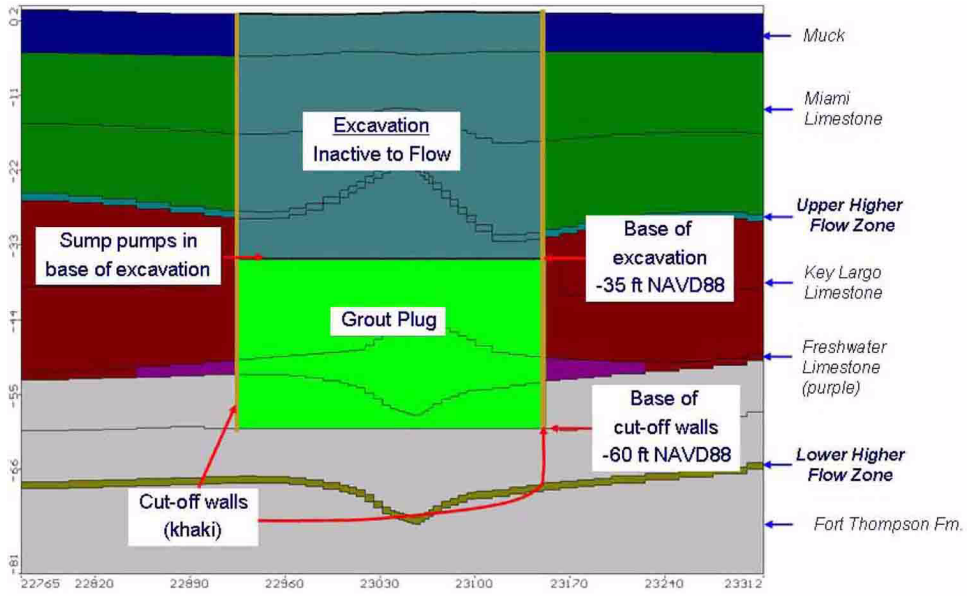

Notes: Cut-off walls extended to top of model domain for illustration only
Section Across Row 218. Vertical Exaggeration 5:1. Excavation for Unit 6 has similar configuration. Vertical axis represents elevation in ft NAVD 88. Horizontal axis represents model coordinates in ft. Model origin at easting 852766, northing 362512 (in State Plane Coordinates, North American Datum of 1983/ Adjustment of 1990, Florida East, Zone 0901, US ft).

Figure 2CC-239 Grouting Holes Spacing and Frequency during Proposed Grouting Method

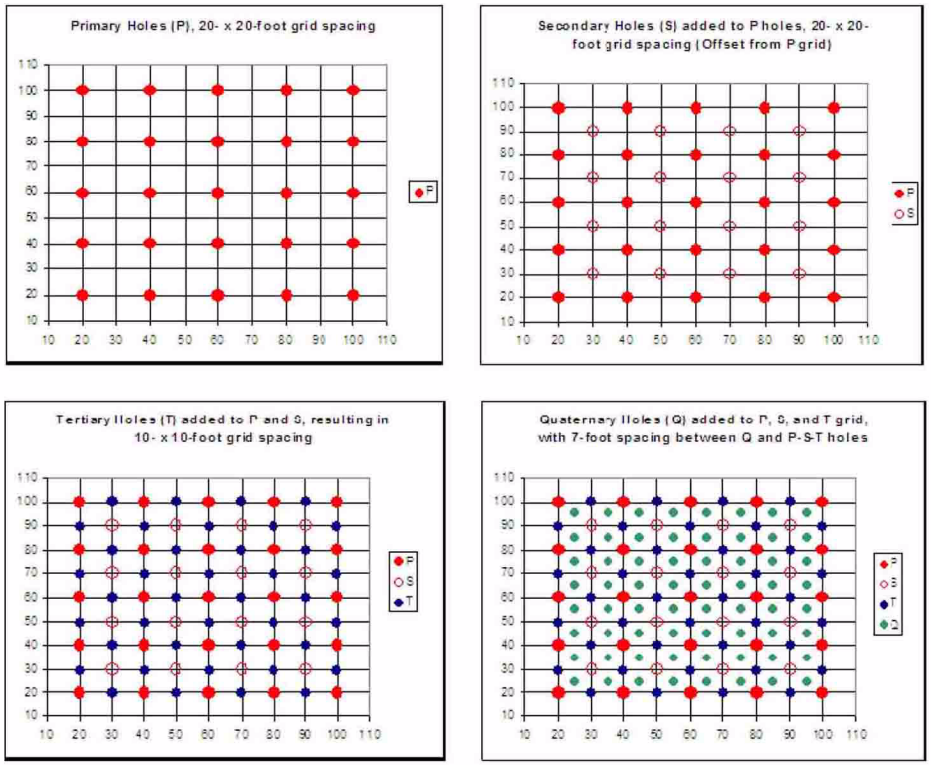

Figure 2CC-240 Comparison of Pumping Rates under Different Grouting Scenarios

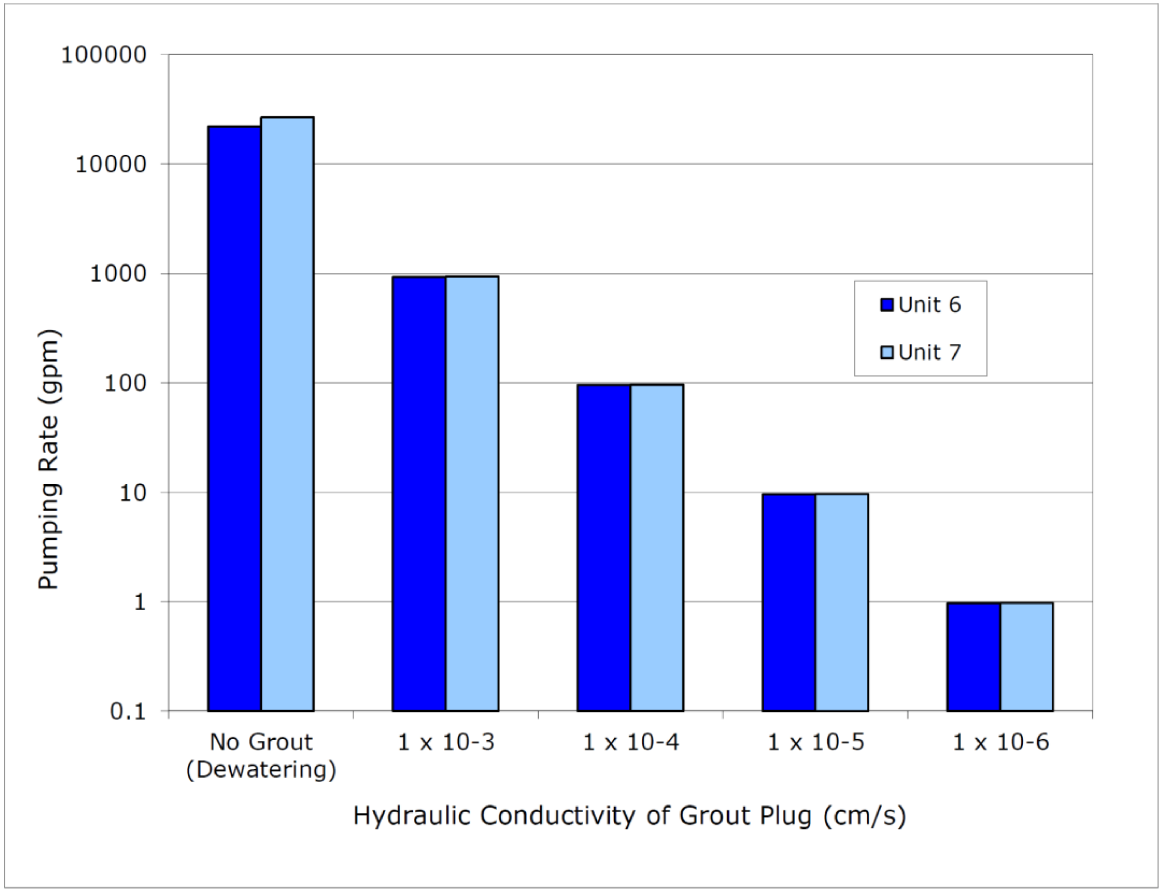

Figure 2CC-241 Phase 1 Post-Construction Recharge Zones for Units 6 & 7

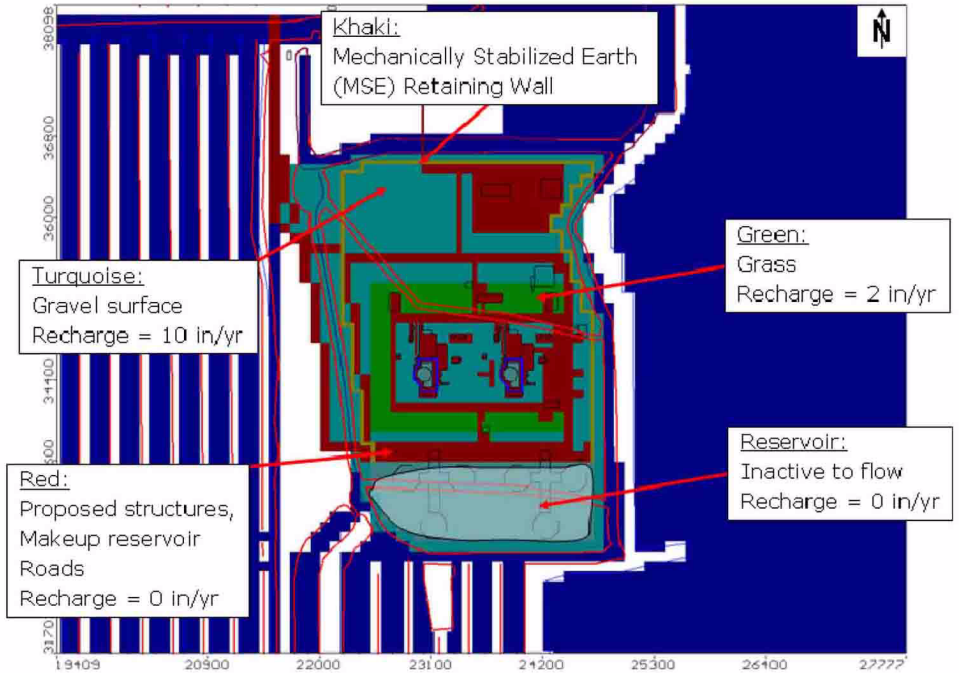

Note: Vertical and horizontal axes represent model coordinates in ft. Model origin at easting 852766, northing 362512 (in State Plane Coordinates, North American Datum of 1983/Adjustment of 1990, Florida East, Zone 0901, US ft).

Figure 2CC-242 Location of Radial Collector Wells and Laterals, with Finite-Difference Grid and Pumping Well Locations

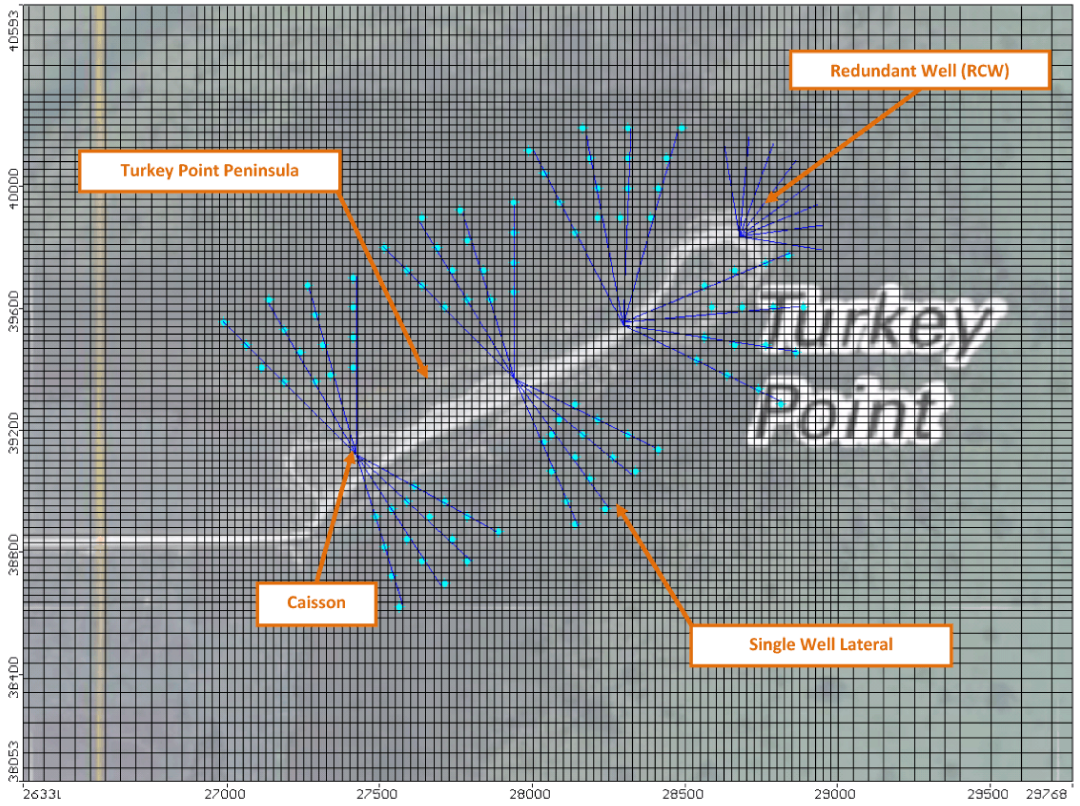

Note: Dark blue lines = radial collector well arms. Light blue symbol = pumping well node.

Figure 2CC-243 Potentiometric Surface within the Upper Higher Flow Zone during Radial Collector Well Simulations

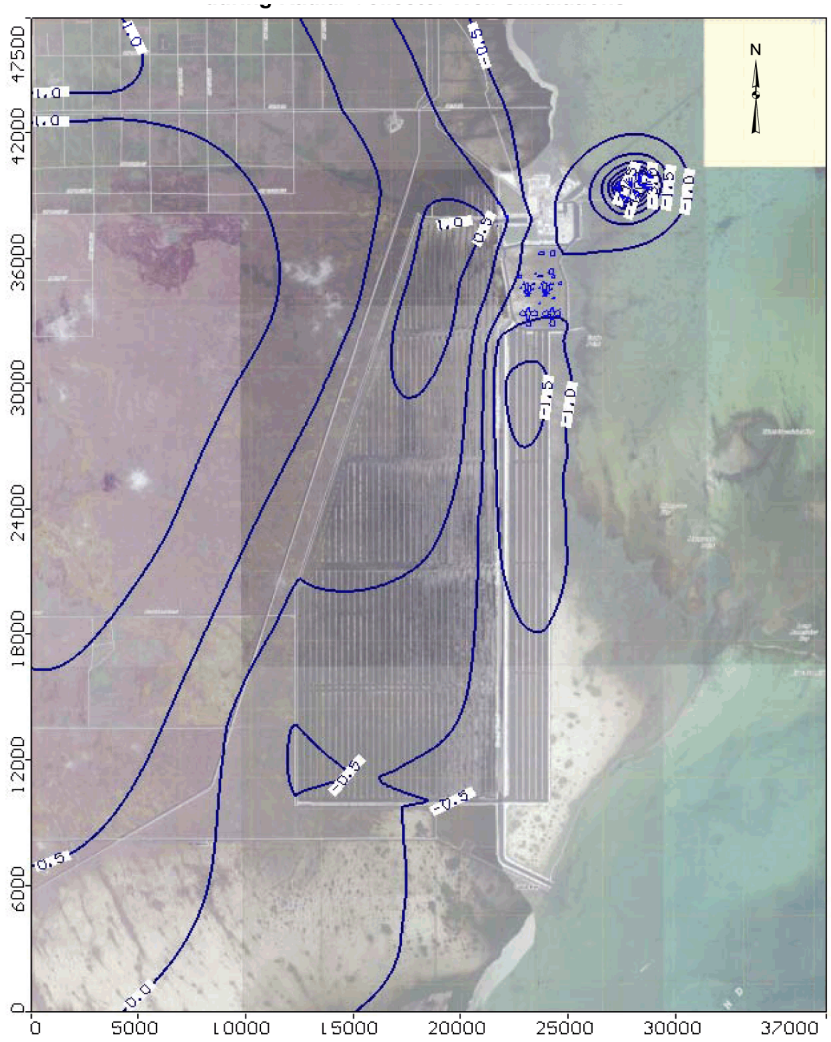

Legend: Blue lines are equipotentials in 0.5 ft increments.
Notes: The Upper Higher Flow Zone is above the Key Largo Limestone and is the zone from which the RCW system is pumped. Light yellow portion in top right is where aerial imagery is not available. Vertical and horizontal axes represent model coordinates in ft. Model origin at easting 852766, northing 362512 (in State Plane Coordinates, North American Datum of 1983/Adjustment of 1990, Florida East, Zone 0901, US ft).

Figure 2CC-244 Head Contours in Layer 1 during Radial Collector Well Simulations

Legend: Blue lines are equipotentials in 1 foot increments.
Notes: Light yellow portion in top right is where aerial imagery is not available.

Vertical and horizontal axes represent model coordinates in ft. Model origin at easting 852766, northing 362512 (in State Plane Coordinates, North American Datum of 1983/Adjustment of 1990, Florida East, Zone 0901, US ft).

Figure 2CC-245 Cross Section through Turkey Point Peninsula Showing Groundwater Contours Resulting from Operation of the RCW System

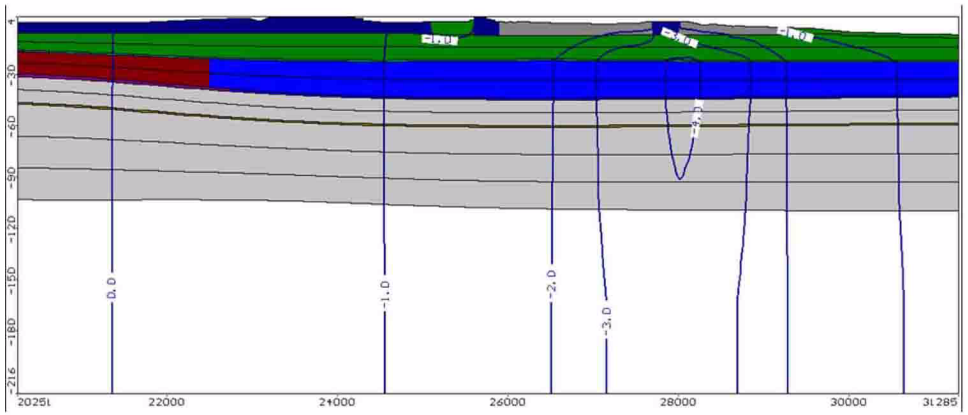

Legend: Blue lines are equipotentials in 1 foot increments.

Notes: Section Across Row 120, Vertical Exaggeration = 20:1
Vertical axis represents elevation in ft NAVD 88. Horizontal axis represents model coordinates in ft. Model origin at easting 852766, northing 362512 (in State Plane Coordinates, North American Datum of 1983/Adjustment of 1990, Florida East, Zone 0901, US ft).

Figure 2CC-246 RCW Drawdown within the Top Layer

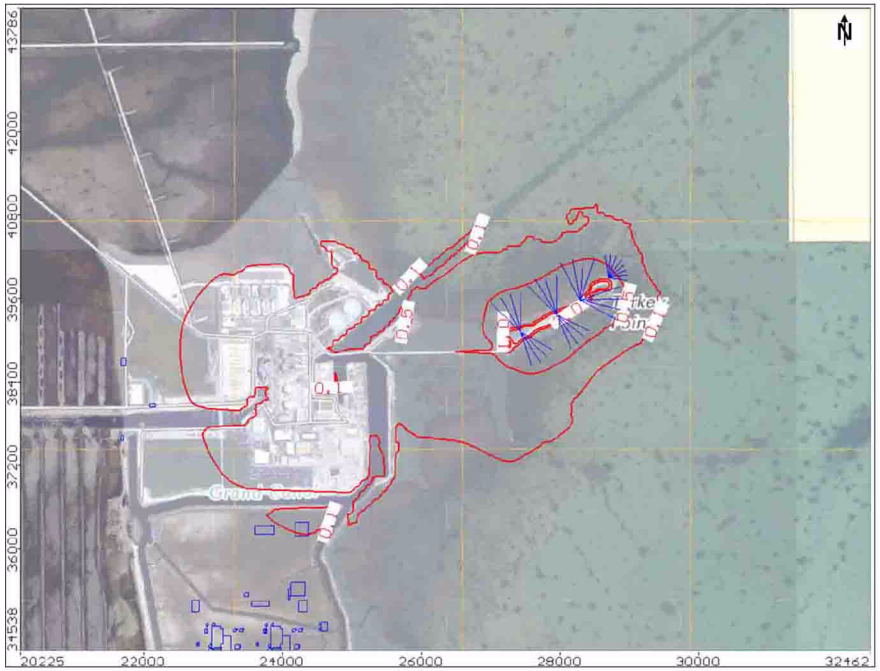

Notes: Thin red line = 0.1, 0.5, 1.0, and 2.0 foot drawdown contours. Light yellow portion in top right is where aerial imagery is not available.

Vertical and horizontal axes represent model coordinates in ft. Model origin at easting 852766, northing 362512 (in State Plane Coordinates, North American Datum of 1983/Adjustment of 1990, Florida East, Zone 0901, US ft).

Figure 2CC-247 RCW Drawdown within the Pumped Layer (Upper Higher Flow Zone)

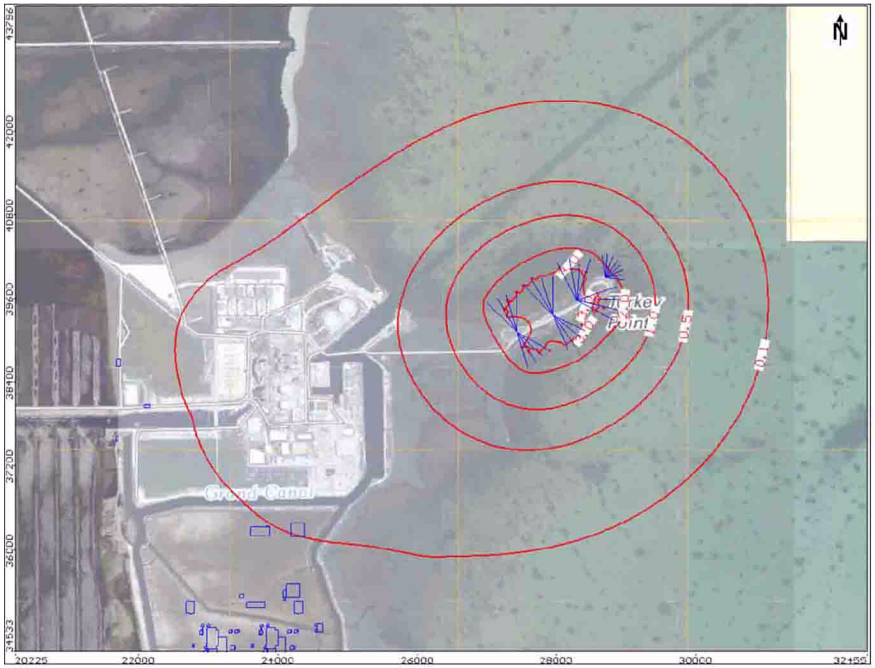

Notes: Thin red line = 0.1, 0.5, 1.0, 2.0, and 3.0 foot drawdown contours. Light yellow portion in top right is where aerial imagery is not available. Approximate elevation of Upper Higher Flow Zone underneath Turkey Point Peninsula is -22 ft NAVD 88.

Vertical and horizontal axes represent model coordinates in ft. Model origin at easting 852766, northing 362512 (in State Plane Coordinates, North American Datum of 1983/Adjustment of 1990, Florida East, Zone 0901, US ft).

Figure 2CC-248 Origin of Flow to the RCW System (Layer 1)

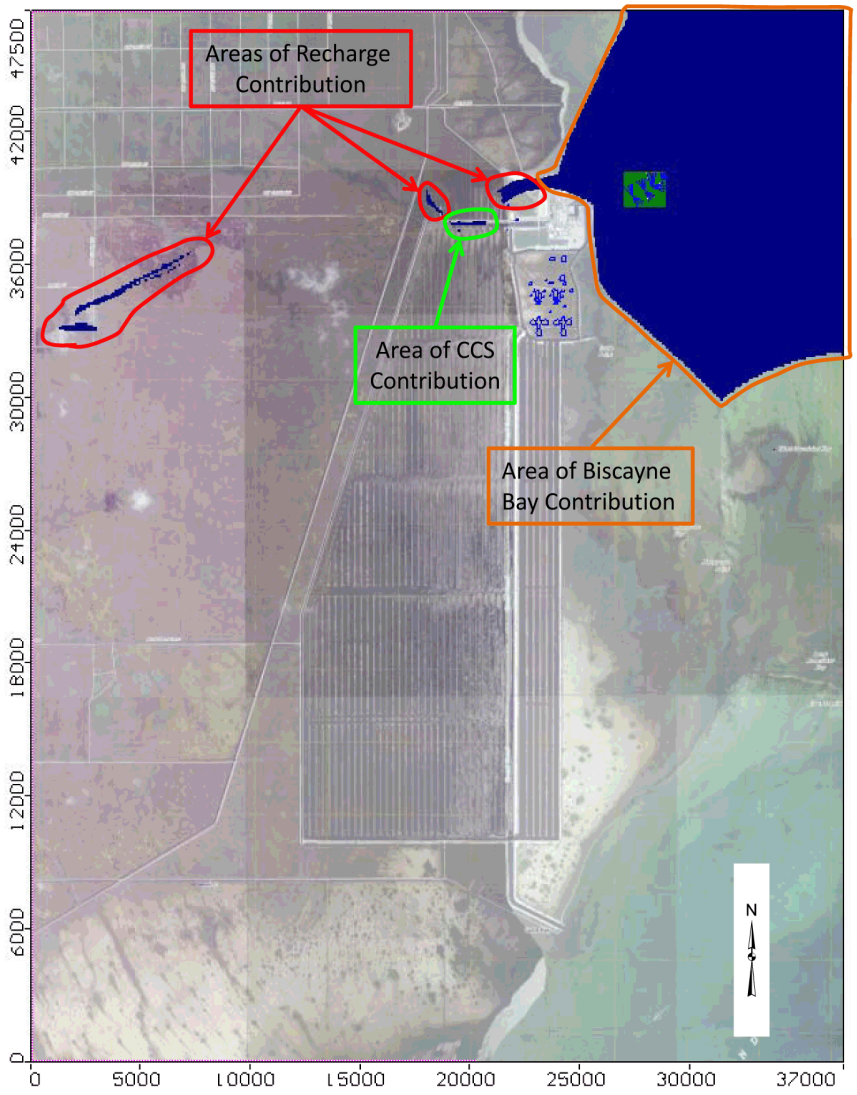

Note: Blue areas show origins of water contributing to RCW system.

Figure 2CC-249 Origin of Flow to the RCW System (Layer 2)

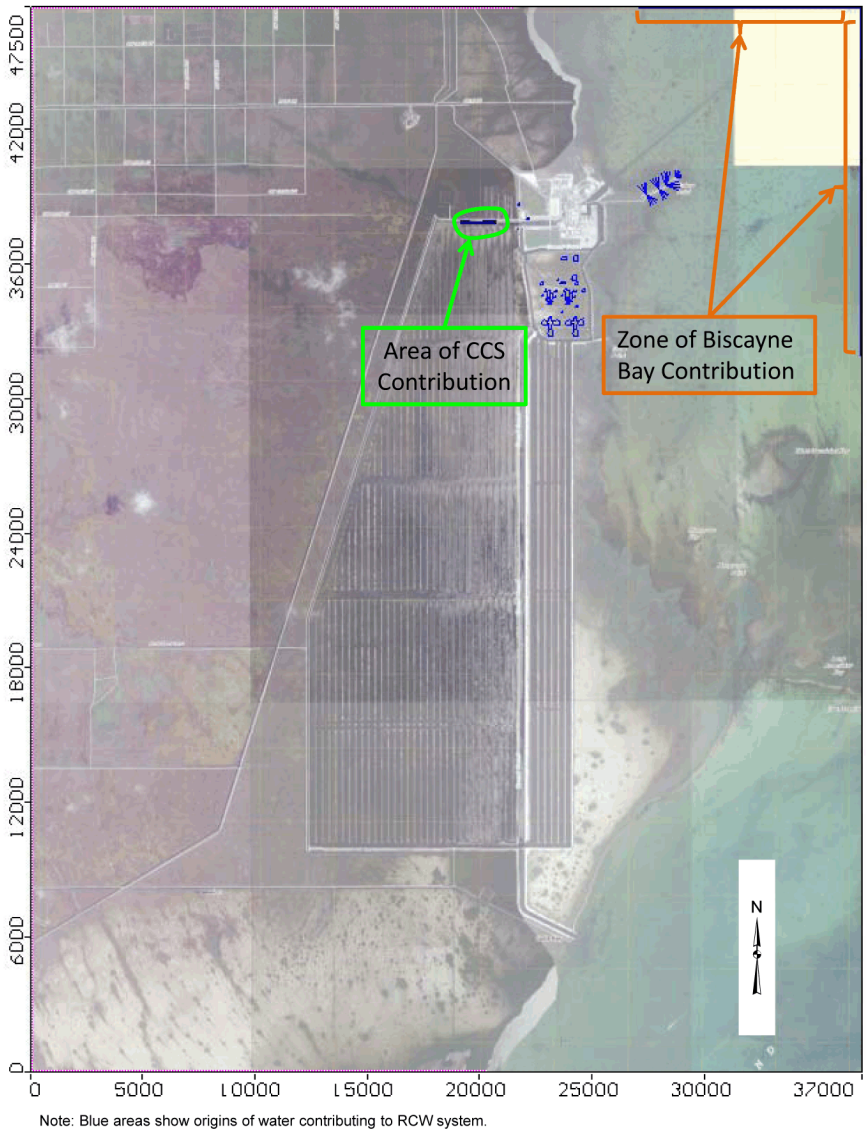

Note: Blue areas show origins of water contributing to RCW system.

Notes:
1. Blue areas show origins of water contributing to RCS system.
2. Light yellow portion in top right is where aerial imagery is not available.

Figure 2CC-250 Additional Areas for RCW Approach Velocity Calculation

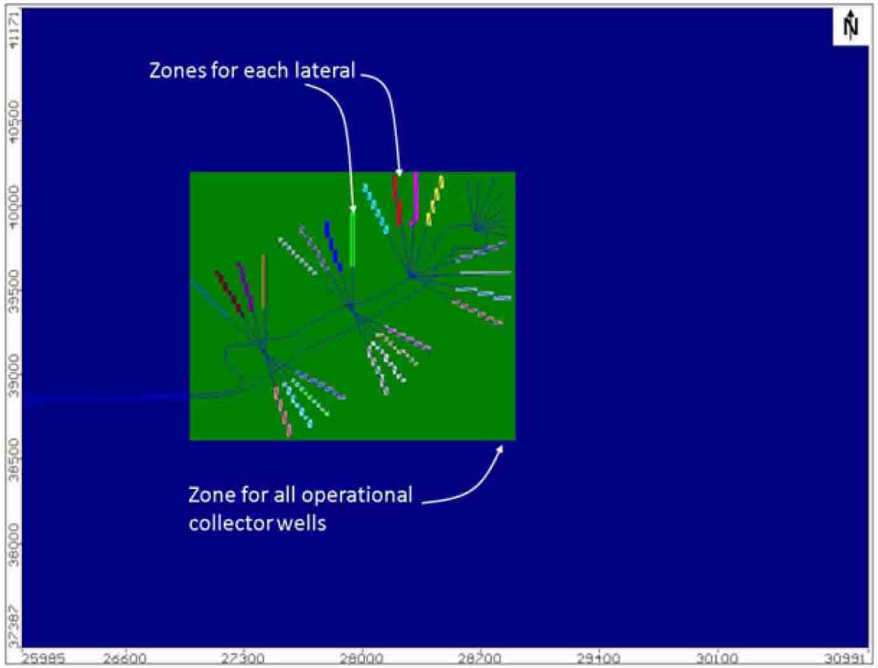

Note: Vertical and horizontal axes represent model coordinates in ft. Model origin at easting 852766, northing 362512 (in State Plane Coordinates, North American Datum of 1983/Adjustment of 1990, Florida East, Zone 0901, US ft)

Figure 2CC-251 Calculated Flux of Water between Layers 1 and 2 (Darcy Velocity)

Notes: Units in ft/day. Light yellow portion in top right is where aerial imagery is not available.
Vertical and horizontal axes represent model coordinates in ft. Model origin at easting 852766, northing 362512 (in State Plane Coordinates, North American Datum of 1983/Adjustment of 1990, Florida East, Zone 0901, US ft).

Figure 2CC-252 RCW Drawdown within the Top Layer — Seasonal High and Low Water Level Biscayne Bay

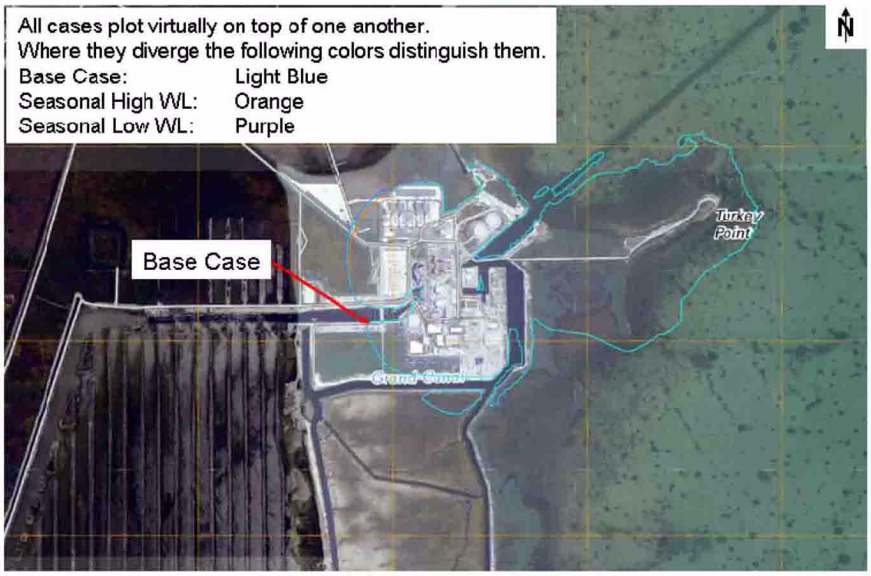

Notes:

1. 0.1 ft drawdown contour.
2. Divergence of drawdown lines is seen to the west and northwest of the existing Turkey Point plant where the drawdown contour for the seasonal high water level is to the east of the base case contour and the seasonal low water level contour is to the west of the base case contour where distinguishable.

Figure 2CC-253 RCW Drawdown within the Top Layer - Sensitivity Case Biscayne Bay Vertical Hydraulic Conductivity

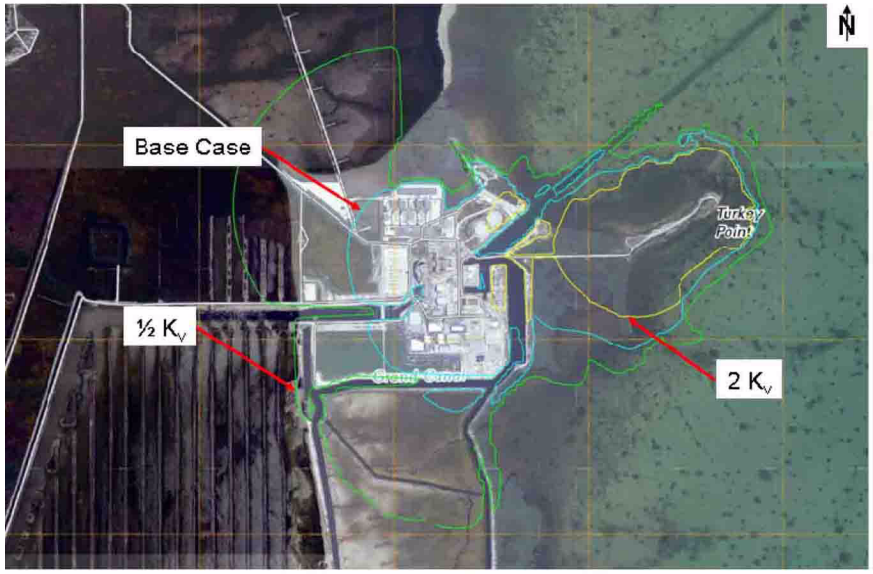

Note: 0.1 ft drawdown contour.

Figure 2CC-254 RCW Drawdown within the Top Layer — Hydraulic Conductivity of Key Largo Limestone

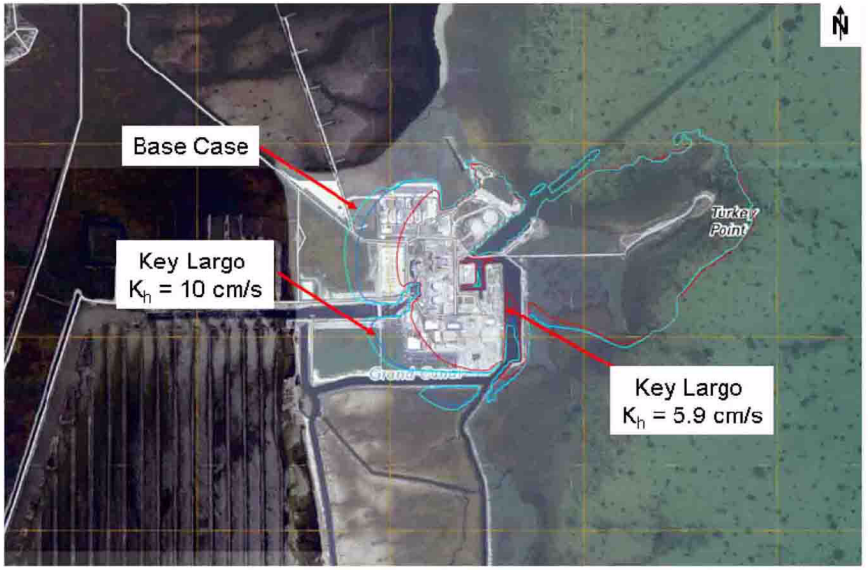

Note: 0.1 ft drawdown contour.

Figure 2CC-255 Hydrostratigraphic Units and Location of Diaphragm Walls (Row 219)

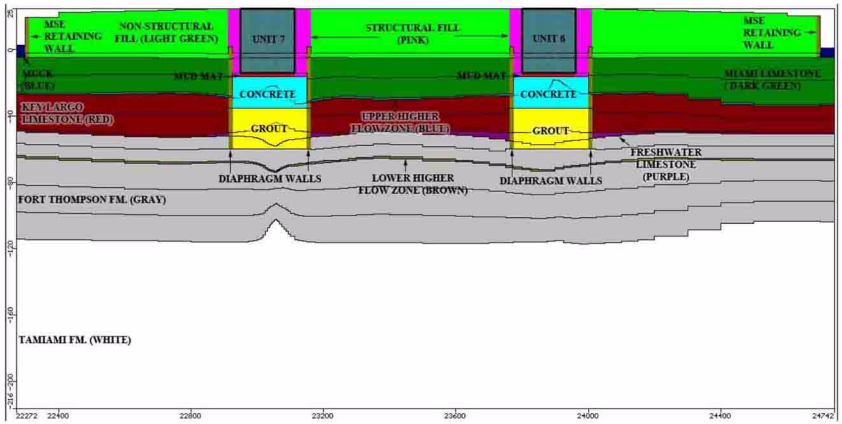

Note: Vertical axis represents elevation in ft NAVD 88. Horizontal axis represents model coordinates in ft. Model origin at easting 852766, northing 362512 (in State Plane Coordinates, North American Datum of 1983/Adjustment of 1990, Florida East, Zone 0901, US ft).

Figure 2CC-256 Layer 2 Diaphragm Walls Relative to Layer 1 Recharge Zones

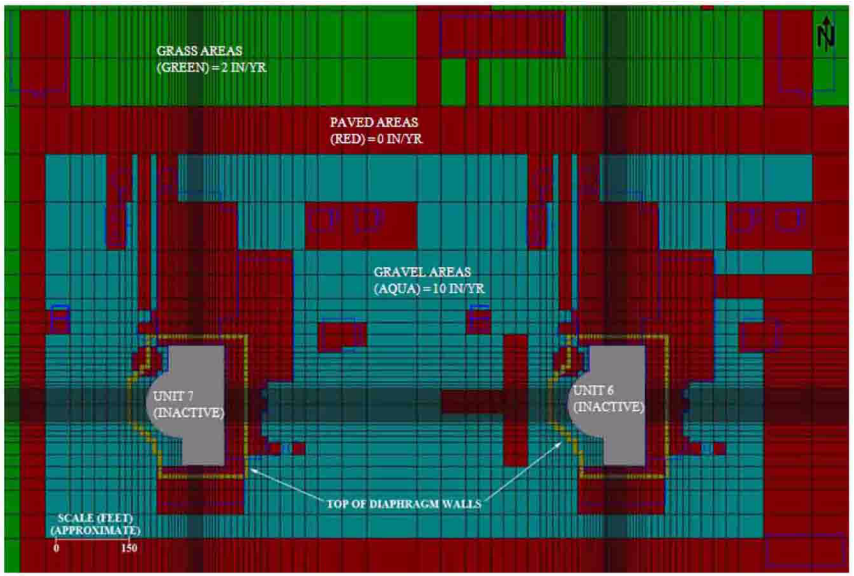

Notes: Diaphragm walls are shown in brown; gravel recharge zones are shown in aqua; paved recharge zones are shown in red; and grass recharge zones are shown in green.

Figure 2CC-257 Phase 2 Post-Construction Recharge Zones for Units 6 & 7

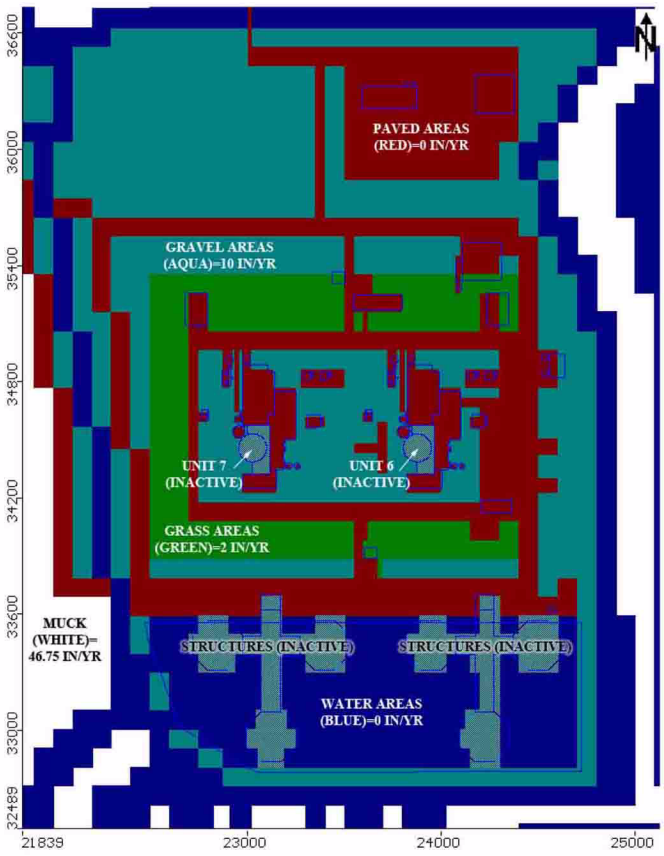

Note: Vertical and horizontal axes represent model coordinates in ft. Model origin at easting 852766, northing 362512 (in State Plane Coordinates, North American Datum of 1983/Adjustment of 1990, Florida East, Zone 0901, US ft).

Figure 2CC-258 K95 and K92 Hydraulic Conductivity Zones

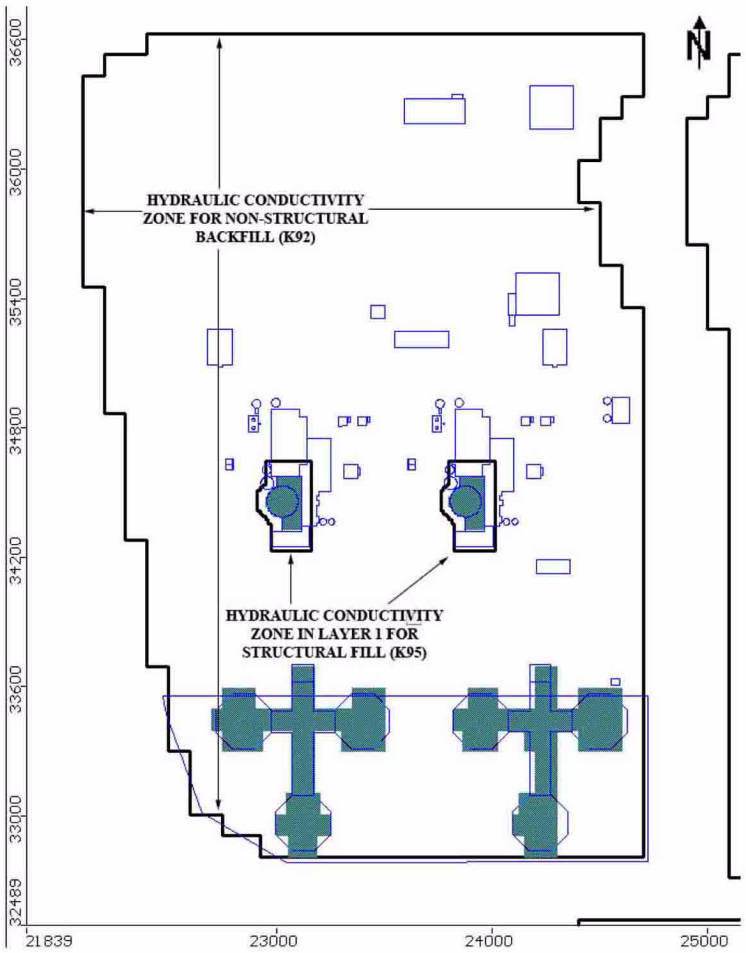

Notes: The Units 6 & 7 plant area is shown by the outer ring (shown as a black line). The inner ring near Units 6 & 7 (also shown as a black line) represents structural backfill (K_{95}).

Vertical and horizontal axes represent model coordinates in ft. Model origin at easting 852766, northing 362512 (in State Plane Coordinates, North American Datum of 1983/Adjustment of 1990, Florida East, Zone 0901, US ft).

Figure 2CC-259 MWR Model Configuration (Row 251)

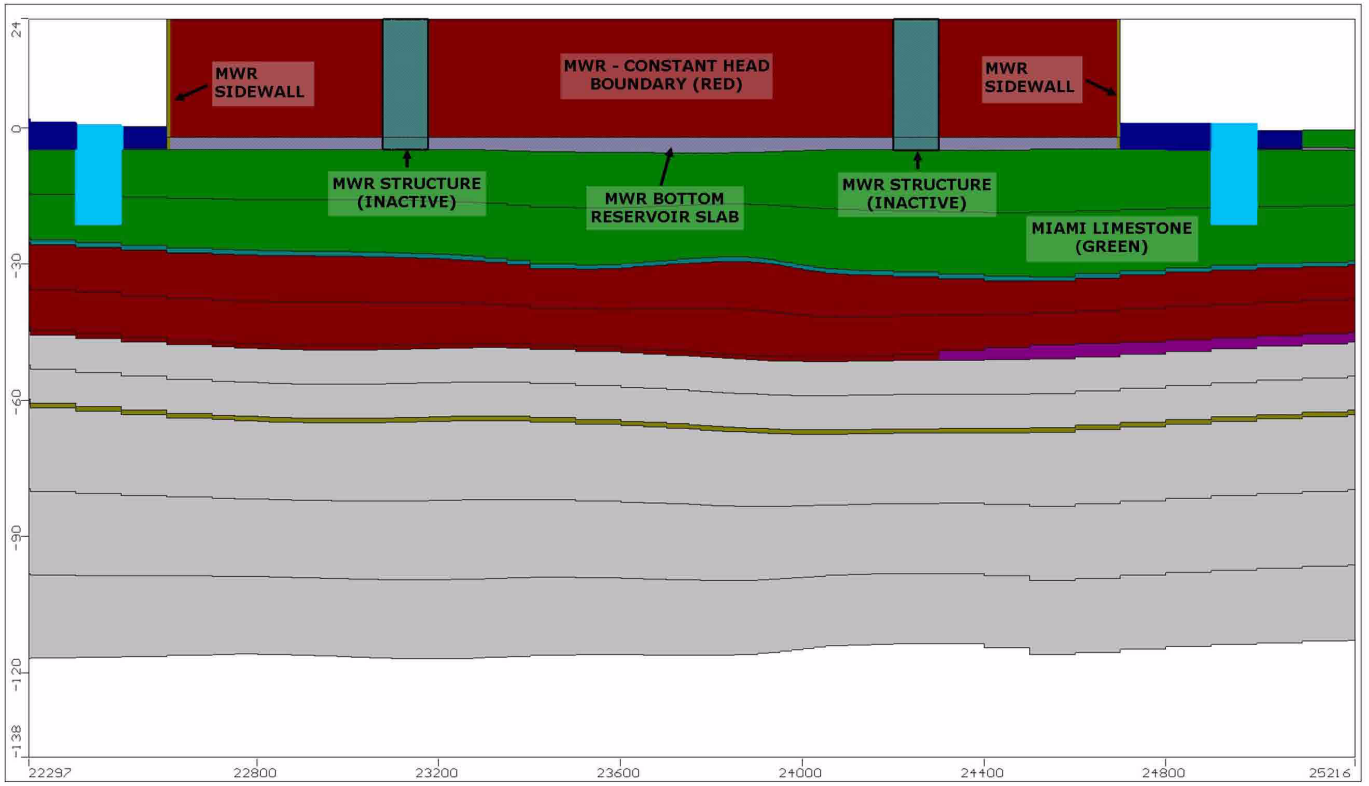

Note: Vertical axis represents elevation in ft NAVD 88. Horizontal axis represents model coordinates in ft. Model origin at easting 852766, northing 362512 (in State Plane Coordinates, North American Datum of 1983/Adjustment of 1990, Florida East, Zone 0901, US ft).

Figure 2CC-260 Phase 2 — Observation Point Locations Near Unit 6 and Unit 7

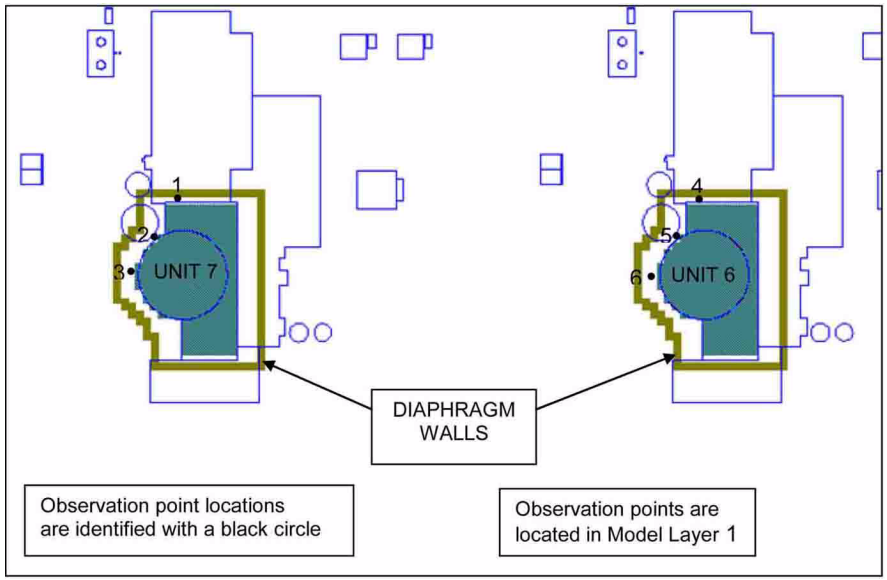

Figure 2CC-261 Phase 2 — Boundary Conditions in Model Layer 1

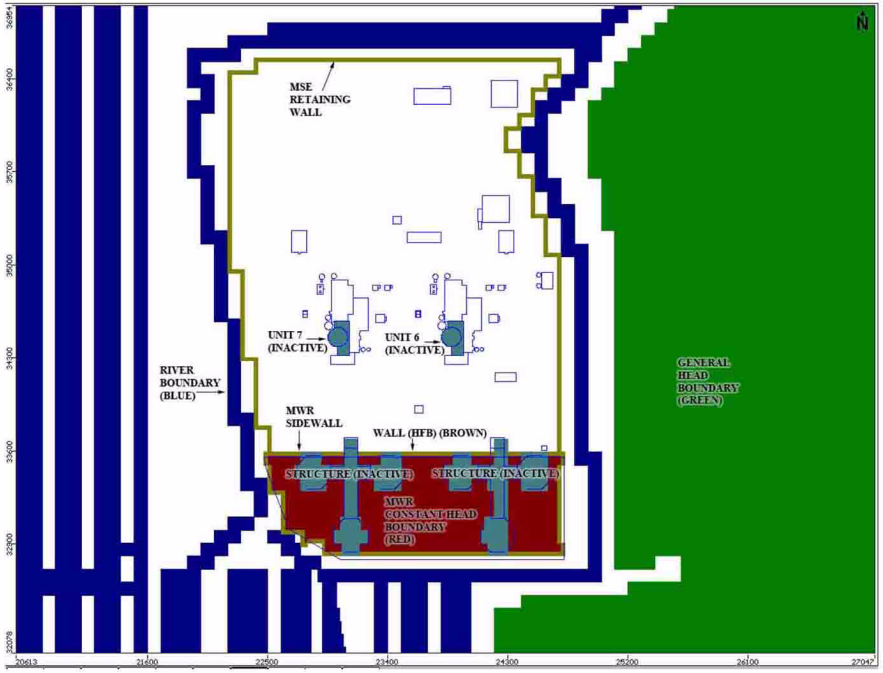

Note: Vertical and horizontal axes represent model coordinates in ft. Model origin at easting 852766, northing 362512 (in State Plane Coordinates, North American Datum of 1983/Adjustment of 1990, Florida East, Zone 0901, US ft).

Figure 2CC-262 Phase 2 Case 1 Simulated Groundwater Contours — Model Layer 1 Under Base-Case MWR Conditions

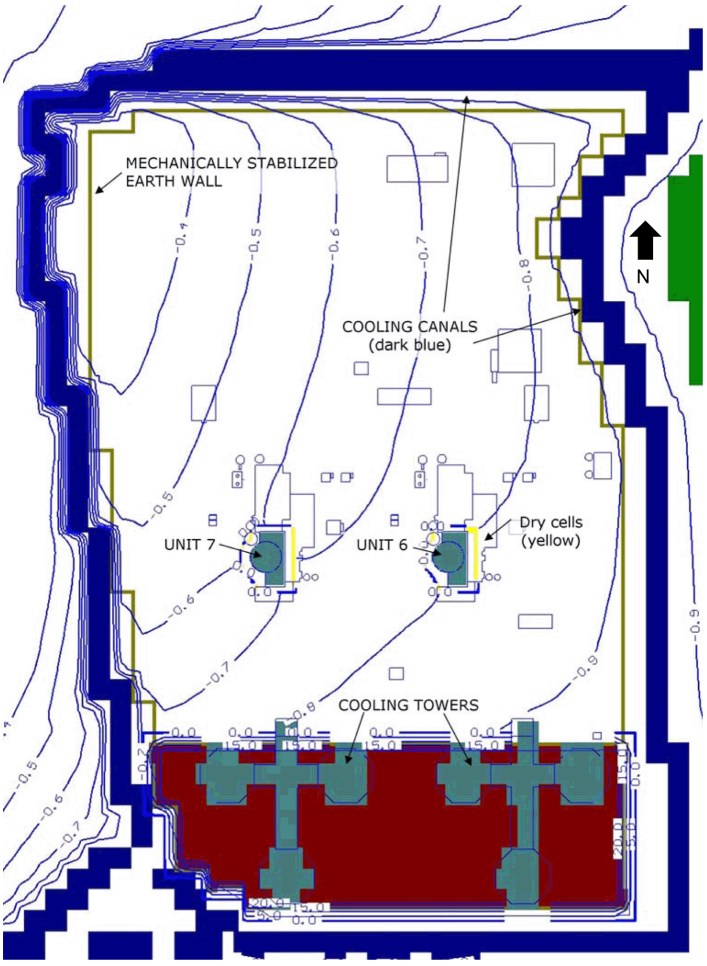

Note: Groundwater level contours in ft NAVD 88.

Figure 2CC-263 Phase 2 Case 3 Simulated Groundwater Contours — Model Layer 1 Under MWR Failure

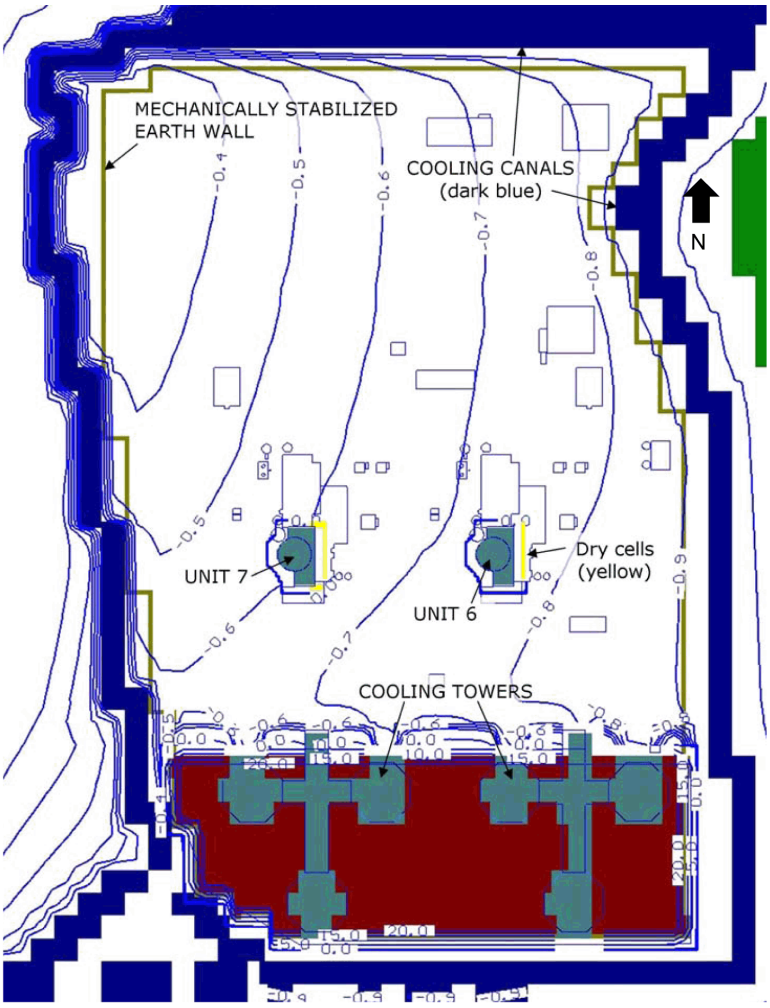

Note: Groundwater level contours in ft NAVD 88.

Figure 2CC-264 Phase 2 Case 4 Simulated Groundwater Contours — Model Layer 1 Under Sea-Level Rise Conditions

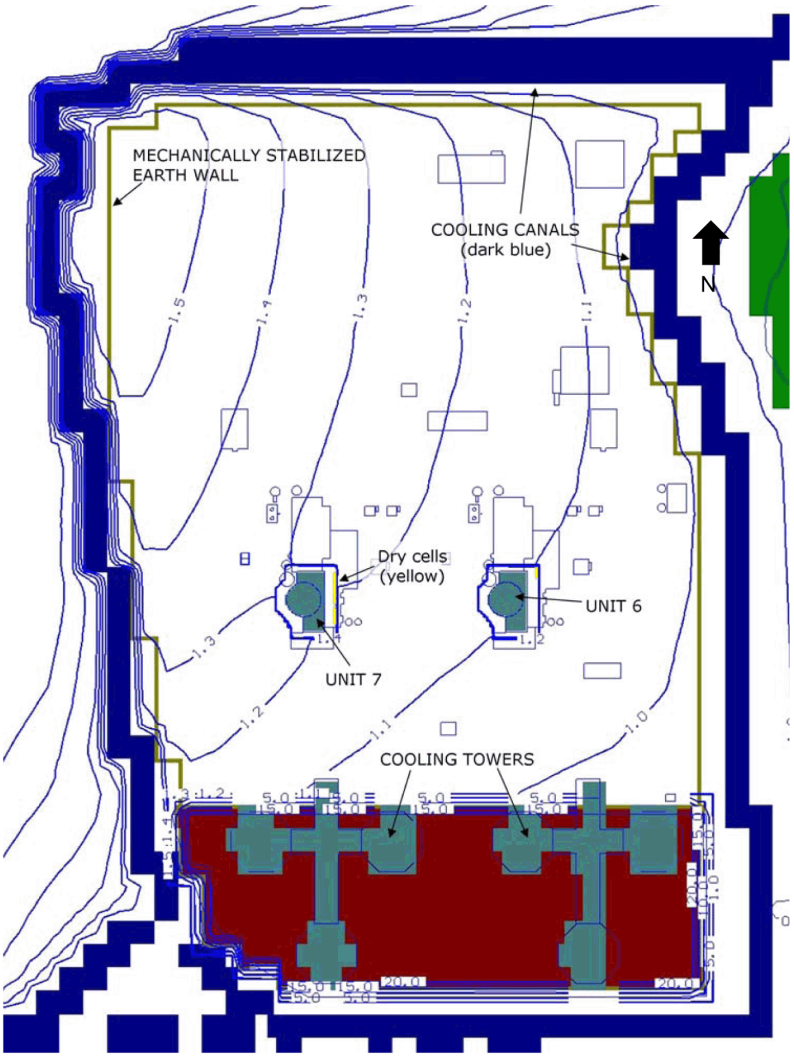

Note: Groundwater level contours in ft NAVD 88.